Optimal Design of Slotless Permanent Magnet Generators

OTT PABUT

TUT
PRESS

TALLINN UNIVERSITY OF TECHNOLOGY
Faculty of Mechanical Engineering
Department of Machinery

This dissertation was accepted for the defence of the degree of Doctor of Philosophy in Engineering on June 15, 2015.

Supervisor: Professor Martin Eerme, Department of Machinery,
Tallinn University of Technology, Estonia.

Opponents: Andrey Aniskevich, PhD, Leading Researcher,
Institute of Polymer Mechanics, University of Latvia, Latvia.

Toomas Lepikult, PhD, Associate Professor,
The Estonian Information Technology College, Estonia.

Andrus Salupere, PhD, Director, Institute of Cybernetics,
Tallinn University of Technology, Estonia.

Defence of the thesis: August 26, 2015.

Declaration:

Hereby I declare that this doctoral thesis, my original investigation and achievement, submitted for the doctoral degree at Tallinn University of Technology has not been submitted for doctoral or equivalent academic degree.

/ Ott Pabut /

Uurdevabade püsimagnetgeneraatorite optimeerimismeetodid

OTT PABUT

TTÜ
KIRJASTUS

CONTENTS

LIST OF PUBLICATIONS

This PhD thesis is based on the following publications, presented in Appendix A and referred in the text to as "Paper 1", "Paper 2", "Paper 3", "Paper 4" and "Paper 5".

Paper 1   **Pabut, O.**; Lend, H.; Tiirats, T. Load Sensitivity Analysis of a Large Diameter Permanent Magnet Generator for Wind Turbines. *In: Proceedings of the 9th International Conference of DAAAM Baltic Industrial Engineering: 24–26th April 2014, Tallinn, Estonia*, 59 – 64.

Paper 2   **Pabut, O.**; Eerme, M.; Kallaste, A.; Vaimann, T. Multi-Criteria Design Optimization of Ultra Large Diameter Permanent Magnet Generator. *Elektronika ir Elektrotechnika*, vol. 21, no. 3, 2015, 43 – 48.

Paper 3   **Pabut, O.**; Kirs, M.; Lend, H.; Tiirats, T. Optimal Structural Design of a Slotless Permanent Magnet Generator. *In: Proceedings of the 10th International Conference of DAAAM Baltic Industrial Engineering: 12–13th May 2015, Tallinn, Estonia*, 1 – 7.

Paper 4   Tiirats, T.; **Pabut, O.**; Kallaste, A.; Herranen, H.; Naar, H.; Vaimann, T. Analysis of Mechanical Vibrations Caused by Eccentricity in a Slow-Speed Slotless Permanent Magnet Generator. *In: Electric Power Quality and Supply Reliability Conference PQ 2014: 11–13th June, Rakvere, Estonia*, 237 – 241.

Paper 5   Patent application EP14192176, Priority date 06.07.14. Placement and Replacement System and Method for Placing and Replacing the Electrical Components of Electromagnetic Rotary Machine. Owner: Goliath Wind OÜ. Inventors: **Pabut, O.**; Zingg, R.; Kisseljov, I.

INTRODUCTION

The current paper focuses on the development process of an electrical generator for wind turbine applications in order to optimise the machine layout in terms of maximum energy yield and minimal system cost. The design of an electrical generator is a complex task involving several different disciplines including mechanical and electrical engineering. Furthermore, very often the used systems incorporate variables of different nature, magnitude and gradient, while being subjected to strict economic, technical and safety related constraints.

The wind energy sector has developed rapidly during the past decades, with the main focus being on larger turbine capacities and rotor diameters [1]. Although more attractive in terms of produced energy, the increase of wind loads and energy output has led to a number of technical challenges related to cooling methods, high component masses and inertias [2]. Even though several turbine sub-systems have gone through a standardisation process, the most optimal concept for the electrical generator remains open [3]. Numerous scientific papers have been presented regarding the electromagnetic layout of such a machine [4–6]. Researchers have also developed analytical and probabilistic methods for the prediction of structural properties of the generator, including electromagnetically active and passive mass [7–8]. Overall weight of the machine is crucial for the so-called direct-drive generators, which have high reliability and power density but also feature high mass and production costs [9–10]. For these particular reasons, the mature technology of a high speed generator in combination with a gearbox still dominates the market [11]. Nevertheless, many researches acknowledge that direct-drive technology still has considerable potential for optimisation and component integration while keeping its known advantages of robustness and efficiency [12–13].

Most of the mass of the described units results from the mechanical carrier structure of the machine [14]. In the past, electromagnetically active materials had high relative prices and, consequently, the focus on decreasing their volume was justified. With the increase of wind energy, the relative price of the active components has steadily declined and at higher turbine capacities, cost composition is dominated by the mechanical part [15–16]. Therefore, a more structured approach, in connection with novel technologies and optimisation procedures tailored for this particular problem, is necessary to reduce the cost of direct-drive generators and the price tag of the produced energy. Established methods employed in other industries have already been used at a small scale to aid in the process of selecting initial design parameters. Isfahani *et al.* [17] have utilised a genetic algorithm to optimise the electromagnetic layout of a direct-drive permanent magnet generator. The same method was used by Li and Chen [18] to match generators with different power ratings and rotational speeds to proposed wind turbine sites.

Main objectives and activities

The main objective of the current study is the development of a methodology for the design optimisation of an electrical generator in a wind turbine. The proposed approach consists of multiple sub-steps to handle the complexity of the task. Furthermore, the investigated electromagnetic and mechanical layouts of the generator have not been utilised previously for machines with capacities in the megawatt ranges and are thus also novel. Since no ready-made analytical methods have been developed for detailed structural modelling, various design tools and meta-modelling techniques including finite element analysis, artificial neural networks and a hybrid genetic algorithm are combined to create the mathematical response model of the machine [19–22]. For effects that are related with manufacturing, small scale and full scale prototype machines are constructed and tested. Even though the proposed approach is illustrated based on one specific layout of the generator, the general principles are applicable to a wide range of layouts, when necessary changes considering the nature of the used parameters are implemented. The featured electromagnetic and mechanical layouts are investigated as they aspire to provide solutions to reduce the transportation problems of direct-drive generators.

Scope and limitations of the research

The main focus of the research is aimed at the mechanical configuration of the machine and especially the weight reduction of the carrier structure. However, as the mechanical setup of such a generator goes hand in hand with the electrical layout, its principle characteristics are also investigated and an analytical procedure is proposed for the initial definition of design parameters. Due to this, a detailed analysis of the magnetic flux and electromotive force is not presented. Only the parameters that are necessary for the investigation of the mechanical properties are described. It has to be noted that for each electromagnetic configuration there exists an optimal mechanical solution, as the acting forces and overall dimensions of the machine are dependent primarily on the electromagnetic layout. In the engineering process, each chosen solution incorporates a unique set of challenges and thus requires a specific approach. During the development of the proposed configurations, practical problems including the influence of eccentricities and the precise positioning of the electromagnetically active elements are studied in detail. This has to be considered as an inseparable part of the research in order to solve the existing problems associated with direct-drive machines.

Novelty

The thesis presents and discusses the following novel solutions and methods:

- a new design approach for an electrical generator in a wind turbine and the methodology for determining the optimal design parameter values;
- the implementation of a slotless electromagnetic circuit and a novel lattice type support structure for a permanent magnet generator at the megawatt scale;
- concepts for improving the transportability of large diameter permanent magnet generators;
- methods for predicting and solving assembly related problems of modular large diameter generators.

Dissemination of results and publications

The results of this doctoral thesis have been presented by the author at six international peer-reviewed conferences. The author has published seven international scientific papers directly associated with the thesis, four of which as the first author. These papers are indexed in databases such as the ISI Web of Knowledge and IEEE. Based on the conducted research, one patent application has been submitted to the European Patent Office.

ABBREVIATIONS AND SYMBOLS

Abbreviations

AEP	Annual energy production
AFPM	Axial flux permanent magnet
ANN	Artificial neural networks
ANOVA	Analysis of variance
COE	Cost of energy
DD	Direct-drive
DFIG	Double-fed induction generator
DOE	Design of experiments
DYN	Machine with dynamic eccentricity
EESG	Electrically excited synchronous generator
EMAS	Machine with unbalanced mass
FEA	Finite element analysis
FEM	Finite element method
FFE	Full factorial experiment
GA	Genetic algorithm
HGA	Hybrid genetic algorithm
IGBT	Insulated-gate bipolar transistor
LEP	Lifetime energy production
MPR	Multiple polynomial regression
MSE	Mean square error
NdFeB	Neodymium magnet
OP	Operational profit
PM	Permanent magnet
PMSG	Permanent magnet synchronous generator
RFPM	Radial flux permanent magnet
SCIG	Squirrel cage induction generator
SmCO	Samarium-cobalt magnet
SN	Signal-to-noise
STAT	Machine with static eccentricity
ZERO	None eccentric machine
TFPM	Transverse flux permanent magnet

Symbols

A_s	linear current density
B_{ecc}	flux density of an eccentric pole
B_n	normal direction air-gap flux density
B_{rm}	remanent flux density of magnets
C	model parameter
$cos\varphi$	power factor between active and apparent power
C_p	rotor power coefficient
c_r	scale parameter of the Weibull distribution
d	eccentricity magnitude
$f(v)$	probability density function of the Weibull distribution
$F(\bar{x})$	objective function of optimisation
$F_C(\bar{x})$	cost characteristic
$F_E(\bar{x})$	efficiency characteristic
$f_i(\bar{x})$	normalised form of the characteristic
$F_M(\bar{x})$	mass characteristic
$F_{SR}(\bar{x})$	structural response characteristic
$F_\varepsilon(\bar{x})$	stiffness characteristic
$F_\sigma(\bar{x})$	strength characteristic
g_{air}	mechanical air-gap
g_{eff}	effective air-gap
G_{fe}	iron conductance
G_g	air-gap conductance
G_l	leakage conductance over magnet edge
g_{mag}	magnetic air-gap
G_{pm}	permanent magnet conductance
G_s	leakage conductance from magnet to magnet
h_c	coil height
h_{iso}	isolation layer height
h_m	magnet height
h_y	total air-gap height
k_a	generator aspect ratio
k_{coil}	coil height to the total air-gap ratio
k_{mag}	magnet height to the total air-gap ratio
k	number of factors
k_p	magnet width and pole pitch ratio
k_r	shape parameter of the Weibull distribution
k_{str}	structural aspect ratio
k_w	total air-gap and pole pitch ratio
l	generator axial length
l_c	coil length
l_m	magnet length
l_{str}	structural axial length

m_{con}	conductor mass
m_{cprf}	cooling profile mass
m_{fixR}	mass of structural fixing items for the rotor
m_{fixS}	mass of structural fixing items for the stator
m_{gen}	generator mass
m_{lam}	lamination mass
m_{mag}	permanent magnet mass
m_{rot}	rotor mass
m_{rot}^{oR}	mass on the rotor's outer electromagnetic radius
m_{rot}^{str}	mass of the structural material for the rotor
m_{stat}	stator mass
m_{stat}^{iR}	mass on the stator's inner electromagnetic radius
m_{stat}^{str}	mass of the structural material for the stator
m_{str}	structural mass
m_{yok}	rotor yoke mass
n_c	number of coils
N_h	number of neurons in the hidden layer
N_{in}	number of neurons in the input layer
N_L	number of hidden layers
n_{life}	turbine lifetime
n_m	number of magnets (poles)
n_{ph}	number of phases
N_{tr}	capacity of the training data
O_r	rotor symmetry centre
O_s	stator symmetry centre
P	power in the wind
ρ_{air}	air mass density
p_{con}	specific cost of the conductor
p_{cprf}	specific cost of the cooling profile
P_{el}	turbine's electrical power
P_{elN}	turbine's nominal electrical power
p_{gen}	generator cost
p_{gen}^{str}	structural material cost for the generator
p_{kWh}	price of electric energy
p_{lam}	specific cost of laminations
p_{mag}	specific cost of permanent magnets
P_{meh}	turbine's mechanical power
p_{rot}^{act}	active material cost for the rotor
p_{stat}^{act}	active material cost for the stator
p_{str}	specific cost of structural material
p_{work}	specific cost of assembly work
p_{yok}	specific cost of the rotor's yoke
q	total magnetic attraction force

q_{ecc}	unbalanced magnetic attraction force
r	turbine rotor radius
R	generator air-gap radius
R^2	coefficient of determination
R_r	rotor's electromagnetic radius
R_s	stator's electromagnetic radius
t	time
v_c	cut-out wind speed of the turbine
v_i	cut-in wind speed of the turbine
v_r	rated wind speed of the turbine
v_{tip}	blade tip speed
v_{wind}	wind speed
w_c	coil width
w_i	weight coefficient for a characteristic
w_m	magnet width
w_p	pole pitch
x_i	design parameter
$\bar{x}_i$	vector of design parameters
X_i	independent design variable
X_j	independent design variable
Y	measured response
β	eccentricity angle
β_0	regression coefficient for intercept
β_i	regression coefficient for linearity
β_{ii}	regression coefficient for square
β_{ij}	regression coefficient for interaction
Δ	range of SN values of the Taguchi method
ε^{max}	sum of the rotor and stator air-gap deformations
ε_{rot}^{max}	maximum rotor air-gap deformation
ε_{stat}^{max}	maximum stator air-gap deformation
θ	coil angle
μ_0	permeability of vacuum
μ_{rm}	relative permeability of the PM material
σ_{rot}^{max}	maximum rotor stress
σ_{stat}^{max}	maximum stator stress
σ_{tan}	tangential component of the Maxwell stress
η	generator efficiency
τ	generator torque
Φ	magnetic flux
ω	rotational speed of the machine

1. STATE OF THE ART

1.1 Wind turbine layout

A wind turbine typically consists of rotor blades to capture the wind and convert it to mechanical rotation, a generator to convert the mechanical energy into electrical energy and a power converter system to convert the electrical energy into a suitable format for the power distribution grid and to control the generator loading [23]. Even though not necessary in principle, historically a gearbox has been used between the rotor blades and the generator, since available standard electrical generators including a double-fed induction generator (DFIG) or squirrel cage induction generator (SCIG) have been used [24]. In order to keep the mechanical wear and noise emission of the rotor blades at an acceptable level, wind turbines rotate at low rotational speed. The above-mentioned generator types are typically operated at a high speed in the range of 1000–3000 rpm, while a 1 MW wind turbine would be limited to a rated speed of 25–28 rpm [25]. Many turbine producers have solved this issue by neglecting the gearbox and introducing a nonstandard generator with a high number of poles to compensate for the low rotational speed [26–28]. The two most common generator types used for this application are the permanent magnet synchronous generator (PMSG) and the electrically excited synchronous generator (EESG). These usually require a power converter for the full power rating, while the DFIG needs a converter with a rating of 25 % of the nominal power [29]. In the case of the PMSG and EESG, the generator is directly connected to the wind turbine rotor and therefore the concept is in general referred to as a direct-drive (DD) solution. The principle schemes of the four most common turbine power conversion types are presented in Figure 1.1.
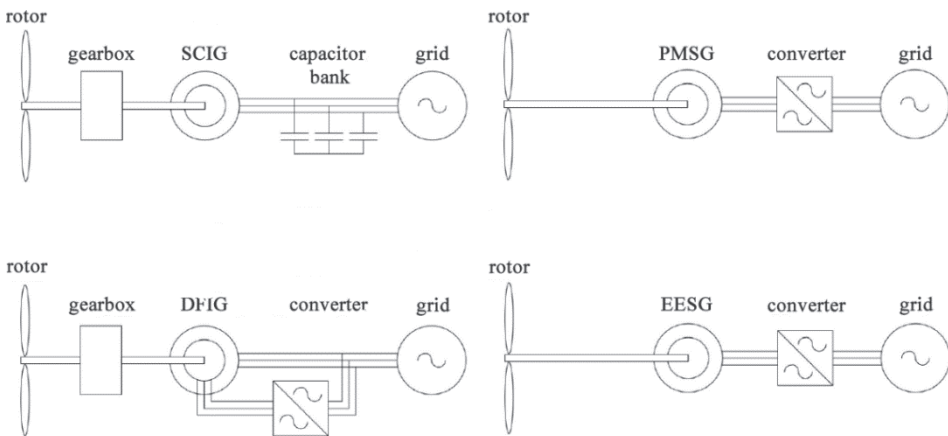

Figure 1.1. Most used wind turbine power conversion systems [29].

1.2   Gearbox or direct-drive

Electrical generators for wind turbines are located on top of tall towers and hence their overall weight from the lifting and loading point of view is one of the most important parameters to be considered. The size and weight of a generator are proportional to the developed torque and since high speed machines develop smaller torque, they tend to be relatively light and inexpensive [30]. At the time when the first commercial wind turbines were introduced to the market, the DFIG and SCIG technologies were already mature and perfectly suitable for smaller capacities. As the turbine nominal power grows, the high speed of these machines is actually becoming one of the largest problems for the described concept. The rotational speed of the turbine rotor is reducing along with the power growth and thus the transmission ratios for the used gearboxes become more unfavourable, while the transferred torque continues to grow. In order to distribute the loading and torque conversion, it is necessary for the gearbox to have multiple stages. This has a well-known negative effect on reliability and energy conversion efficiency [31]. Due to harsh environment, difficult serviceability and the variable nature of loading, gearbox failures have become one of the most noticeable and discussed problems in the wind energy sector [32]. Nevertheless, high speed machines still dominate the market. For example, in the offshore market the most used power conversion principle includes a DFIG or SCIG accompanied by a gearbox [16]. The typical setup of such a turbine is shown in Figure 1.2.
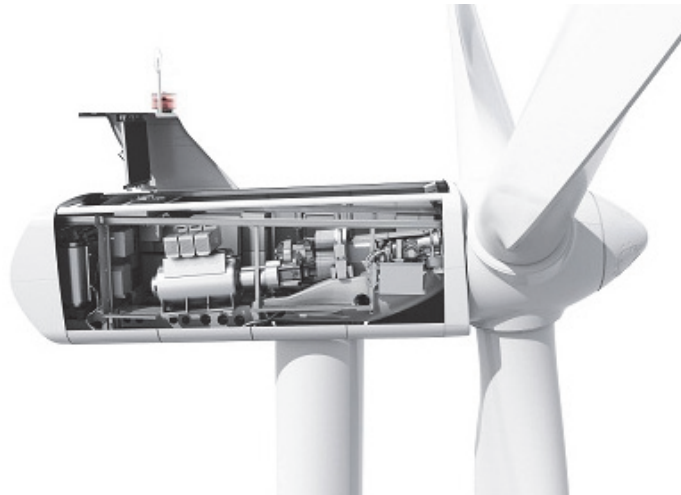

Figure 1.2. A turbine with a DFIG and a gearbox [33].

Many scientific papers have been published on the topic of the DD *vs.* gearbox conundrum. Polinder *et al.* [34] have compared two DD generator systems with three geared solutions in terms of cost and the produced energy, and established that the DFIG with a gearbox remains the most interesting choice in terms of energy yield divided by cost, while the PMSG has the largest energy yield and

thus the greatest future potential. Tavner *et al.* [35] have investigated the reliability aspect of both concepts. Even though failure numbers for the DD and gearbox configurations are fairly similar, the down time caused by repairs is significantly higher for gearbox concepts. Similarity in failure incidents is mainly caused by the increase of failure rates in the full power converter and electrical system. McMillan and Ault [36] have stated that economically gearbox-driven machines are still preferable but there could be a technical advantage in deploying DD machines, which can be turned into commercial advantage if manufacturing costs are reduced. In conclusion, it can be seen that the DD is still considered to be an immature technology with a great potential and pressing need for optimisation and system integration.

1.3 Direct-drive generators

The main advantage of a DD machine is the low number of moving parts prone to wear, especially due to mechanical contact. This enables to reach high mechanical reliability and energy conversion efficiency figures [37]. However, in order to compensate for the low rotational speed, the machine has to feature a high number of poles. Usually, a relatively large outer diameter for the machine is required and as the generator takes part in the full torque conversion process, more structural material is needed to combat the acting forces. The used generator types are generally designed for a specific purpose, since the direct coupling to the turbine rotor leads to a number of special design constraints. The nominal speed of the generator should match the rotational speed of the turbine and in many cases it also has to participate in the transfer of wind loads. The approach mentioned offers many new opportunities for structural optimisation and system integration with other turbine components [8]. A typical, fairly integrated setup of such a machine is presented in Figure 1.3.
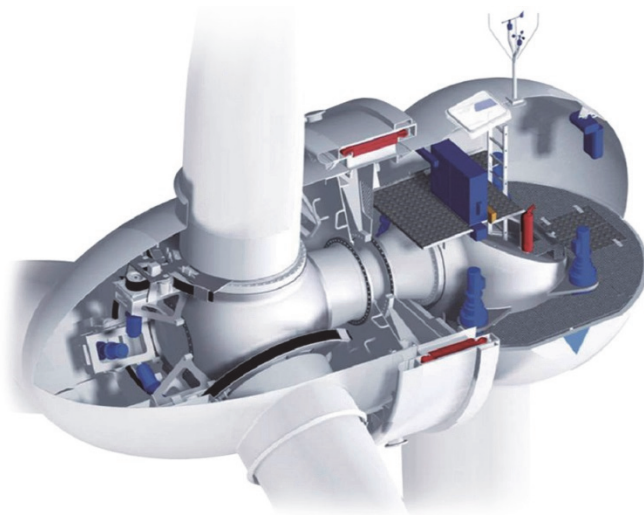

Figure 1.3. A turbine with a PMSG [38].

Among DD generators, the PMSG technology is considered to be more promising in contrast to the EESG. As a rule, the PM excitation allows building lighter machines and results in smaller specific energy cost [39]. The initial cost disadvantage of the PM excitation has faded away, since the relative price of magnets has considerably decreased compared to the times when DD machines first entered the market. Furthermore, the partial load efficiency of PM machines is higher compared to electrically excited machines and thus the total energy yield of the turbine is also increased [34]. The main disadvantage from the technical point of view is the uncontrollable excitation, which can propose problems during assembly and operation.

1.4 PMSG's electromagnetic layout

There are several principle choices and options when the electromagnetic layout of the PMSG is considered. These include flux direction, rotor and stator positions, the magnet layout on the rotor and the winding layout on the stator.

1.4.1 Flux direction

From the viewpoint of the magnetic flux direction with a reference to the rotor rotational axis, the machines can be classified into (see Figure 1.4): radial flux (RFPM), axial flux (AFPM) and transverse flux permanent magnet machines (TFPM). For large scale DD generators, the RFPM configuration seems to be more favoured as the design is relatively simple and the structural stability is easy to achieve [40]. Compared with the RFPM, the AFPM has a lower torque to mass ratio and therefore, these machines tend to be heavier on the active side. For large diameters, the structural stability is more difficult to achieve. This usually leads to larger mass also on the passive side. The TFPM machines have been studied in many scientific publications [41–42] but have not found application in large capacity wind turbines. Reasons for this can be mainly associated with considerable flux leakage and a complicated structural setup in the case of machines with large air-gaps [10]. Most of the manufactures that have chosen the PMSG technology are also using the RFPM configuration due to the described advantages [27–28, 43].
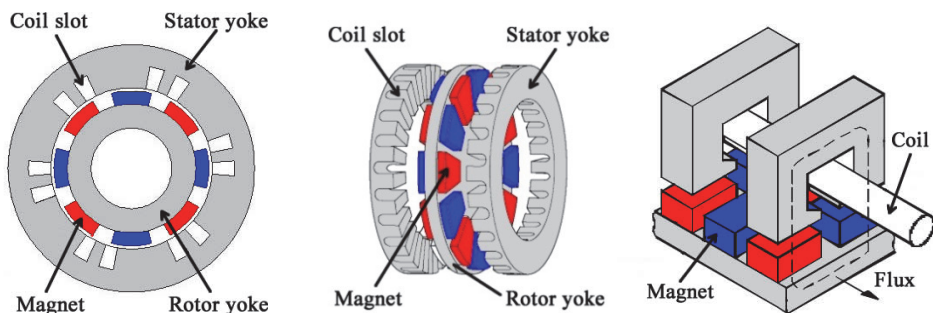

Figure 1.4. Radial, axial and transverse flux generators.

1.4.2 Rotor elements

The main parts of the RFPM machine are the rotor and stator, consisting of a rotor yoke and permanent magnets and a stator yoke and electrical windings, respectively. Permanent magnets on the rotor can be mounted either onto the rotor yoke's surface or buried into the yoke. When the magnets are positioned onto the yoke, materials with high flux densities like NdFeB or SmCo have to be used in order to achieve the desired magnetic field [44]. With buried magnets, the magnetic flux concentration can be employed and higher electromagnetic conversion efficiencies can be achieved or magnetic materials with a lower grade can be used. However, with high grade magnets, flux concentration often leads to high magnetic attraction forces between the rotor and stator, resulting in the built machines becoming very sensitive to radial movements between the rotor and stator. Thus, for large diameter machines surface mounted high grade magnets with curved surfaces are used, as the corresponding rotor can be built with a rather simple structure [45].

1.4.3 Stator elements

Electrical windings in the stator can be either concentrated or continuous, embedded in the stator yoke slots or mounted on the stator yoke, in which case no slots are featured in the stator structure [40]. Usually, the slotted configuration with continuous winding is used, as it provides high flux densities and is a mature technology. The main drawbacks of the configuration include large cogging torque between the rotor and stator and restrictions for the generator diameter upscaling when reaching higher capacities [2]. Many alternatives are offered in the literature to overcome the mentioned deficits. For example, one option is to use a slotless stator construction with negligible cogging torque [46]. Spooner *et al.* have proposed an ironless modular stator, which features no cogging torque at all and can be combined with a lightweight structure due to the absence of magnetic attraction forces [47]. Vaimann *et al.* have developed the concept further with the addition of iron in the stator yoke (see Figure 1.5) to increase the air-gap flux density and reduce the machine dimensions [48]. Such a generator features a simple electromagnetic structure and can be built with ambient air-cooling also for megawatt scale wind turbines.
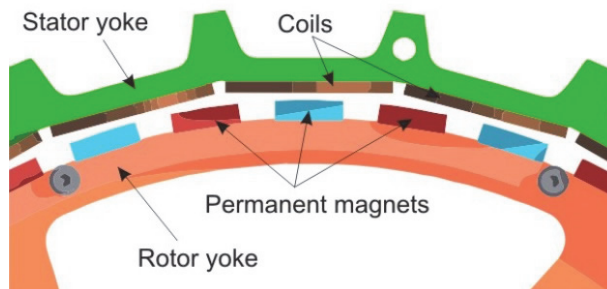

Figure 1.5. A slotless PMSG for wind applications [48].

1.4.4 Inner or outer rotor

The rotor of the RFPM generator can be positioned either inside or outside the generator stator. In the case of an outer rotor some of the active material can be saved or the generator diameter can be reduced, as the magnets have higher linear velocity [27]. As the majority of the heat of a PMSG is generated in the stator windings, most of the turbine manufacturers have opted for an inner rotor. In such an arrangement, the stator windings can be easily cooled by the ambient air, which passes the generator structure. The power produced by a wind turbine generator is connected with the ambient air speed and consequently such a concept is technically well justified.

1.5 PMSG's structural layout

As turbine power outputs and generator sizes rise, the design of the inactive support structure of the PMSG becomes an increasingly more prominent topic, as it starts to dominate the costs composition of the generator. The mechanical structure mainly provides support for the active elements and participates in the transfer of electromagnetic forces. Design requirements usually include the following: adequate rigidity for maintaining the air-gap clearance, sufficient strength properties to resist ultimate and fatigue loads, features to support the auxiliary components, low mass, low cost and size small enough for road transportation [49].

1.5.1 Acting forces

Forces acting on an electrical machine are common for various generator types. However, as the unit is positioned onto the wind turbine tower's top, additional loads have to be taken into account. The main force components to be considered include:

- gravity;
- tangential/shear component of the Maxwell stress (generator torque);
- normal component of the Maxwell stress (the rotor and stator magnetic attraction force);
- rotor centrifugal force;
- turbine tower top accelerations (front-to-back, side-to-side);
- wind load on the generator structure.

Load components and their directions for a RFPM machine with an inner rotor and a cantilever stator are presented in Figures 1.6a and 1.6b, respectively. An arrangement of active elements and the direction of the electromagnetic forces for a slotless RFPM generator with an inner rotor and outer stator is presented in Figure 1.6c.

In order to create more clearance for the turbine blades when they pass the tower, the rotor axis of a wind turbine is tilted compared to the vertical axis (typically about 4°). Therefore, the gravity load has two components which cause widening and narrowing of the air-gap and also the rotor and stator misalignment in the axial direction [9]. Commonly, the RFPM generators have a mechanical air-gap clearance of $1/1000^{th}$ of the air-gap diameter and the allowed deflections are in the range of 10–20 % [39]. As a result, for large diameter machines it is not the load magnitudes that pose a problem, but the small allowed deformations where the gravity component can play a major role.
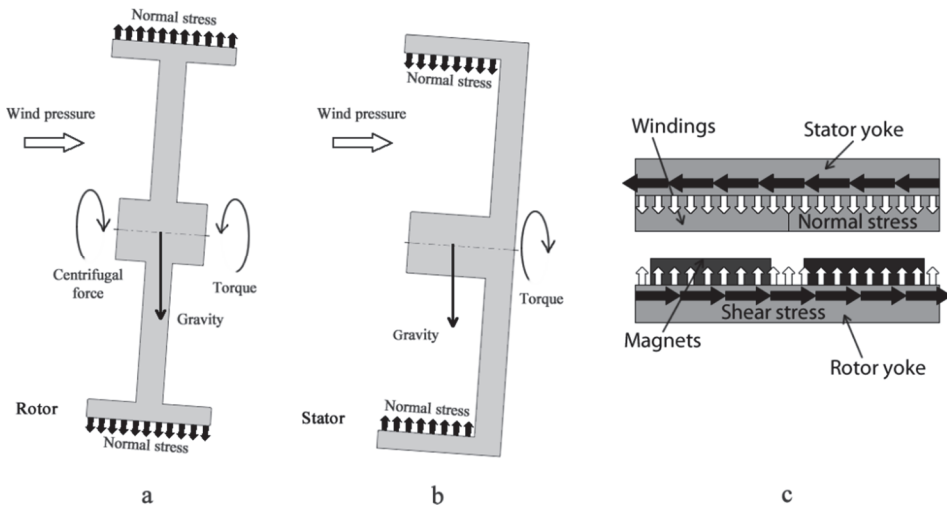

Figure 1.6. RFPM generator forces for the rotor (a) and stator (b) and electromagnetic forces for a slotless RFPM generator (c).

1.5.2 General topology

Depending on the relative positions of the rotor and stator, the chosen bearing concept and level of integration, various topology configurations are possible for the generator. With the elimination of a gearbox, the only primary components subjected to mechanical wear are the bearings between the rotor and stator [50]. All the bending moments resulting from the turbine rotor are transferred through the bearings into the stationary structure and therefore the chosen concept for these also determines the generator topology. Commercial turbines tend to use single or double bearing arrangements. When only one bearing is used, the cantilever design has to be used for either the rotor or stator or for both. If two bearings are utilised, the outer element is usually of the cantilever nature, while the inner element has central support. Even though the cantilever design results in an unfavourable load bath, it is used as a standard approach to ease the assembly process. As an exception, the Spanish producer MToi has utilised the double supported concept for both the rotor and stator [51]. In contrast to usual solutions of placing the bearings near the rotational

axis, Engström *et al.* [52] have proposed the *NewGen* concept where the bearings are located inside the generator air-gap. Although mass and stiffness requirements for the generator are greatly reduced, the high component count and wear of roller elements has a severe negative effect on the reliability of the overall system. The most commonly used bearing and corresponding rotor and stator configurations are presented in Figure 1.7.
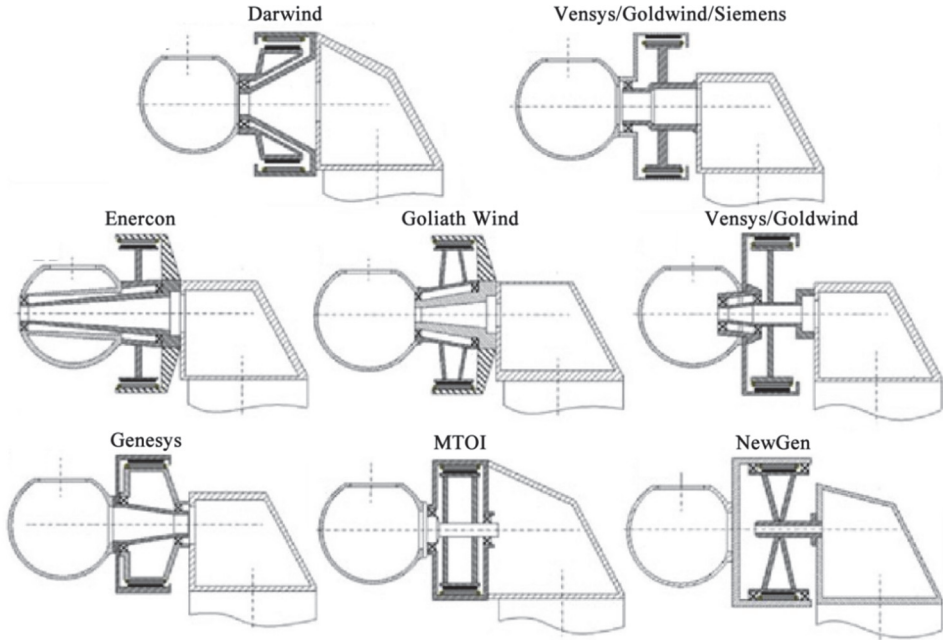

Figure 1.7. RFPM generator topology on a wind turbine [49]*.*

1.5.3   Substructure options

In most cases, the passive structure for a DD generator consists of sheet metal plates arranged as discs, structurally profiled spokes, support arms or discs with stiffness ribs [49]. As previously mentioned, the main task of the mechanical structure is to resist air-gap deformations and as a result, the described structures are in most cases radially stiffened (see Figure 1.8). Rigidity is commonly achieved by rearranging the material placement rather than employing materials with higher stiffness properties. With lower capacity turbines, designs remain compact and structures can be rather simple without a high weight penalty. However, for output powers over several megawatts, the support structures of DD machines are often contributing the highest amount of mass for the turbine tower top. According to scaling laws developed by Shrestha *et al.* [7], torque of a DD machine increases more than proportionally, compared with the power level increase.

Figure 1.8. Radially stiffened rotor structure of Enercon GmbH [53].

Since the mass of a generator is proportional to the developed torque, the upscaling of existing technologies eventually leads to unnecessarily heavy and expensive designs. For example, the mass of the now obsolete Enercon E-112 with the power output of 4.5 MW was already 220 tons [54].
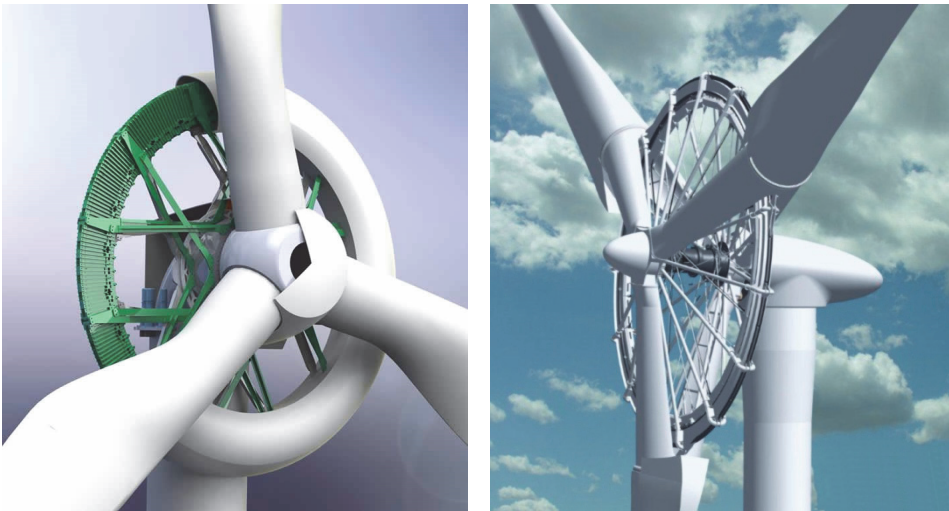
Figure 1.9. Lightweight air-core ultra large diameter generators [55–56].

In order to break the technological barrier, alternative options for lightweight structures are being researched. For reducing the structural mass dominating at higher capacities, designs with an ironless stator and ultra large radiuses supported by pre-stressed tension rods and a bicycle like arrangement of spokes (see Figure 1.9) have been offered in academic research [47, 57] and are being developed by the commercial companies Boulder Wind Power [55] and Sway Turbine [56]. Unfortunately, until now no full scale turbine prototypes have

been successfully erected. With diameters far greater than usual, an additional set of technical challenges needs to be solved. Due to the size of the components, transportation restrictions need to be taken into account, which leads to mechanically and electromagnetically segmented assemblies. In many cases, the full machines are also too large for the mechanical treatment of the air-gap diameter and additional methods for controlling the manufacturing tolerances need to be taken into account [58]. For PM machines, the assembly of magnetically active rotor segments needs to be carefully planned even for air-core machines and it often proves to be the most difficult of the technical challenges.

1.6   Objectives of the research

Based on the state of the art review, <u>the main objective</u> of the current study is the development of a methodology for the design optimisation of an electrical generator in a wind turbine. The main novel features of the process are the inclusion of a pre-design block containing an in-depth analysis and simplification of the initial problem and decomposition of the overall task into sub-optimisation routines. The goal of the procedure is the reduction of the generator's weight and increase of the energy output.

<u>Secondary objective</u> is the implementation of novel electromagnetic and mechanical configurations, with the aim to reduce the transportation and weight problems associated with direct-drive machines. As the described layouts feature their specific problems, several subtasks of the study can be outlined:

- the development of analytical methods for defining initial design parameters;
- the compilation of a mathematical response model for the novel structural layout through FEA;
- the development of solutions for reducing the effect of assembly accuracy for a modular structural layout;
- the investigation of assembly accuracy and resulting operational problems for the large diameter generator.

Hypotheses

The main hypotheses of the thesis can be described as follows:

H1: The weight of a generator designed by conventional methods can be reduced with the proposed optimisation process while increasing the energy output and keeping costs within reasonable limits.

H2: Decomposing the optimisation problem in to pre-analysis, electrical design and mechanical design blocks reduces the complexity of the proposed problem without a significant penalty on the achieved results.

H3: The proposed novel electromagnetic and mechanical layouts reduce the transportation problems associated with direct-drive machines.

H4: The proposed generator layout can be assembled with an accuracy that does not compromise the output characteristics and mechanical safety of the machine.

In the following chapters of the thesis, the results are offered and investigation is carried out to prove the proposed hypotheses.

2. GENERATOR DESIGN METHODOLOGY

In the wind energy sector, engineers are facing the challenge of selecting design parameters that influence the performance of the wind turbine throughout aerodynamic, electromagnetic and mechanical design phases. Different optimisation algorithms and fitness functions have been utilised to reduce the design space, depending on the specific goals and constraints of the particular system. These can range from the reduction of active mass to the increase of efficiency. However, the primary fitness functions of interest for a renewable energy system are usually the cost of energy (COE) and operational profit (OP) [59–60]. During design activities, analytical models are often combined with the finite element method (FEM) [61] while approximating methods like GA are used to solve the proposed [62] optimisation problem. The fitness functions also differ in nature and can be either one-dimensional [63] or multi-criteria [64] ones. There are several ways to set up the optimisation problem and the focus is shifting towards the decomposition and simplification of the actual modelling work in order to reduce the need for complex analytical and numerical analyses.

2.1 Used methods

In the current research, analytical equations are used to set up a number of designs for the meta-modelling approach. Back-propagation ANN and multiple polynomial regression (MPR) are used for meta-modelling due to their general high accuracy and simplicity. The quality of these methods depends on the design data used as the basis for learning. Therefore, the population of initial designs is created following the guidelines set by the Taguchi method and the full factorial experiment (FFE) technique [65]. In order to find the optimal solutions within the design space, HGA is employed [66]. When multiple contradicting criteria are considered, the Pareto optimality criterion is applied to describe the achieved results and provide information for the selection of optimal solutions.

2.1.1 Artificial neural networks

In this paper, the response modelling and optimisation of the electromagnetic layout (Section 4.2) is carried out by the combination of ANN and HGA. Input data for the procedure are determined by analytical equations and FEM analysis. No specific rules for the appropriate architecture of the ANN, considering the current application, can be found in the literature as it has to be configured for each particular problem. The minimisation of the mean square error (MSE) and general robustness of the network can be and are used as acceptance criteria for the ANN. Various different methods exist for determining the architecture of the network for the approximation of different functions [67]. It has been proven that an ANN with a single hidden layer can approximate any continuous function accurately on a compact set and an ANN with two hidden layers can approximate any function to arbitrary accuracy [68]. In the current study, the

rules of thumb have been omitted and the following formulae are considered to involve the capacity of the training data [67]:

$$N_h = \left(N_{in} + \sqrt{N_{tr}}\right)/N_L, \tag{2.1}$$

$$N_h = C(N_{tr}/(N_{in}\log(N_{tr}))^{1/2}, \tag{2.2}$$

where N_L is the number of hidden layers and N_{tr} the capacity of the training data, N_h, N_{in}, stand for the numbers of neurons in the hidden and input layers, respectively. The expression (2.2) contains the parameter C, which has to vary for determining N_h. Consequently, the formula (2.1) is used for determining the starting point and the number of hidden layers is increased up to the upper bound set by the right hand side of the formula (2.2) (see [67]):

$$N_h \le N_{tr}/N_{in}. \tag{2.3}$$

The tuning process of the neural network has been interrupted if increasing the number of neurons further does not improve the accuracy. The MPR model described in the next section has been considered as an alternative algorithm.

2.1.2 Multiple regression model

Response surface modelling and the optimisation of the structural layout (Section 4.3) is carried out by MPR modelling. Input data for the procedure are determined by the FEM of the generator structure and the corresponding responses. Structural modelling combined with a sufficient amount of learning data do not involve highly non-linear effects but the interactions of the design parameters can be significant. Therefore, the quadratic model is chosen to represent the objective functions with the following general form [65]:

$$Y = \beta_0 + \sum_{i=1}^{k} \beta_i X_i + \sum_{i=1}^{k} \beta_{ii} X_i^2 + \sum_i \sum_j \beta_{ij} X_i X_j, \tag{2.4}$$

where Y is the measured response, k is the number of factors, β_0, β_i, β_{ii} and β_{ij} are the regression coefficients for intercept, linearity, square and interaction and X_i and X_j are the independent design variables. Values for the regression coefficients are determined by the least square method. Fitness of the model is kept in mind and assessed by using the analysis of variance (ANOVA) and investigating the coefficients of determination (R^2). In this study, the achieved values for R^2 for all of the objective functions are above 0.95 (maximum value 1), thus the quadratic models exhibit sufficient accuracy for the described analysis [69]. It is possible to raise the accuracy of the models by using higher order regression. However, it has to be observed that for increased order the number of experiments necessary has to be increased as the models will otherwise become aliased [65]. The optimisation procedure is carried out in the *Design Expert 9* software environment.

2.1.3 Hybrid genetic algorithm

The HGA has been applied successfully by the Tallinn University of Technology's research group for solving the optimality problems of composite and sheet metal structures [20–22]. In the current study the algorithm is adapted for optimising the wind turbine generator design.

The HGA utilised for the optimisation procedure contains:
- the mixed integer GA for global search;
- the gradient method combined with branch and bound algorithm for finding the local optimum in the predefined design space.

The local search is carried out only for the individuals complying with the following requirements:
- individuals belong to the first 15 % of the population based on the values of the fitness function;
- the distance between individuals is not less than the given value (diversity condition).

The proposed HGA is less time and calculation effort consuming than the traditional GA and will not feature problems with convergence to the exact minimum by reaching an infinite loop near the minimum. The entire procedure is carried out with the use of the *MATLAB* neural networks toolbox.

2.2 Problem formulation

The minimisation of the COE and maximisation of the OP of a wind turbine and therefore also the employed generator is the desired goal for any wind energy converter. This task can be achieved in various ways, out of which one happens to be the improvement of technology and the engineering process. Based on the state of the art review it can be concluded that there are a number of key factors influencing the above-mentioned objectives and thus a multi-criteria optimisation problem in the general form can be given as follows:

$$F(\bar{x}) = (F_\varepsilon(\bar{x}), F_\sigma(\bar{x}), F_M(\bar{x}), F_C(\bar{x}), F_E(\bar{x})), \qquad (2.5)$$

subjected to the constraints

$$g_i(\bar{x}) \le g_i^*, \qquad i = 1, \dots, n_1, \qquad (2.6)$$

$$h_j(\bar{x}) = h_j^*, \qquad j = 1, \dots, n_2, \qquad (2.7)$$

$$x_i \le x_i^*, \quad x_{i^*} \le x_i \le x_i^*, \quad -x_i \le -x_{i^*}, \quad i = 1, \dots, n, \qquad (2.8)$$

where $F(\bar{x})$ is the chosen objective function of optimisation,

$F_\varepsilon(\bar{x})$ is the stiffness characteristic subjected to maximisation,

$F_\sigma(\bar{x})$ is the strength characteristic subjected to maximisation,

$F_M(\bar{x})$ is the mass characteristic subjected to minimisation,

$F_C(\bar{x})$ is the cost characteristic subjected to minimisation,

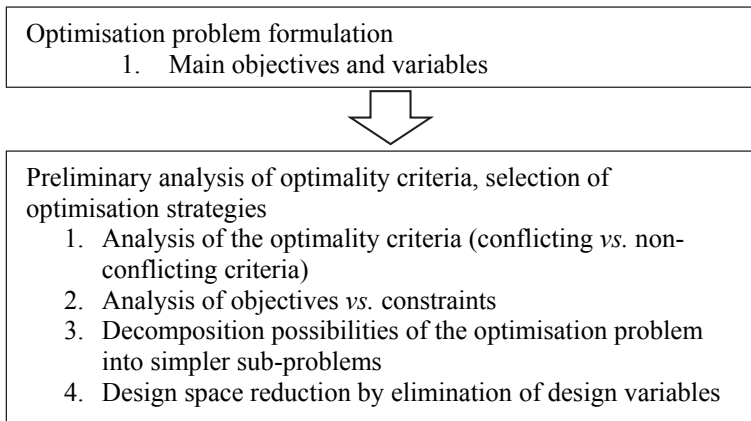$F_E(\bar{x})$ is the efficiency characteristic subjected to maximisation,

$\bar{x} = [x_1, \dots, x_n]$ is the vector of design variables,

g_i^*, h_i^*, x_{i^*}, x_i^* are the given constants.

For a generator in a wind turbine with the given power output the COE and OP are mainly dependent on the cost of the machine $F_C(\bar{x})$ and the electrical conversion efficiency $F_E(\bar{x})$. The end values of these functions are influenced by all choices made by the design team and usually the direct consequences on a global level are difficult to understand. The approach proposed in the following chapters allows decomposing the solution of the optimal generator design into less complicated subtasks while taking into account multiple criteria.

2.3   Optimisation procedure

In the case of a complex multi-criteria optimisation problem, the preliminary analysis of the optimality criteria and possible simplification options are extremely important, such as the pre-processing in the FEA. The general approach for handling the optimality criteria is presented by Velsker [70]. However, for a specific problem no unique rules can be found in the literature. The preliminary analysis of the criteria and the corresponding simplifications allow to avoid principle miscarriages in the selection of optimisation strategies, reduce computational effort and the complexity of the task [71–73]. Therefore, in the current study the main focus is turned to the simplification of the initial global optimisation problem through preliminary analysis of optimality criteria and the decomposition of the problem into electromagnetic and structural optimisation blocks. The proposed procedure for solving the optimal design problem of an electrical generator in a wind turbine is described in Figure 2.1.

| Optimisation problem formulation |
| 1.   Main objectives and variables |

⇩

| Preliminary analysis of optimality criteria, selection of optimisation strategies |
| 1. Analysis of the optimality criteria (conflicting *vs.* non-conflicting criteria) |
| 2. Analysis of objectives *vs.* constraints |
| 3. Decomposition possibilities of the optimisation problem into simpler sub-problems |
| 4. Design space reduction by elimination of design variables |

Reformulation of the optimisation problem and sub-problems
1. Definition of objectives, variables, constraints, design space and key characteristics

Electromagnetic optimisation block
1. Electromagnetic parameters considered as variables, structural parameters as constants
2. Determination of responses for efficiency, cost and structural response
3. Check for constraints, optimality conditions, sensitivity of the solution

Optimal electromagnetic relative/actual dimensions of the machine in terms of efficiency, cost and structural response

Structural optimisation block
1. Structural parameters considered as variables, electromagnetic parameters as constants
2. Determination of responses for structural mass, cost, deformations and stresses
3. Check for constraints, optimality conditions, sensitivity of the solution

Optimal structural relative/actual dimensions of the machine in terms of structural mass, cost, deformations and stresses

Estimation of generator energy production and final price

Satisfactory   Unsatisfactory

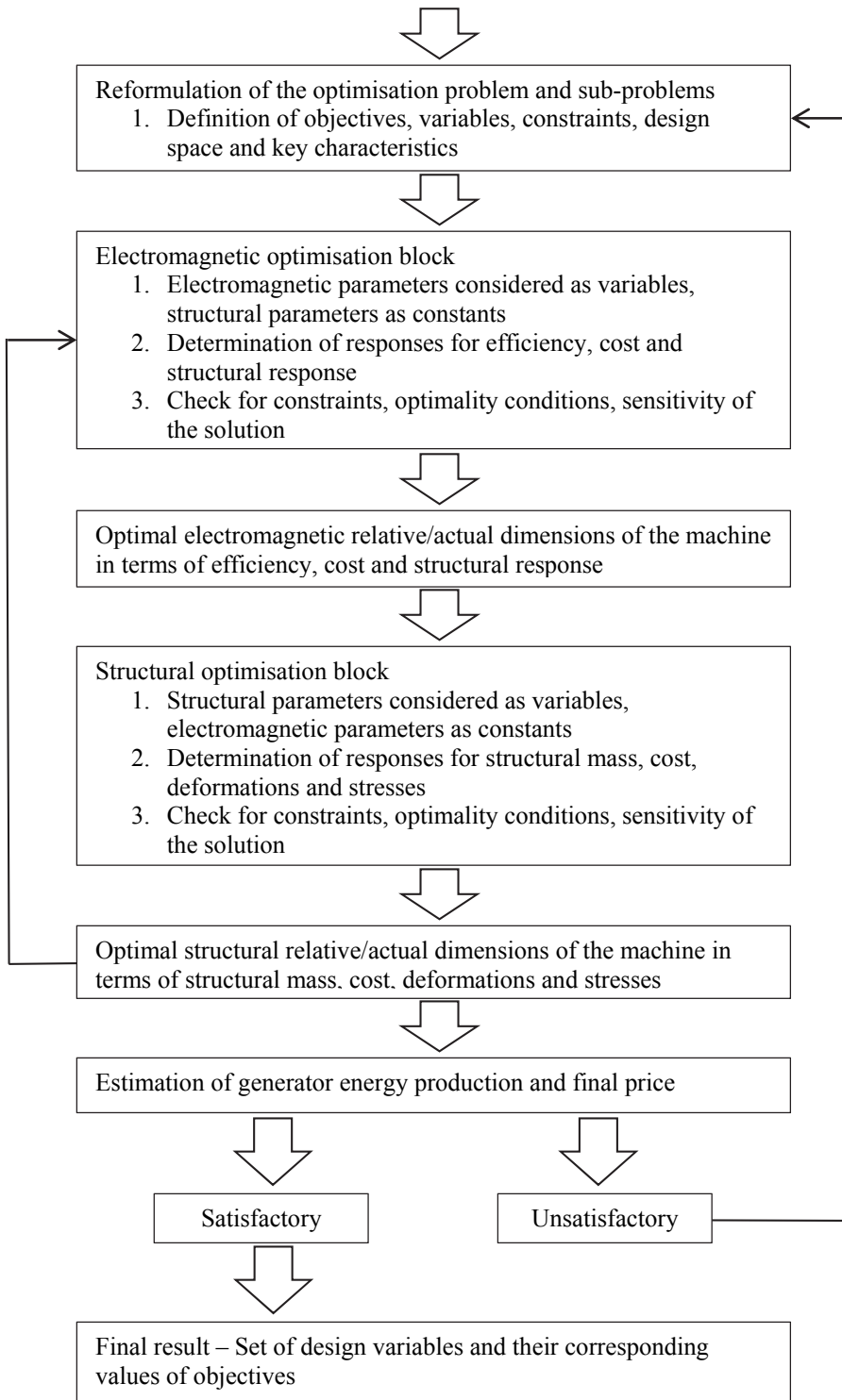Final result – Set of design variables and their corresponding values of objectives

Figure 2.1. The general optimisation procedure.

In general, the optimisation problems for a certain goal can often be formulated in several ways and considering different aspects. Thus, the selection of optimality criteria, constraints and objectives has to be thoroughly investigated to reach a qualified solution with the smallest amount of effort. In structural engineering, the question often lies in the optimal structural shape and the acting forces can be treated as constants. For an electrical generator, the acting forces depend greatly on the electromagnetic layout and thus they should be considered as parameters. This increases the number of required experiments to achieve a reasonable accuracy for the response modelling. The electromagnetic layout also determines the efficiency of the generator system and influences the cost structure. The cost $F_C(\bar{x})$ and efficiency $F_E(\bar{x})$ functions are contradicting in nature and cannot be combined into a single objective. Therefore, a simultaneous optimisation that takes into account electromagnetic and structural parameters demands a high number of parameters and simulations/experiments to reach acceptable sensitivity and accuracy values for the objective functions. Nevertheless, as the interaction between the electromagnetic and mechanical parameters exists, a fully separate analysis does not naturally provide the best solutions in terms of optimality.

The approach presented above allows handling these processes and sets of parameters separately while considering the interaction of the design variables. In the electromagnetic optimisation block, structural parameters are treated as constants and the effect of the chosen configuration on the mechanical structure is assessed via combining the rotor and stator stiffness characteristic $F_\varepsilon(\bar{x})$ and strength characteristic $F_\sigma(\bar{x})$ into a single structural response characteristic $F_{SR}(\bar{x})$. The basis for the given simplification results from the fact that the configurations which evoke the lowest structural response will also lead to the lightest structural designs in later stages. In the electromagnetic optimisation block, the cost $F_C(\bar{x})$ and structural response $F_{SR}(\bar{x})$ are non-contradicting and thus evaluated against the efficiency characteristic $F_E(\bar{x})$ based on the Pareto optimality criteria. The values of electromagnetic design variables which lead to the most favourable results in terms of all considered criteria are implemented in the structural optimisation block as constants. Further analysis is directed towards finding the best combination of variables leading to the lowest structural mass $F_M(\bar{x})$ and cost $F_C(\bar{x})$ characteristics, which in the structural analysis block are non-contradicting and combined into a single criterion. Once the optimal solution is achieved in the structural optimisation block, a full generator design can be compiled or the found structural parameters can be used as input for a revised electromagnetic optimisation, creating an iterative procedure.

In the case of an unsatisfactory overall outcome or a violation of constraints, the whole procedure is reverted to the formulation of the optimisation problem and sub-problems. In general, it is possible to simply exclude the solutions that do not fit into the design space. However, as the goal is to produce suitable solutions during every optimisation run, it is more beneficial to review the

optimality criteria or apply additional design parameter restrictions to keep the future results within the desired range.

The optimisation procedure for the electromagnetic block is given in Figure 2.2 and for the structural block in Figure 2.3. The procedures are depicted together with specific methods employed for solving each of the steps in the block for the described generator. However, in general the proposed procedure is not linked with any specific method. These can be chosen freely according to the specificities of the generator layout, demands set by accuracy and the number of used variables. An overview of the methods and a description of their application criteria is given in [70].
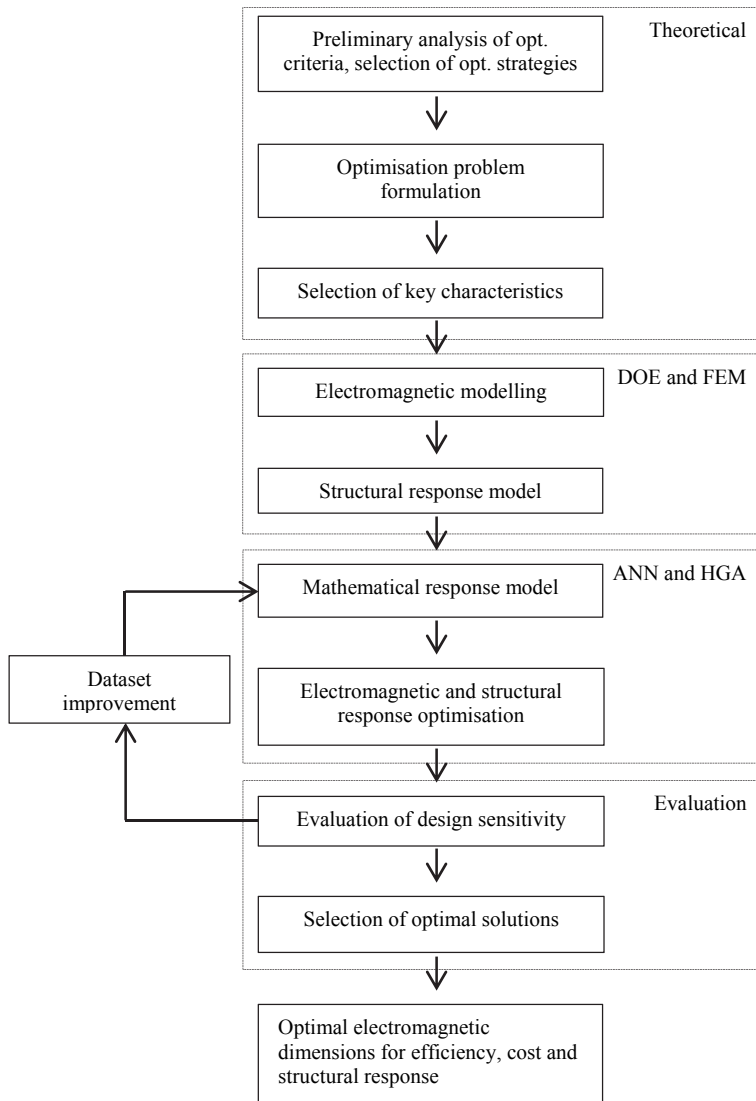
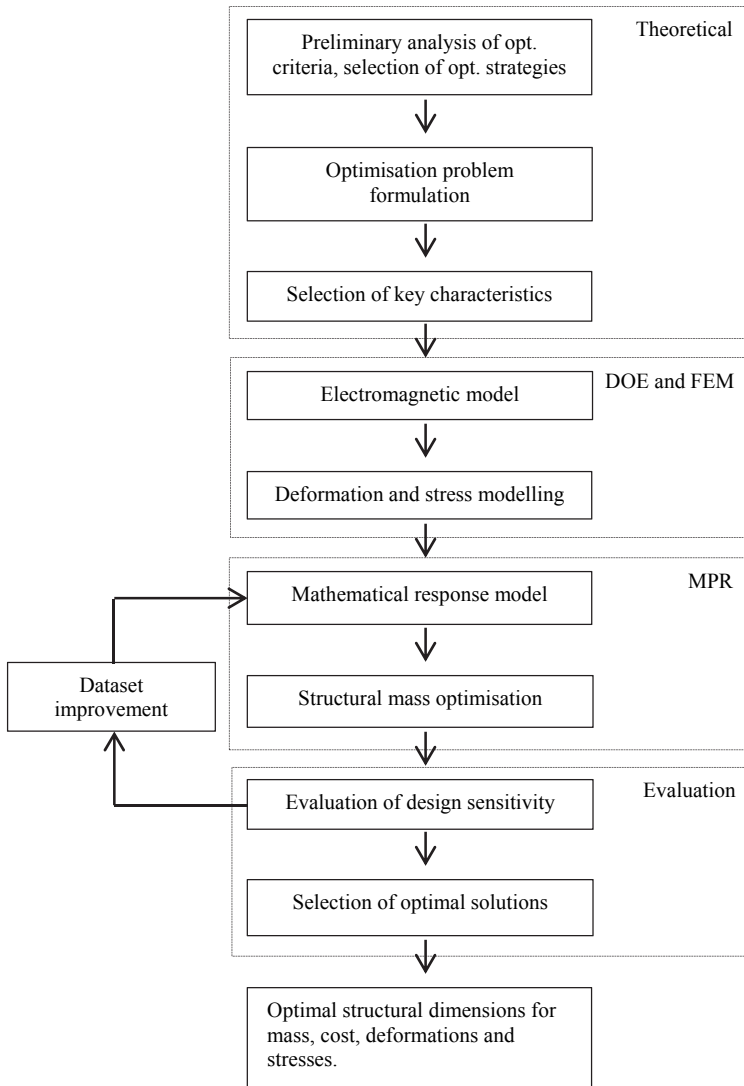*Figure 2.2. The electromagnetic optimisation block and used methods.*

Figure 2.3. The structural optimisation block and used methods.

When unsatisfactory results or conversion problems occur in the electromagnetic and structural optimisation blocks, the procedure reverts to the build-up of the mathematical model. Conversion issues can be dealt with by increasing the learning data and thus the number of performed experiments. It is also possible to improve the procedure by modifying the parameters of the applied optimisation and mathematical modelling methods. For ANN, this could be the number of layers or the nature of used transfer functions. However, this should be decided separately for each particular case as the results are highly dependent on the exact methods used for gathering the learning data.

2.4   Analysis of acting loads

As the investigated electromagnetic configuration and structural setup are novel, no literature is available regarding their main structural design drives. The forces presented in Section 1.5.1 depend both on the electromagnetic and structural parameters of the generator. As an example, the current machine features an unusual relation between the tangential and normal components of the Maxwell stress. Therefore, all the acting forces should be considered either in the actual modelling work as variables or state variables, or a qualified decision regarding their influence is necessary. In the current work, the ANOVA and Taguchi methods are used to rank the acting forces according to their contribution to overall stress and deformation levels. This enables to exclude the components with a low influence in order to reduce the design space by the reduction of the variables. Furthermore, the signal-to-noise (SN) ratio analysis of the Taguchi method gives further information about favourable and unfavourable design decisions. This knowledge can be utilised in order to reach a reasonable structural layout before the exact and time consuming modelling work of the optimisation process takes place. The procedure for the analysis of acting loads is presented in Figure 2.4.
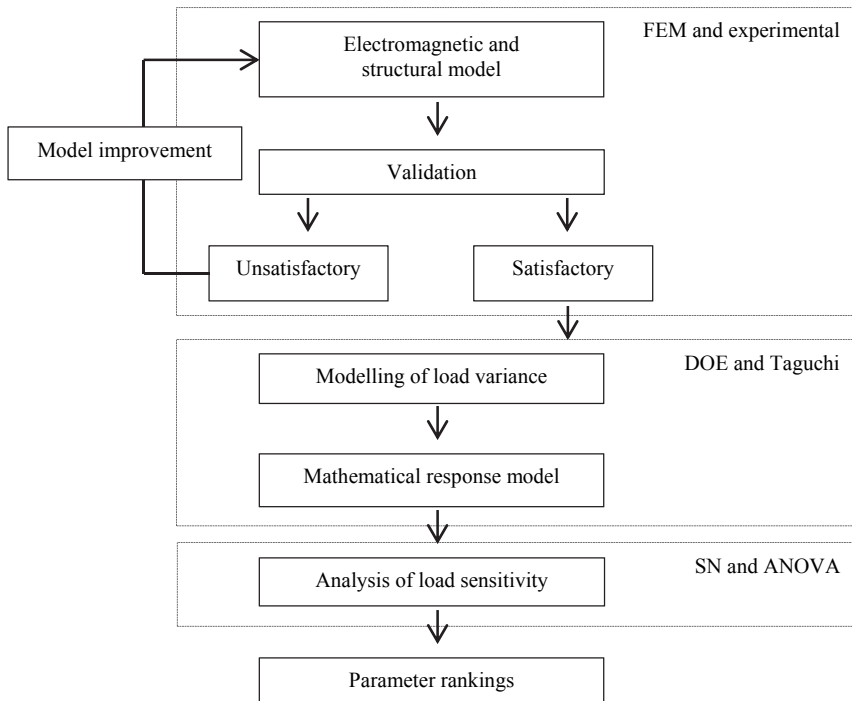

Figure 2.4. The load analysis block and used methods.

In the next chapters, the basic blocks of the proposed optimisation procedure and used considerations are described in detail.

3. MACHINE DESIGN

In terms of electromagnetic and mechanical layouts, it is possible to utilise various types of generators for windmills even if the restrictions of a PM DD machine are applied. The design of the machine should in general comply with the following criteria [74]:

- simple construction;
- low weight;
- low rotational speed;
- high output power capability;
- variable speed capability;
- low starting torque;
- low cost.

One of the theoretical designs that takes into account the above-mentioned criteria is the RFPM machine with air-gap windings and the slotless stator yoke. This configuration features properties fairly similar to the iron-free machine developed by Gordon [75] but leads to a higher magnetic flux density in the air-gap and is easier to build, as steel can be used to support stator windings. The ferromagnetic surfaces of the rotor and stator are practically equal and magnetic resistance in the generator is the same in all rotor positions. As a result, no magnetic cogging torque appears in the machine and the start-up torque of the generator is very low. This is an especially important feature for wind applications, as most of the time, the generator operates at a relatively small torque, compared to the rated value. Thus, cogging effects can be noticeable and cause unwanted changes in the machine behaviour or impede the starting procedure. So far, such a construction has been successfully employed by Kallaste [76] in small windmills and consequently it is a good candidate for reducing some of the drawbacks of DD machines for large industry scale turbines. Therefore, the described concept has been chosen as the subject for the previously described optimisation process.

3.1 Electromagnetic layout

Equations describing the basic geometry of the machine are given in [Paper 3]. Below, only the acting force components and dimensions of the active elements are found. When the basic geometrical dimensions of the machine have been set and the desired magnetic flux density is known, it is possible to find the relative electromagnetic dimensions of the machine by using reluctance networks. A simplified equivalent magnetic circuit of the machine is presented in Figure 3.1. The magnetic circuit can be divided into three paths: the main path from the rotor to stator, the leakage baths on top and between the magnets, and the leakage over the magnet edges. It is important to note the additional conductivities G_{g2} and G_{g3}. These are the results of the modular design of the

magnet and winding units and add additional resistance to the flux path in the rotor and stator yokes.
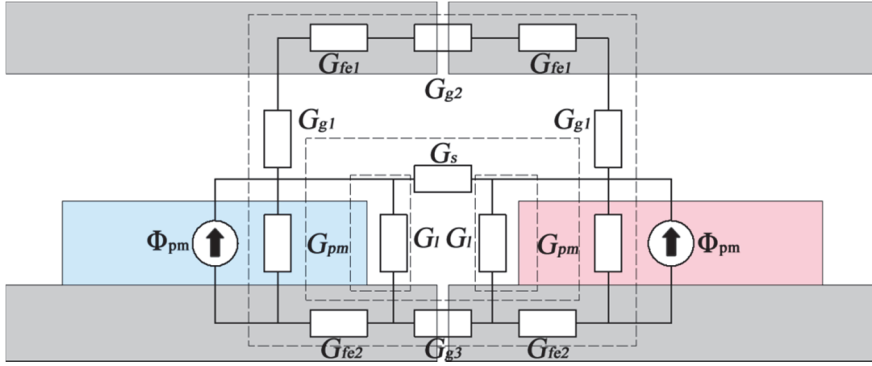

Figure 3.1. Equivalent magnetic circuit for one pole pair of the generator.

Each generator's electromagnetic circuit usually features several ratios that remain fairly similar for most optimal solutions in terms of efficiency and the used material. For this particular machine type, the relative dimensions are given as follows [76]:

$$k_p = \frac{w_m}{w_p}, \qquad k_w = \frac{h_y}{w_p},$$

$$k_{mag} = \frac{h_m}{h_y}, \qquad k_{coil} = \frac{h_c}{h_y}, \qquad (3.1)$$

where k_p is the magnet width and pole pitch ratio, w_m is the magnet width, w_p is the pole pitch, k_w is the total air-gap ratio to the pole pitch, h_y is the total air-gap height, k_{mag} is the magnet height ratio to the air-gap, h_m is the magnet height, k_{coil} is the coil height ratio to the air-gap and h_c is the coil height. The main parameters of the active components are described in Figure 3.2.
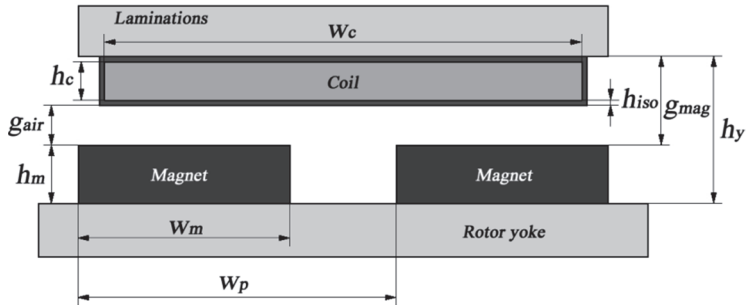

Figure 3.2. Air-gap layout and parameters.

Prior to using the relative dimensions, some initial conditions and estimations about the parameter values have to be made. There are several ways how to start

the design process but the most common is to derive the generator's mechanical air-gap according to machine's radius or diameter. From the electromagnetic point of view, minimum values are desired, thus the actual size of the air-gap is in general set by the occurring mechanical deformations and the reachable assembly precision. As a rule of thumb, the value of $0.002R$ is a good starting point for a RFPM generator. The exact gap height has to be refined during the magnetic field calculations and optimisation process. The magnet height h_m can be found based on the air-gap flux density and the total effective air-gap [77]:

$$h_m = \frac{B_n \mu_{rm} g_{eff}}{B_{rm}},$$ (3.2)

where μ_{rm} is the relative permeability of the PM material, B_{rm} is the remanent flux density of the magnets and g_{eff} is the effective air-gap. As the machine has no slots and the coil units are located in the air-gap, the magnetic air-gap of the machine is relatively large and the following simplification can be made:

$$g_{eff} = h_y + 2h_{iso},$$ (3.3)

where h_{iso} is the isolation layer height around the concentrated winding. By combining the equations (3.1), (3.2) and (3.3), the magnet height dependency on the desired mechanical air-gap can be expressed as:

$$h_m = \frac{g_{air} + 2h_{iso}}{\left(\frac{B_{rm}}{B_n \mu_{rm}} \frac{k_{coil}}{k_{mag}} - 1 \right)}.$$ (3.4)

If the machine's torque has been defined, the most interesting remaining electromagnetic force for the structural design is the normal component of the Maxwell stress q. It results from the magnetic attraction forces of the rotor and stator and can be found as a function of the air-gap flux density over the active surface area:

$$q = 2\pi R l k_p \frac{B_n^2}{2\mu_0},$$ (3.5)

where μ_0 is the permeability of vacuum. For permanent magnet machines with surface mounted magnets, the commonly used value providing near optimal weight to the energy density ratio for k_p is 0.65. For simplification purposes the magnet length l_m is considered to be equal to the axial length l of the machine.

In order to calculate the masses of magnets, concentrated windings and fixation elements, their quantity should be found. The number of n_m magnets (poles) is determined by the defined generator radius:

$$n_m = \frac{2\pi R}{w_p}.$$ (3.6)

The number of coils is influenced by the required number of phases. If a three phase system is required, the shift between phases must be granted and the

symmetry of the system has to be achieved. For determining the number of coils n_c, the following system of equations must hold [78]:

$$\sin\left(\frac{0.5n_m}{n_c}\right) = \left|\frac{\sqrt{3}}{2}\right|, \qquad n_c = 3n_{ph}, \qquad (3.7)$$

where n_{ph} is the number of phases.

As it is not the goal of the current thesis to present a detailed electromagnetic design but merely describe the design principles, the process of solving the introduced reluctance network is not conducted. Equations applicable for the used generator type are given in [79]. The values of relative dimensions derived during the magnetic field calculation are presented in Section 4.2. By using the Maxwell equations or FEA, the magnetic circuit calculations can be refined and the generator parameters including the generated electromotive force and losses can be derived. In this particular case, the vector potential method developed by Bumby *et al.* has been utilised [80].

3.2   Structural layout

The design of the mechanical carrier structure for a PM generator is in general driven by the allowable air-gap deflection. For machines with high flux densities ($B_n = 1.1$ T) and large aspect ratios ($k_a > 0.4$) well studies mechanical layouts can be found from the literature. As the machines are usually compact, carrier structures can be rather simple without a high weight penalty.

3.2.1   General topology

Utilising the relatively low air-gap flux density ($B_n = 0.5$ T) for the slotless RFPM generator results in a machine with a small normal force magnitude but a considerably larger air-gap radius. For example, a 3 MW generator would require a radius of 6 metres, while the conventional slotted machines can be built with a radius of approximately 2.5 metres. The resulting inactive support structure would be too large for regular transportation methods and likely too heavy if the industry's standard structural design utilising sheet metal is used. One option not considered in the available literature is the utilisation of a lattice structure. It has been used in bridge, crane and building constructions for centuries and is generally characterised by its light weight, high loading capacity and stiffness to length ratio [81]. The machine under investigation has a small aspect ratio, a large air-gap radius and a medium normal force envelope by which it differs from the previously described state of the art. In order to bypass the transportation restrictions, the carrier structure will be segmented.

The general topology of the novel lattice based generator is depicted in Figure 3.3a. The overall layout and considered segmentation lines of the utilised lattice structure are shown Figure 3.3b.

Based on the state of the art, the following structural considerations are made:
- a double bearing arrangement – the possibility for central support for one of the elements;
- central support for the rotor, cantilever support for the stator – ease of assembly and lower expected fatigue problems for the rotating rotor;
- inner rotor, outer stator – allows utilisation of ambient air-cooling;
- segmentation of the rotor and stator – allows overcoming the transportation limits of large diameter machines.
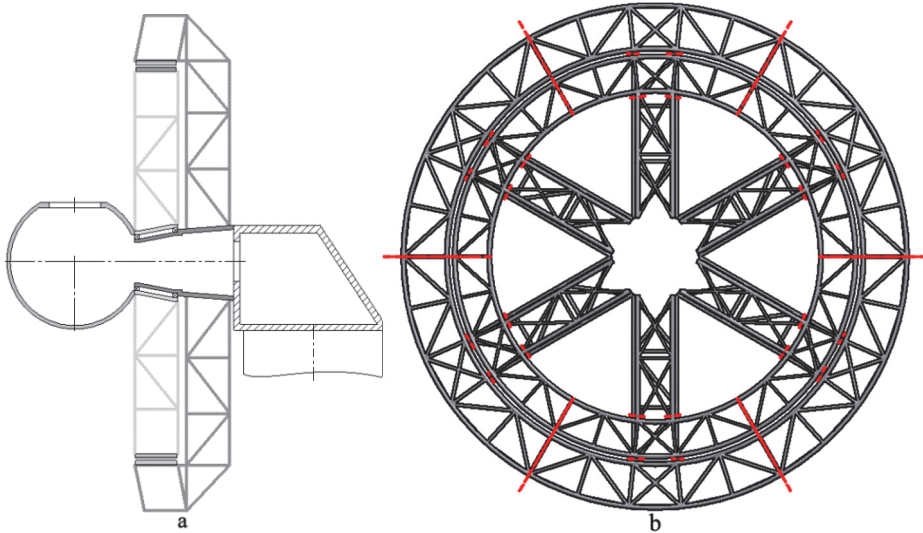

Figure 3.3. The generator's structural layout (a) and lattice structure layout with segmentation lines (b).

The principle layouts of one rotor segment and stator segment both consisting of a spoke and a sector are depicted in Figures 3.4a and 3.4b, respectively.
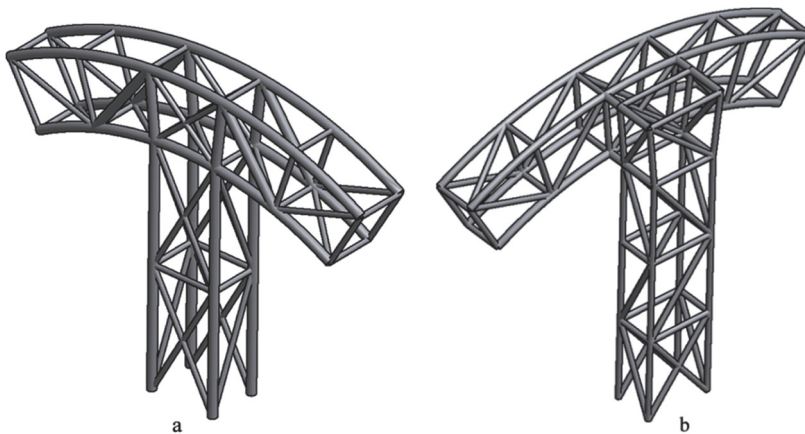

Figure 3.4. The rotor sector and spoke (a) and the stator sector and spoke (b).

The main bearing assembly, rotating and stationary shafts are mainly dimensioned by the bending moments originating from the turbine rotor. In general, their overall weight and cost are not connected to the particular electromagnetic and structural layouts of the generators. Therefore, they have been neglected from the detailed structural analysis.

3.2.2 Calculation model

Generators with standard sheet metal structures are well studied and analytical tools exist for determining the air-gap deflections and maximum stresses [82–83]. These tools can be effectively used as long as they meet the design space and simplification criteria imposed by their authors. As the lattice structure has so far not been employed in such an application, no ready-made methods can be found from the literature. It would be possible to use known truss calculation methods including the Maxwell-Cremona diagram, the method of joints and the method of sections for determining the internal forces and deflections of the members [84]. However, these are best suited for simple planar structures and cannot be easily adjusted in the case of layout changes. Therefore, FEM is used in the current research to estimate the resulting deformations and stresses.

The framework of the generator is modelled in the *ANSYS Workbench 14.5* environment using beam elements (BEAM188). These are based on the Timoshenko beam theory and include shear-deformation effects. The elements consist of two nodes and have six degrees of freedom at each node. They are well-suited for linear, large rotation and large strain nonlinear applications [85]. Different beams are connected by shared nodes that automatically transfer all moments and forces. The nodes are therefore treated as having the same carrying capacity as the profiles and no special considerations are taken for the treatment of connection stiffness. From the structural elements, only the framework of the generator is modelled, while the rest of the items including the magnet and coil units are approximated by point masses. Their influence on the stiffness characteristics is therefore neglected and they are treated solely as an additional load. The resulting model is depicted in Figure 3.5.

Figure 3.5. Structural mesh with beam elements.

The mass on the rotor's outer radius m_{rot}^{oR} applied in the simulations is found according to:

$$m_{rot}^{oR} = m_{mag} + m_{yok} + m_{fixR}, \qquad (3.8)$$

where m_{mag} is the permanent magnet mass, m_{yok} the rotor yoke mass and m_{fixR} the constant lump sum mass of smaller structural fixing items and flanges for the rotor. It is considered that m_{fixR} is not dependent on the exact electromagnetic parameters and the structural loading of the generator. The mass on the stator's inner electrical radius m_{stat}^{iR} is found according to:

$$m_{stat}^{iR} = m_{con} + m_{lam} + m_{cprf} + m_{fixS}, \qquad (3.9)$$

where m_{con} is the conductor mass, m_{lam} the lamination mass, m_{cprf} the cooling profile mass and m_{fixS} the constant lump sum mass of smaller structural fixing items and flanges for the stator. It is considered that m_{fixS} is not dependent on the exact electromagnetic parameters and the structural loading of the generator.

The acting loads are applied to the structure considering their nature as described in Section 1.5.1. The normal force and torque are applied to the frame nodes where the permanent magnets and coils are attached to the generator structure. The normal force components are aligned in a cylindrical coordinate system in a manner that for the rotor they are directed outwards (positive values along the polar axis x) and for stator inwards (negative values along the polar axis x). For global analysis, the increase of the normal force from the air-gap value reduction is not considered. As the magnetic air-gap for the current configuration is relatively large and structural deformations are kept at a reasonable limit, the increase or decrease of the normal force does not significantly influence the simulation results. However, for a separate eccentricity analysis the described phenomenon is taken into account. The generator torque direction is modelled to act counter-clockwise for the rotor and clockwise for the stator, according to the operating principle of the actual machine. The load induced by the rotation is applied to all of the rotor's structural parts as a built in function of *ANSYS*. Tower top accelerations and gravity are applied to all of the structural items. Gravity acts in the y-axis direction, while the back-to-front and side-to-side accelerations are taking effect in the z-axis and x-axis directions, respectively. As it is assumed that the stationary and rotating shafts are much stiffer than the generator structure, fixed boundary conditions (all 6 degrees of freedom remover) are applied to the corresponding structural elements facilitating the connection. The structural FEA model with all the described boundary conditions is given in Figure 3.6.
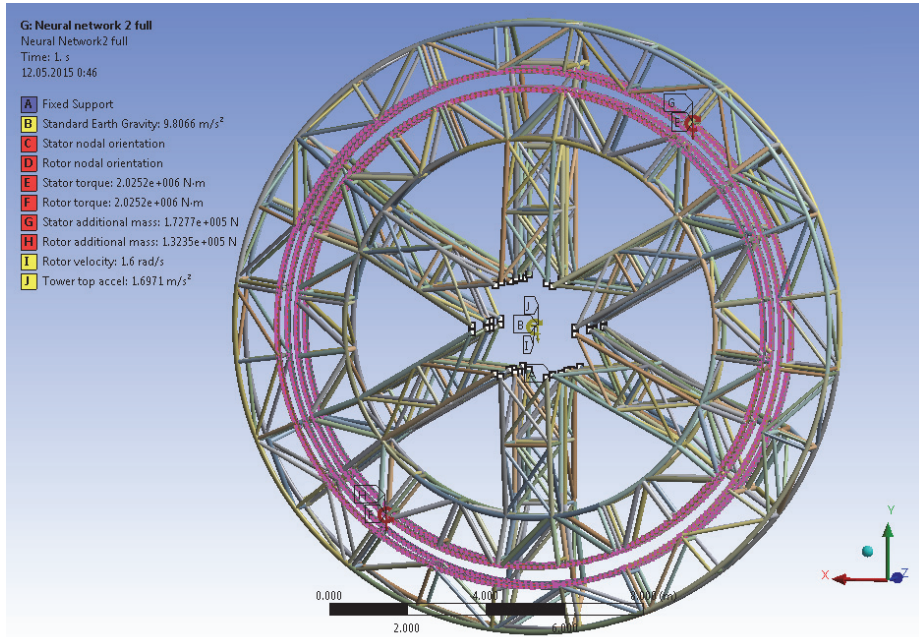
Figure 3.6. Structural model with boundary conditions.

As the DOE block of the electromagnetic optimisation requires multiple load cases with the same structural model, the time stepping method is used to realise the loading, while all results are computed as stationary solutions. For the structural optimisation block, the parametric geometrical model is used together with *ANSYS*'s built in *Design Exploration* function.

The mechanical behaviour of the structure is assessed based on the resulting deformations and stresses. Deflections are evaluated in a cylindrical coordinate system in a manner that for the rotor only positive (deforming outside) and for the stator only negative (deforming inside) values along the polar axis x are considered. This has been found to be the most accurate manner to describe the closing of the air-gap for a circular structure. An example of the rotor's and stator's air-gap deformations is given in Figure 3.7. As beam elements are used for structural modelling, the standard approach of observing *von Mises* stresses is not possible. Instead, the maximum absolute value of linear stress's combination of the axial stress and bending stress is used. The bending stress is taken as the maximum absolute value of the bending stresses in the top and bottom layers for both local axes [85]. In all simulations, the stresses and deformations are kept in such limits that the nonlinear effects of strain stiffening or large deformations do not occur. Examples of the rotor's and stator's minimum and maximum combined stresses are given in Figures 3.8 and 3.9, respectively. For fatigue analysis the stress envelope between the maximum and minimum combined stresses is used as shown in Figure 3.10.

Figure 3.7. The rotor's and stator's air-gap deformations.

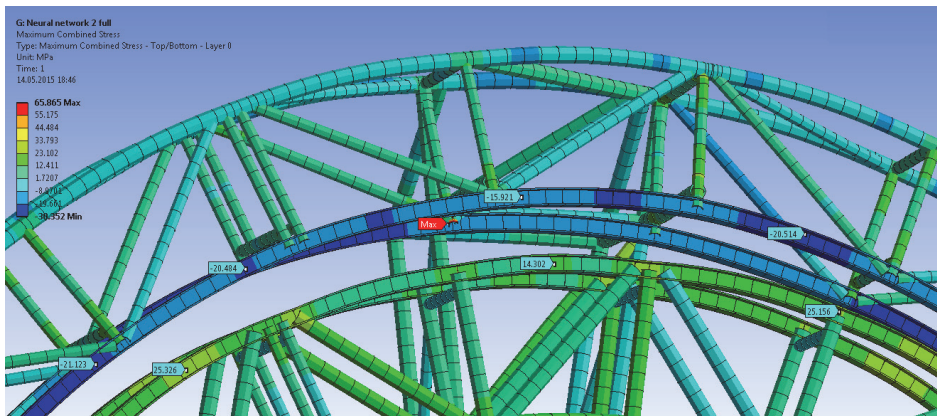*Figure 3.8. The rotor's and stator's minimum combined stress.*

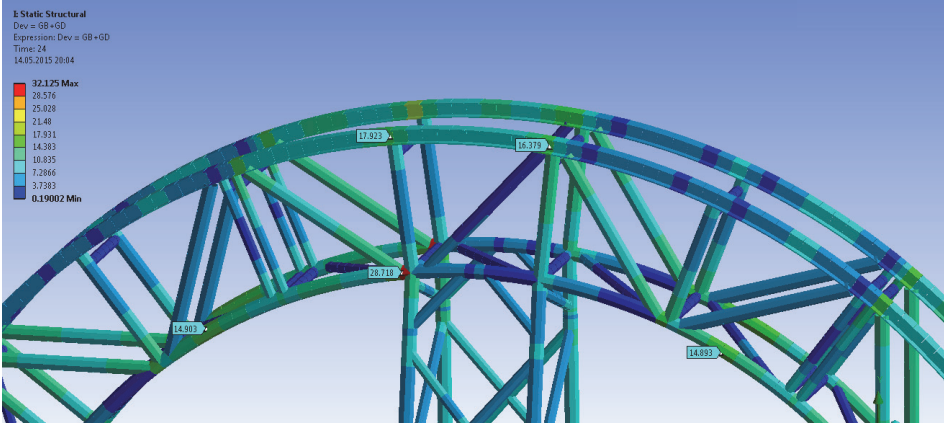*Figure 3.9. The rotor's and stator's maximum combined stress.*

43

Figure 3.10. The rotor's stress envelope for fatigue analysis.

3.3 Cost model

In order to find the most optimal solution for the generator in terms of price, the cost of structural and active materials p_{gen} can be approximated as:

$$p_{gen} = p_{rot}^{act} + p_{stat}^{act} + p_{gen}^{str}, \tag{3.10}$$

where p_{rot}^{act} and p_{stat}^{act} are the active material costs for the rotor and stator and p_{gen}^{str} is the structural material cost for the generator. Active material costs for the rotor are determined by the weight of the rotor yoke, permanent magnets and the corresponding assembly work:

$$p_{rot}^{act} = p_{mag}m_{mag} + p_{yok}m_{yok} + p_{work}(m_{mag} + m_{yok}), \tag{3.11}$$

where p_{mag}, p_{yok} and p_{work} are the specific costs of permanent magnets, the rotor yoke and the work done for assembly, respectively. The stator's active material costs can be found according to the weights of the conductor, laminations, the cooling profile and the corresponding assembly work:

$$p_{stat}^{act} = p_{con}m_{con} + p_{lam}m_{lam} + p_{cprf}m_{cprf} +$$

$$+p_{work}(m_{con} + m_{lam} + m_{cprf}), \tag{3.12}$$

where p_{con}, p_{lam} and p_{cprf} are the specific costs of the conductor, laminations and the cooling profile, respectively. The cost of the structural material can be approximated according to the overall structural weight of the generator:

$$p_{gen}^{str} = p_{str}(m_{rot}^{str} + m_{stat}^{str}), \tag{3.13}$$

where p_{str} is the specific cost of structural material, m_{rot}^{str} and m_{stat}^{str} are the structural material masses for the rotor and stator, respectively.

3.4 Energy production model

In order to assess the generator solution, system energy production over the lifetime has to be estimated. It can be assumed that for the same turbine, energy output depends only on the generator characteristics. Direct assessment of the production is difficult due to the unknown parameters of the turbine rotor and the variable nature of wind. However, comparisons between similar systems by using statistical distribution functions and standard equations can be made. The most commonly used starting point is the calculation of annual energy production (AEP).

As the goal of this study is to assess mainly the generator part of the turbine, efficiencies of the converter and transformer systems are excluded from the energy production estimations. The same applies for the turbine availability factor, as this is highly dependent on the production quality and producer. It is assumed that even with these simplifications, the comparisons of different layouts of the same principle generator configuration are still valid.

The electrical power of the turbine P_{el} for a given wind speed can be approximated by:

$$P_{el}(v) = P_{meh}(v)\eta(v), \tag{3.14}$$

where P_{meh} is the turbine's mechanical power and η is the generator's efficiency. The *AEP* can be found by integrating the product of the electrical output power $P_{el}(v)$ and the probability density function of the Weibull distribution $f(v)$ [86]:

$$AEP = 8760 \int_{v_i}^{v_c} P_{el}(v)f(v)dv =$$

$$= 8760 P_{elN} \left[\frac{1}{(v_r - v_i)^3} \int_{v_i}^{v_r} (v - v_i)^3 f(v)dv + \int_{v_r}^{v_c} f(v)dv \right], \tag{3.15}$$

where v_i is the cut-in wind speed of the turbine, v_c the cut-out wind speed, P_{elN} the rated output power, v_r the rated wind speed and the density distribution can be found according to:

$$f(v) = \frac{k_r}{c_r}\left(\frac{v}{c_r}\right)^{k_r - 1} e^{\left(-\left(\frac{v}{c_r}\right)^{k_r}\right)}, \qquad (k_r > 0, \ c_r > 1), \tag{3.16}$$

where k_r is the shape and c_r is the scale parameter of the Weibull distribution.

In the current case, the rated wind speed of the turbine v_r is not defined as it depends on the efficiency of the generator. This value is established when the turbine's output power P_{el} reaches the nominal value. Above v_r the output power is kept at the rated level. The *OP* of the generator can be found by:

$$OP = AEP \cdot n_{life} \cdot p_{kWh} - p_{gen}, \tag{3.17}$$

where n_{life} is the turbine's lifetime and p_{kWh} is the price of electric energy.

4. RESULTS OF THE DESIGN OPTIMISATION

In order to better illustrate the optimisation procedure, it is carried out on the exact configuration of the machine, which was designed and built for the overall proof of the concept of the electromagnetic and structural models.

4.1 Load sensitivity analysis

The exact methodology and procedure for the load sensitivity analysis of the generator are presented in Section 2.4 and in [Paper 1]. Below, only the most relevant results necessary for further analysis are given.

In the initial assessment, the load components are evaluated based on their contribution to the overall stress and deformation levels at the nominal generator operating mode. Only the parameters that contribute to one of the selected four outputs more than 5 % are included in a further, more thorough analysis with the Taguchi method. These parameters include: deadweight, front-to-back acceleration, normal force and generator torque.

A further analysis of parameter influences is carried out by ranking them according to their Δ values (high SN – low SN) for the minimisation of performance characteristics. Corresponding results for the previously selected variables are given in Table 4.1. Roman numerals I – IV represent the ranking of the parameter for the given characteristic.

Table 4.1. Rakings of force components for all performance characteristics.

Characteristic		Dead weight	Front acceleration	Normal force	Torque
Rotor deformation	Δ	2.30	0.28	3.48	0.32
	rank	II	IV	I	III
Stator deformation	Δ	3.65	0.19	1.72	0.19
	rank	I	III	II	IV
Rotor stress	Δ	0.98	0.39	0.82	4.19
	rank	II	IV	III	I
Stator stress	Δ	2.49	0.06	0.62	2.59
	rank	II	IV	III	I

Dead weight and normal force are determined to be the most influential factors for the air-gap deformations, while torque and again the dead weight contribute most to the stress levels. Frontal acceleration has a minor influence on all of the structural response components. Therefore, for the optimisation procedure only dead weight, normal force and torque are considered as the acting load components in order to reduce the number of variables and the experiments necessary.

4.2 Electromagnetic optimisation

The exact methodology and analysis of optimality criteria for the electromagnetic optimisation of the generator are presented in Section 2.3 and in [Paper 2]. Below, only the final optimisation problem and the most relevant results are given.

Objectives considered for the electromagnetic optimisation block are listed as: cost, efficiency and maximum values of the four structural response characteristics (rotor deformation, stator deformation, the rotor's maximum stress, the stator's maximum stress). After the analysis of optimality criteria, the posed optimisation problem is reduced to the minimisation of two objectives as:

$$f(\bar{x}) = (f_E(\bar{x}), f_{CMB}(\bar{x})) \rightarrow min. \tag{4.1}$$

The combined objective $f_{CMB}(\bar{x})$ in (4.1) is defined as:

$$f_{CMB} = \left[\sum_{i=1}^{4}(w_{SRi}f_{SRi})^c + (w_{Co}f_C)^c\right]^{1/c},$$

$$\sum_{i=1}^{4} w_{SRi} + w_{Co} = 1, \quad 0 < w_{SRi} \le 1, \quad 0 < w_{Co} \le 1. \tag{4.2}$$

In (4.2), the parameter $c \ge 1$ $i = 1, ..., n$ and in the case of $c = 1$, the compromise programming technique reduces to the weighted summation technique. The objectives $f_{SR1}(\bar{x}),..., f_{SRn}(\bar{x})$ describe the normalised structural response of the construction (maximum rotor and stator deformations ε_{rot}^{max}, ε_{stat}^{max} and stresses σ_{rot}^{max}, σ_{stat}^{max}, characterising the stiffness and strength of the structure) and f_C is the normalised cost objective function. The weight coefficients for structural response characteristics w_{SRi} and cost w_{Co} depend on the active and passive material contributions to the overall cost structure and the chosen final objective (COE or OP). In the current example, OP is defined as an objective and the coefficients are selected as: $w_{SR} = 0.2$ and $w_{Co} = 0.8$.
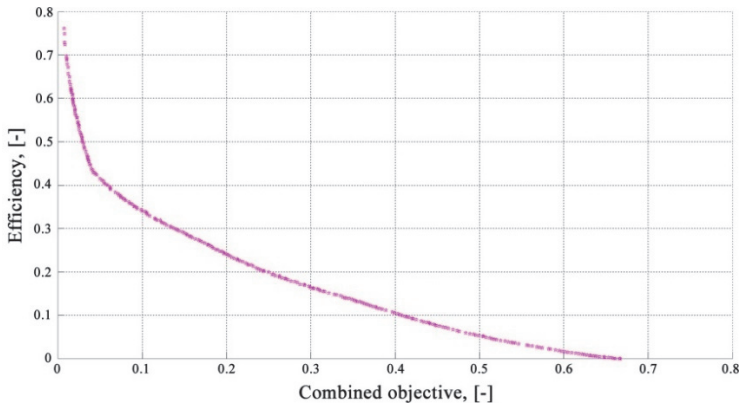

Figure 4.1. The Pareto front: combined objective vs. efficiency.

Taking into account the above-mentioned criteria, the Pareto front is developed since it provides more information compared to physical programming techniques. The front for "combined objective *vs*. efficiency" is depicted in Figure 4.1. In the case of efficiency, the lowest normalised values correspond to the highest non-normalised values. It can be seen that the increase rate of the efficiency is slowing down with the increasing values of the combined objective. Since all the points in the Pareto curve are optimal to some extent, additional information is required for making the final decision. As efficiency is more valuable than the system cost, one meaningful selection of the optimal solution is point (0.37; 0.12). There the efficiency reaches near an ideal value and further improvement leads to a rapid increase (worsening) of the combined objective. The optimal set of design variables corresponding to the selected point is presented in Table 4.2.

Table 4.2. Possible optimal solution for structural response vs. efficiency.

Air-gap, mm	Magnet thickness, mm	Magnet length, mm	Coil thickness, mm	Point
11.5	22	790	14	(0.37; 0.12)

4.3 Structural optimisation

The exact methodology and analysis of optimality criteria for the structural optimisation of the generator are presented in Section 2.3 and in [Paper 3]. Below, only the final optimisation problem and the most relevant results are given.

For the structural optimisation block, only the framework mass $F_m(\bar{x})$ is chosen as an objective subjected to minimisation, while the air-gap deformation ε is defined as a constraint. Therefore, the single criterion optimisation problem can be formulated:

$$F_m(\bar{x}) \rightarrow min, \tag{4.3}$$

subjected to linear constraints applied to the design variables vector $\bar{x}$:

$$x_i \leq x_i^*, \qquad -x_i \leq x_{i*}, \quad i = 1, \dots, n, \tag{4.4}$$

and nonlinear constraint applied to the sum of the rotor and stator air-gap deflections ε^{max} as:

$$\varepsilon^{max}(\bar{x}) \leq \varepsilon^*, \tag{4.5}$$

where the indices * in the equations (4.4) and (4.5) refer to the upper limit value of the variable.

Taking into account the above-mentioned criteria, the most optimal configurations for the rotor and stator structures are found. The results of the

final values for the parameters are presented in Table 4.3. It can be seen that the lattice rotor prefers a high aspect ratio and axial length, while the stator is most optimal with minimum axial length and an aspect ratio near 1. This has mainly to do with the cantilever nature of the stator, where additional overhang due to the increased axial length leads to larger deformations. Increasing the aspect ratio beyond 1 does not yield any benefits, as the bending is mostly seen in the stator spokes.

Table 4.3. Structural layout determined by the optimisation procedure.

Factor	Symbol	Unit	Stator	Rotor
Structural axial length	l_{str}	mm	700	1000
Structural aspect ratio	k_{str}	-	1.04	1.30
Air-gap deformation	ε^{max}	mm	2.5	0.85
Maximum stress	σ^{max}	MPa	54	43
Structural mass	m_{str}	kg	16 850	13 740

4.4 Conclusions to the chapter

The multicriteria optimisation procedure has been developed and applied successfully for solving the complex problem of a wind turbine generator design. Firstly, load sensitivity analysis was performed and the key impact factors for performance were detected. Secondly, an analysis of optimality criteria were performed and corresponding optimisation strategies were applied. Finally, the optimal electromagnetic and structural configurations of the generator were determined by applying the developed procedure. A comparison of the initial rule of thumb design values and values obtained through the optimisation procedure is given in Table 4.4.

Table 4.4. Generator configuration determined by the optimisation procedure.

Parameter	Symbol	Unit	Initial	Optimised
Electrical power	P_{el}	kW	3 000	3 000
Rotational speed	ω	rpm	15.3	15.3
Torque	τ	kNm	2 090	1 980
Efficiency	η	%	91.2	94.5
Air-gap radius	R	m	6.3	6.3
Air-gap width	g_{air}	mm	9	11.5
Magnet height	h_m	mm	18	22
Magnet width	w_m	mm	100	100
Magnet length	l_m	mm	600	800
Coil height	h_c	mm	17	14
Coil width	w_c	mm	200	200
Coil length	l_c	mm	800	1 000
Mag. width/pole pitch	k_p	-	0.65	0.65
Total air-gap/pole pitch	k_w	-	0.30	0.32
Mag. height/total air-gap	k_{mag}	-	0.39	0.44
Coil height/total air-gap	k_{coil}	-	0.37	0.29
Total normal force	q	kN	1 265	2 040
Rotor air-gap mass	m_{rot}^{oR}	kg	12 900	16 800
Stator air-gap mass	m_{stat}^{iR}	kg	19 600	19 500
Rotor mass	m_{rot}	kg	26 600	13 700
Stator mass	m_{stat}	kg	18 400	16 900
Generator mass	m_{gen}	kg	77 500	66 900
Price	p_{gen}	EUR	417 500	479 600
Annual energy production	*AEP*	MW/h	12 501	12 702
Operational profit	*OP*	kEUR	13 291	13 427

By taking into account the structural response characteristic in the electromagnetic optimisation, the generator's mass has been considerably reduced. Although, the generator's overall price has increased, so has the energy production, which leads to an increased OP. Thus, the proposed optimisation procedure has been successfully implemented to improve the machine design. The machine can compete with the machines available on the market and further improvement of the design is possible with another optimisation loop with refined input parameters.

5. APPLICATION OF THE MODULAR DESIGN

Although the theoretical electromagnetic and structural layouts of the generator show great promise, a series of practical issues have to be addressed. Due to the low air-gap flux density of the machine, an unconventionally large electrical radius is required for the generator. For example, the machine with a 3 MW capacity results in an overall physical generator diameter of 16 metres. In order, to deal with the real world transportation requirements, segmentation of the carrier structure is necessary. For structures in the construction industry, this is a routine task but in the case of generators, much stricter requirements have to be considered. Firstly, the generator air-gap diameter needs to be achieved with a high accuracy to avoid rotor-stator collision, unbalanced magnetic forces and mass distribution. Secondly, for PM machines, the handling of the magnetically active segments must be considered. The issues regarding assembly precision could be handled by machining the segments after assembly or individually, but this would have a severe penalty on the manufacturing costs. In order to assess the achievable precision, the influence of unbalanced forces and assembly procedure, a series of tests have been performed on small scale and full scale prototypes.

5.1 Eccentricity analysis

As the effects of the mass unbalance of rotating structures are well studied, the main emphasis in the current sections is directed towards the unbalance of electromagnetic forces. In order to assess the vibrational behaviour of the described generator, a small scale 5 kW laboratory test model was built and different eccentricity faults were introduced. The exact experimental methodology and procedure of the assessment are presented in [Paper 4]. Below, only the eccentricity types are described and a summary of the most relevant results is given. The small scale model is shown in Figure 5.1.
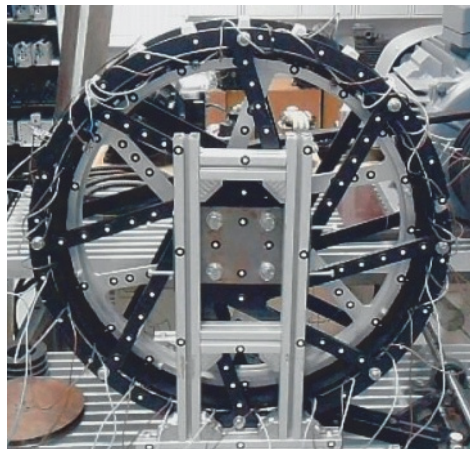

Figure 5.1. The small scale test model

There are multiple eccentricity types, which can occur during the production phase of the machine. These are presented in Figure 5.2 and can be classified geometrically into static, elliptic, dynamic and mixed eccentricities. Static eccentricity takes place when the rotor symmetry axis coincides with the axis of rotation but is displaced from the stator symmetry axis. The pure elliptic form of eccentricity occurs when the rotor is not built as circle and has an elliptic shape. In the case of dynamic eccentricity, the centre point of rotor symmetry is shifted from the stator symmetry point and the rotation occurs around the stator symmetry point. Mixed eccentricity is an obvious combination of the faults mentioned before (87). In addition, a pure rotor mass unbalance towards the centre of rotation can occur to a certain degree.
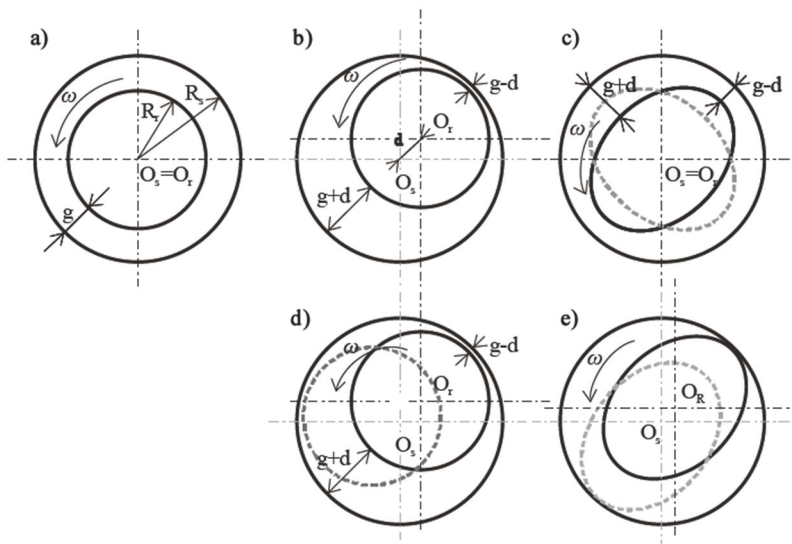

Figure 5.2. Generator eccentricity types: a) healthy machine, b) static, c) elliptic, d) dynamic and e) mixed [87]. O_r and O_s are rotor and stator symmetry centres, g is the width of the air-gap and d represents the eccentricity magnitude.

In order to assess the relative influence of the eccentricity faults, four test runs with the prototype were carried out. These included healthy (ZERO), static (STAT), dynamic (DYN) and mass unbalance (EMAS) configurations. The goal of the tests was to observe the transitions of marker points located on the air-gap radius of the rotor. The results for axial displacements at nominal rotational speed are presented in Figure 5.3 and the results for radial displacements in Figure 5.4. Measurements were carried out with the calibrated Pontos 4M optical measurement system, at the accuracy of ± 0.015 mm (coverage factor 2).
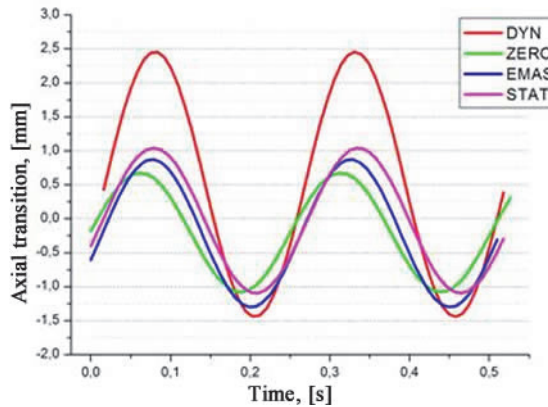
Figure 5.3. Rotor vibrations in the axial direction for different eccentricities.
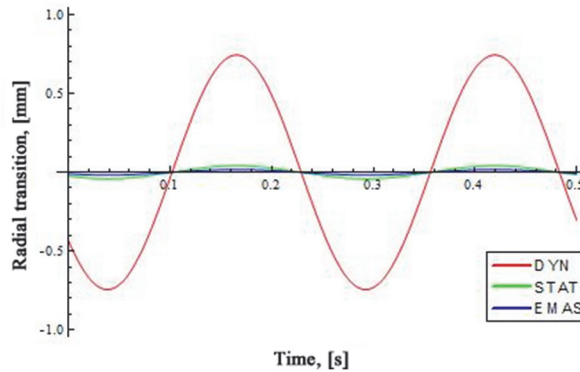

Figure 5.4. Rotor vibrations in the radial direction for different eccentricities.

According to the experimental result, only dynamic eccentricity has a noticeable effect on the generator's behaviour. It amplifies the normal vibration amplitudes in both axial and radial direction by the factor of two and can pose a serious risk of air-gap closure. Noticeable effects of the eccentricity faults can be seen only for the rotor. However, due to the fixing conditions in the test bench, no real long term conclusions can be made for the stator. As the dynamic eccentricity features both mass unbalance and electromagnetic unbalance, it can be concluded that the combined effect of both faults is causing the large relative movements and should be avoided at all costs. The large amount of rotor mass is located on the outer rim in the form of permanent magnets and the rotor yoke. As the magnets are also generating the magnetic field and are the elements closest to the stator, their correct position after assembly is determined to be the key factor influencing the structural stability and lifetime of the generator.

5.2 Unbalanced magnetic pull

In order to estimate the magnetic force misbalance, it is necessary to find the air-gap of the fault situation. In the case of static eccentricity, the magnetic air-gap g_{mag} can be determined according to [87]:

$$g_{mag} = R_s - R_r + \sqrt{R_r^2 - (d \cdot sin\beta)^2}, \tag{5.1}$$

where R_s is the stator's electromagnetic radius, R_r is the rotor's electromagnetic radius, d is the eccentricity value and β is the eccentricity angle. For dynamic eccentricity, the magnetic air-gap value is additionally dependent on the time t and is given as:

$$g_{mag}(t) = R_s - R_r + \sqrt{R_r^2 - (d \cdot sin\beta(t))^2}. \tag{5.2}$$

When the new air-gap is known, the flux density corresponding to each pole B_{ecc} can be calculated by using vector potentials, and the radial unbalanced force q_{ecc} acting in the rotor centre is found by integrating the radial force density along the rotor's surface:

$$q_{ecc} = \int_0^{2\pi} \frac{1}{2\mu_0} B_{ecc}^2 R \, d\theta, \tag{5.3}$$

where θ is the coil angle. Depending on the electromagnetic concept, the unbalanced magnetic pull can cause serious problems for the stability of the generator structure. As the described machine has a relatively large magnetic air-gap compared to the mechanical air-gap, it is expected that smaller eccentricities do not pose a serious mechanical problem. Nevertheless, due to the dynamic effects, the value of the unbalanced pull has to be taken into consideration. The values on the unbalanced force q_{ecc} for the test machine layout presented in Chapter 3 are given in Figure 5.5.
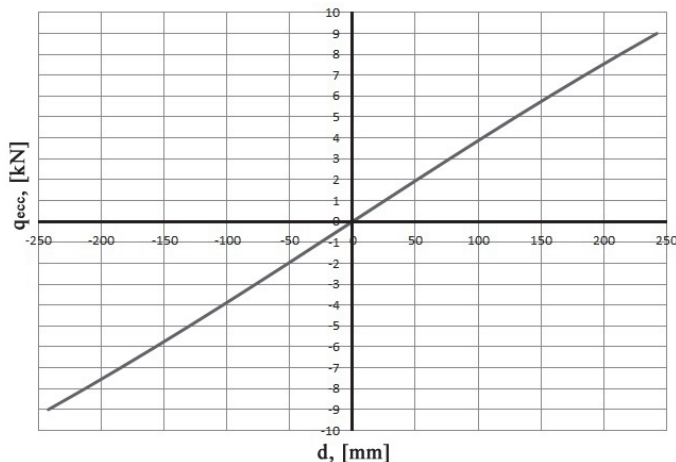

Figure 5.5. Values of the unbalanced force depending on the eccentricity value.

The most dangerous situation for the stability of the air-gap occurs when the direction of the unbalanced force for the stator coincides with the gravity vector direction (negative eccentricity). Due to the cantilever support, the stator is more flexible than the rotor and thus additional downwards deformation is created. Deformations in the described case for the rotor and stator corresponding to the different eccentricity values of the test machine are given in Table 5.1. An illustration of the radial deformations of both structures at the eccentricity value –5 mm can be seen in Figure 5.6.

Table 5.1. Structural deformations according to eccentricity.

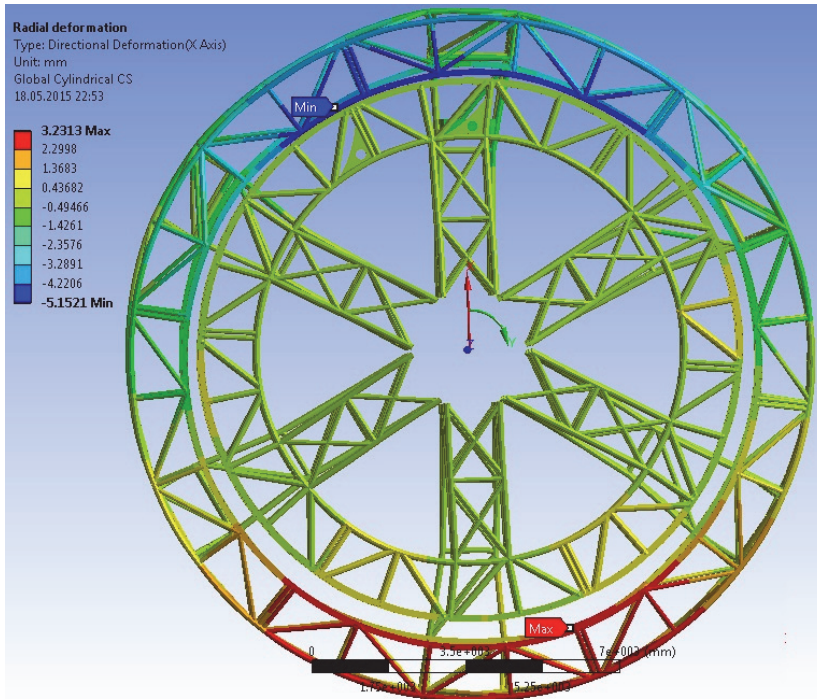| Eccentricity, mm	Stator deformation, mm	Rotor deformation, mm
0	–4.0	1.1
–1	–4.3	1.0
–2	–4.5	1.0
–3	–4.7	1.0
–4	–4.9	0.9
–5	–5.1	0.9

Figure 5.6. Structural deformations at –5 mm eccentricity.

From the presented data, it can be concluded that large eccentricity values of the machine have to be avoided and the assembly precision of the rotor and stator is a key factor in the feasibility of the described generator concept.

5.3   Assembly of the test machine

In order to investigate the achievable air-gap precision for a modular generator structure and prove the feasibility of handling the magnetically active rotor sectors, a prototype machine has been built and tested. The safe handling and precise placement of permanent magnets is described in [Paper 5]. Below, only the results of the achieved air-gap precision are presented. The built full scale prototype generator is given in Figure 5.7

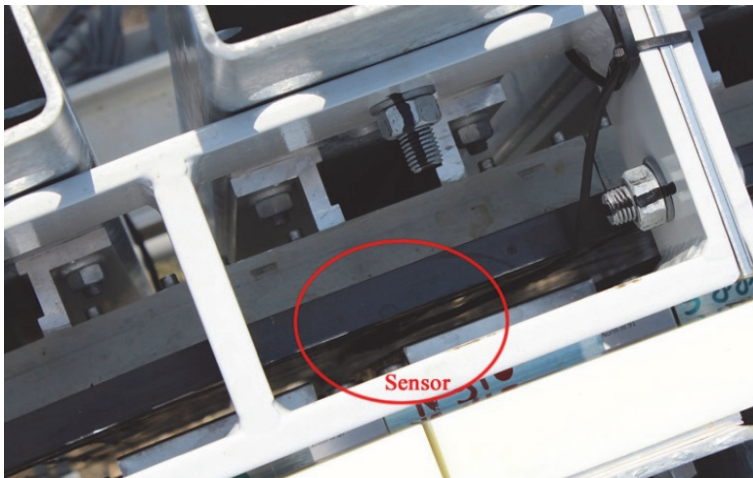*Figure 5.7. The full scale prototype machine.*

Figure 5.8. Placement of the air-gap sensor.

To assess the precision of assembly of the rotor, six *Mikrotrend* low profile capacitive air-gap AGS-25 measuring sensors [88] were placed onto the generator stator and into the air-gap. The sensors were equipped with AGSC-25 signal conditioners and the signals were collected with a common desktop computer. An example of the placement of one sensor is show in Figure 5.8. Measurement results taken at the rotational speed of 1 rpm are shown in Figure 5.9 and the numerical overview of results is given in Table 5.2.
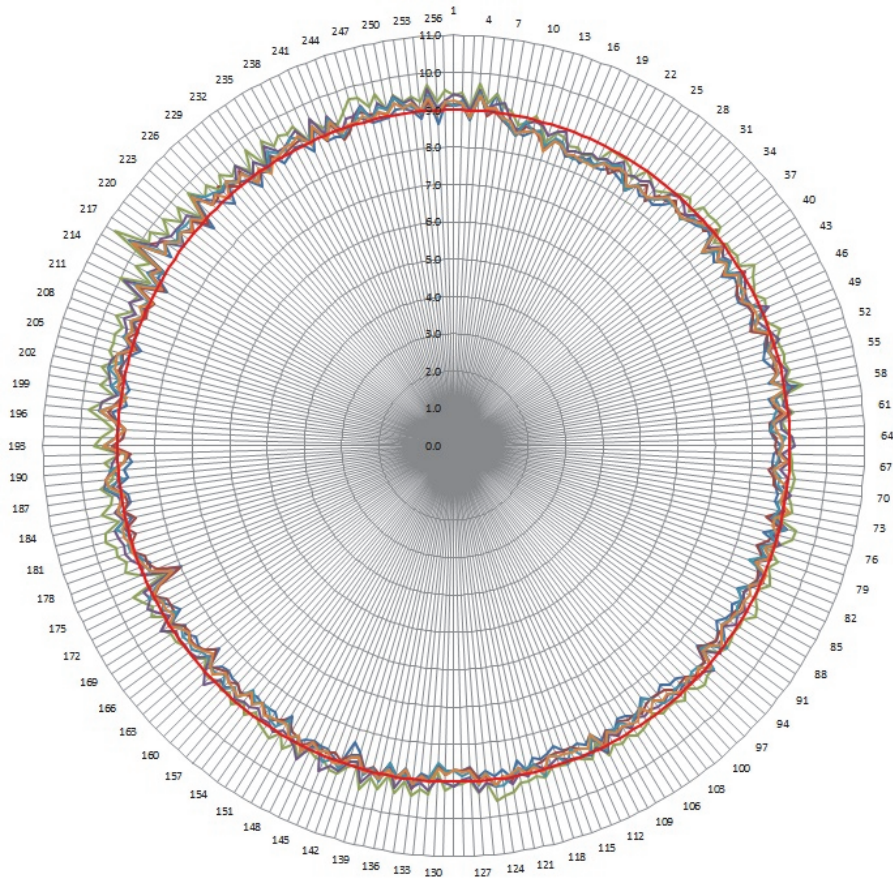

Figure 5.9. Air-gap measurement results for the rotor.

Two larger spikes in the outwards direction (magnet no. 217) and inwards direction (magnet no. 175) can be seen from the radar chart. In certain cases the entire sector has moved either outwards (magnets nos. 217 to 256) or inwards (magnets nos. 4 to 33). However, in general the air-gap precision can be deemed to be satisfactory as the total deviation for the first assembly attempt is 2.8 mm and the average desired air-gap value of 9.0 mm has been achieved. As these measurements are taken only after one adjustment circle, it is natural that a very precise circle cannot be obtained. This is mainly caused by the magnetic forces which change during the adjustment process since the air-gap is changing.

When the adjustment procedure is repeated, the relative change of attraction force will be smaller and thus a higher end precision can be expected.

Table 5.2. Results of air-gap measurements with coverage factor 2.

| Air-gap parameter | Unit | Sensor number | | | | | |
		1	2	3	4	5	6
Maximum	mm	10.1	10.2	10.7	10.3	10.3	10.2
Minimum	mm	8.0	8.0	8.5	8.3	8.2	8.3
Average	mm	8.8	8.9	9.2	9.1	8.9	8.9
Deviation	mm	2.1	2.1	2.3	2.0	2.0	1.9
Standard deviation	mm	0.26	0.27	0.29	0.27	0.28	0.26
Total maximum	mm	10.7 ± 0.3					
Total minimum	mm	8.0 ± 0.3					
Average air-gap	mm	9.0 ± 0.65					
Target air-gap	mm	9.0					

Based on the presented data, it can be concluded that even with the segmented design, the necessary air-gap precision for the generator rotor can be achieved. As it results in a relatively even distribution of magnetic forces and rotor mass, dynamic eccentricity effects and the resulting increased deformations and movements of the rotor can be avoided. As the assembly of the test machine has been performed in a successful manner, the developed method of handling magnetically active rotor poles has also been confirmed in practice. Therefore, the most pressing practical design issues of the presented concept have been solved and the design has taken successfully been taken beyond the theoretical concept.

CONCLUSION

This dissertation concentrated on the development of an optimisation procedure for an electrical generator in a wind turbine. The general conclusions of the work are the following:

1. The design optimisation methodology for an electrical generator in a wind turbine has been introduced and implemented on an example machine.
   - Utilisation of the developed procedure on an example machine has allowed reducing the machine's weight by **14 %** and increasing the annual energy production by **1.6 %**. Even though the overall machine cost has risen, the target objective concerning the increase of operating profit has been achieved.
   - Hypothesis H1 given in Section 1.6 can be considered to be consistent with the findings of the work.
2. The proposed methodology greatly reduces the complexity of the design process of an electrical generator.
   - It was found that the decomposition of the optimisation problem into electromagnetic and structural parts decreases the complexity of the problem. The introduction of the structural response characteristic in the electromagnetic optimisation block enables to optimise the generator's layout in terms of output energy while taking into account the effect on structural stability.
   - The preliminary analysis block and investigation of acting loads enables to reduce the design space of the developed optimisation problem without compromising the practical application of the end result.
   - The utilisation of relative electromagnetic dimensions enables to define the initial machine geometry without a detailed analysis of the electromagnetic circuit with acceptable accuracy. The optimal relative dimensions remain similar for machines with various capacities and thus the design process is accelerated even further.
   - FEM with the parametric geometrical model can be successfully used to determine the most optimal relative and absolute structural dimensions for the mechanical support structure.
   - Hypothesis H2 given in Section 1.6 is found to be mostly consistent with the results of the conducted work. However, the full effect of the decomposed procedure on the achieved results needs further investigation.
3. Novel electromagnetic and structural concepts for the example generator have been introduced and analytical methods have been offered for the initial determination of the design parameters.
   - The proposed lattice type carrier structure can be built with a smaller overall weight than a comparable sheet metal layout. Therefore, the undesired high weight of the direct-drive generator can be reduced for the particular electromagnetic concept.

- The segmentation and modularisation of electromagnetic and structural layouts enables to build large diameter generators without violating transportation restrictions. Therefore, excessive electromagnetic material and expensive cooling systems can be avoided as the linear speed of magnets can be considerably increased.
- Hypothesis H3 given in Section 1.6 is considered to be consistent with the outcomes of the research, as the transportation restrictions of large direct-drive generators can be avoided by utilising the proposed layouts.

4. Practical issues of the introduced layouts have been investigated on prototype machines with satisfactory results.
- Dynamic eccentricity has been found to be the most dangerous machine assembly fault type, leading to the increased radial and axial movements of the machine. FEM analysis has revealed that small eccentricities of the rotor do not pose a danger to the overall structural stability. The full rotor eccentricity of **2 mm** leads to an increased deformation of only **0.5 mm**. The test assembly of the prototype generator has proved that with the described methods the needed accuracy for the air-gap can be achieved. The average value of the real air-gap matched the targeted theoretical value.
- The proposed device and method for the assembly of active magnet modules onto a fully assembled generator have been successfully implemented. Machine assembly has been executed without any harm to personnel or modules.
- Hypothesis H4 given in Section 1.6 corresponds with the experimental findings of this paper.

As a final conclusion, it can be stated that all of the goals of the research work were achieved and the proposed hypotheses were proven to be consistent with the findings of the research. Also all subtasks stated in Section 1.6 were successfully completed.

Novelty

The paper proposes and discusses the following novel solutions:
- A novel design approach and optimisation method for an electrical generator in a wind turbine. The novelty lies in the introduction of the pre-analysis block, thorough load sensitivity analysis, the decomposition of the process into electromagnetic and structural optimisation blocks and the inclusion of the structural response characteristic into the electromagnetic optimisation.
- The implementation of a slotless electromagnetic circuit and a novel lattice type support structure for a permanent magnet generator at the megawatt scale. The described electromagnetic circuit has not been proposed for the megawatt class generator in the available literature and

the lattice structure type has not been utilised for any previous generators.

- The concept for improving the transportability of large diameter permanent magnet generators. The novelty lies in the segmented approach to both structural and electromagnetic units, enabling the full assembly of the generator from modules complying with transportation requirements.

- The methods for predicting and solving the assembly related problems of modular large diameter generators. The introduced device and exact method has not been commercially utilised and thus a patent application has been submitted for the device and method.

Future work

The proposed optimisation methodology needs to be improved by the inclusion of a detailed fatigue analysis block for the generator rotor. In current work, the fatigue characteristics were applied as constraints, yet optimisation directed towards the lifetime might yield better results. In addition, the restrictions and limits of the offered electromagnetic and structural concepts concerning different generator capacity levels must be investigated. For the structural concept, it would also be necessary to investigate the placement of the tubes in the lattice framework. In present paper, only the rules of thumb for the position of tubes were followed.

REFERENCES

[1]   Polinder, H., Ferreira, J.A., Jensen, B.B., Abrahamsen, A.B., Atallah, K., McMahon, R.A. Trends in Wind Turbine Generator Systems. – *IEEE Journal of Emerging and Selected Topics in Power Electronics*, 2013, 1 (3), 174–185.

[2]   Alnasir, Z., Kazerani, M. An Analytical Literature Review of Stand-Alone Wind Energy Conversion Systems from Generator Viewpoint. – *Renewable and Sustainable Energy Reviews*, 2013, 28, 597–615.

[3]   Zhang, Z., Matveev, A., Øvrebø, S., Nilssen, R., Nysveen, A. State of the Art in Generator Technology for Offshore Wind Energy Conversion Systems. – *Electrical Machines & Drives Conference, Niagara Falls*, 2001, 1131–1136.

[4]   Bang, D., Polinder, H., Shrestha, G., Ferreira, J.A. Promising Direct-Drive Generator System for Large Wind Turbines. – *Wind Power to the Grid - EPE Wind Energy Chapter 1st Seminar*, *Delft*, 2008, 1–10.

[5]   Henriksen, M., Jensen, B.B. Induction Generators for Direct-Drive Wind Turbines. – *Electric Machines Drives Conference*, *Niagara Falls*, 2011, 1125–1130.

[6]   Delli Colli, V., Marignetti, F., Attaianese, C. Analytical and Multiphysics Approach to the Optimal Design of a 10-MW DFIG for Direct-Drive Wind Turbines. – *IEEE Transactions on Industrial Electronics*, 2012, 59 (7), 2791–2799.

[7]   Shrestha, G., Polinder, H., Ferreira, J.A. Scaling Laws for Direct Drive Generators in Wind Turbines. *In: Proceedings of the Electric Machines and Drives Conference IEMDC, Miami*, 2009, 797–803.

[8]   Versteegh, C. Design of the Zephyros Z72 wind turbine with emphasis on the direct drive PM generator. *In: Proceedings of the Nordic Workshop on Power and Industrial Electronics, Trondheim*, 2004, paper number 68.

[9]   McDonald, A.S., Mueller, M.A., Polinder, H. Structural Mass in Direct-Drive Permanent Magnet Electrical Generators. – *IET Renewable Power Generation*, 2008, 2 (1), 3–15.

[10] Dubois, M.R. *Optimized Permanent Magnet Generator Topologies for Direct-Drive Wind Turbines* : PhD dissertation. Delft, Delft University of Technology, 2004.

[11] Polinder, M., Mueller, M. *Wind Turbine Drive Systems: A Commercial Overview*. Oxford : Woodhead, 2013, 139–157.

[12] Bang, D., Polinder, H., Shrestha, G., Ferreira, J.A. Possible Solutions to Overcome Drawbacks of Direct-Drive Generator for Large Wind Turbines. *In: Proceedings of European Wind Energy Conference and Exhibition, Marseille*, 2009, 1–10.

[13] Brisset, S., Vizireanu, D., Brochet, P. Design and Optimization of a Nine-Phase Axial-Flux PM Synchronous Generator with Concentrated Winding for Direct-Drive Wind Turbine. – *IEEE Transactions on Industrial Applications,* 2008, 44 (3), 707–715.

[14] McDonald, A.S. *Structural Analysis of Low Speed, High Torque, Electrical Generators for Direct Drive Renewable Energy Converters* : PhD dissertation. Edinburgh, Edinburgh University, 2008.

[15] Asian Metal. [WWW] http://www.asianmetal.com (22.11.2014)

[16] Zhang, Z., Chen, A., Matveev, A., Nilssen, R., Nysveen, A. High-Power Generators for Offshore Wind Turbines. – *Energy Procedia*, 2013, 35, 52–61.

[17] Isfahani, A.H., Boroujerdi, A.H.S., Hasanzadeh, S. Multi-Objective Design Optimization of a Large-Scale Direct-Drive Permanent Magnet Generator for Wind Energy Conversion Systems. – *Frontiers in Energy*, 2014, 8 (2), 182–191.

[18] Li, H., Chen, Z. Design Optimization and Site Matching of Direct-Drive Permanent Magnet Wind Power Generator Systems. – *Renewable Energy*, 2009, 34 (4), 1175–1184.

[19] Karjust, K., Pohlak, M., Majak, J. Technology Route Planning of Large Composite Parts. – *International Journal of Material Forming*, 2010, 3 (1), 631–634.

[20] Majak, J., Pohlak, M., Eerme, M., Velsker, T. Design of Car Frontal Protection System Using Neural Networks and Genetic Algorithm. – *Mechanics*, 2012, 18 (4), 453–460.

[21] Pohlak, M., Küttner, R., Majak, J. Modelling and Optimal Design of Sheet Metal RP&M Processes. – *Rapid Prototyping Journal*, 2005, 11 (5), 304–311.

[22] Herranen, H., Pabut, O., Eerme, M., et al. Design and Testing of Sandwich Structures with Different Core Materials. – *Materials Science-Medziagotyra*, 2012, 18 (1), 45–50.

[23] Polinder, H., de Haan, S.W.H., Dubois, M.R., Slootweg, J.G. Basic Operation Principles and Electrical Conversion Systems of Wind Turbines. *In: Proceedings of the Nordic Workshop on Power and Industrial Electronics, Trondheim*, 2004, paper number 69.

[24] Slootweg, J.G., de Vries, E. Inside Wind Turbines - Fixed vs. Variable Speed. – *Renewable Energy World*, 2003, 30–40.

[25] Dubois, M.R. Review of Electromechanical Conversion in Wind Turbines. Delft, Technical University of Delft, 2000, Report EPP00.R03.

[26] Enercon Gmbh. [WWW] http://www.enercon.de (25.04.2015)

[27] Vensys Energy AG. [WWW] http://www.vensys.de (25.04.2015)

[28] XEMC Dawrind BV. [WWW] http://www.darwind.nl (25.04.2015)

[29] Polinder, H. Overview of and Trends in Wind Turbine Generator Systems. – *Power and Energy Society General Meeting, 2011 IEEE, San Diego*, 2011, 1–8.

[30] Hansen, A.D., Iov, F., Blaabjerg, F., Hansen, L.H. Review of Contemporary Wind Turbine Concepts and Their Market Penetration. – *Journal of Wind Engineering & Industrial Aerodynamics*, 2004, 28 (3), 247–263.

[31] International Energy Agency. Renewables in Global Energy Supply: An IEA Fact Sheet. Paris : OECD/IEA, 2006.

[32] De Vries, E. Trouble spots: Gearbox Failures and Design Solutions. – *Renewable Energy World*, 2006, 9 (2), 37–47.

[33] Windpower Engineering & Development. [WWW] http://www.windpowerengineering.com (25.04.2015)

[34] Polinder, H., van der Pijl, F.F.A., de Vilder, G.J., Tavner, P.,J. Comparison of Direct-Drive and Geared Generator Concepts for Wind Turbines. – *IEEE Transactions on Energy Conversion*, 2006, 21 (3), 725–733.

[35] Tavner, P.J., Van Bussel, G.J.W., Spinato, F. Machine and Converter Reliabilities in Wind Turbines. *In: Proceedings of the 3rd IET*

International Conference on Power Electronics, Machines and Drives, Cork, 2006, 127–130.

[36] McMillan, D., Ault, G.W. Techno-Economic Comparison of Operational Aspects for Direct-Drive and Gearbox-Driven Wind Turbines. – *IEEE Transactions on Energy Conversion*, 2010, 25 (1), 191–198.

[37] Jöckel, S. Gearless Wind Energy Converters With Permanent Magnet Generators - An Option for the Future? *In: Proceedings of European Union Wind Energy Conference, Gothenburg*, 1996, 414–417.

[38] Direct Industry. [WWW] http://www.directindustry.com (25.04.2015)

[39] Grauers, A. *Design of Direct-Driven Permanent-Magnet Generators for Wind Turbines* : PhD. dissertation. Gothenburg, Chalmers University of Technology, 1996.

[40] Bang, D., Polinder, H., Shrestha, G., Ferreira, J.A. Review of Generator Systems for Direct-Drive Wind Turbines. *In: Proceedings of European Wind Energy Conference, Brussels*, 2008, 1–11.

[41] Arshad, W.M., Bäckström, T., Sadarangani, C. Analytical Design and Analysis Procedure for a Transverse Flux Machine. *In: Proceedings of IEEE International Electric Machines and Drives Conference, Cambridge*, 2001, 115–121.

[42] Mueller, M.A. Electrical Generators for Direct Drive Wave Energy Converters. *In: IEE Proceedings of Generation, Transmission and Distribution*, 2002, 149 (4), 446–456.

[43] Leitwind AG. [WWW] http://www.leitwind.com (26.04.2015)

[44] Korn, N., Vaimann, T., Kallaste, A., Belahcen, A. Comparative Study of Slow-Speed Slotless Synchronous Generator Using SmCo and NdFeB permanent magnets. *In: Proceedings of Electric Power Quality and Supply Reliability Conference, Rakvere*, 2014, 225–228.

[45] Lampola, P. *Directly Driven Low-Speed Permanent-Magnet Generators for Wind Power Applications* : PhD dissertation. Helsinki, Helsinki University of Technology, 2000.

[46] Nagrial, M., Rizk, J., Hellany, A. Design and Performance of Permanent Magnet Slotless Machines. *In: Proceedings of 18th International Conference on Electrical Machines, Vilamoura*, 2008, 1–5.

[47] Spooner, E., Gordon, P., Bumby, J.R., French, C.D. Lightweight Ironless-Stator PM Generators for Direct-Drive Wind Turbines. *In: IEE Proceedings - Electric Power Applications*, 2005, 152 (1), 17–26.

[48] Vaimann, T., Kallaste, A., Korn, N., Laurit, S., Belahcen, A. Design of Slow-Speed Slotless SmCo Permanent Magnet Synchronous Generator for Wind Applications. *In: Proceedings of the 2014 15th International Scientific Conference on Electric Power Engineering, Brno*, 2014, 339–342.

[49] Stander, J.N., Venter, G., Kamper, M.J. Review of Direct-Drive Radial flux Wind Turbine Generator Mechanical Design. – *Wind Energy*, 2012, 15 (3), 459–472.

[50] Handler, D. *Investigation on Gearless Wind Turbine Generator Structures - Calculation and Optimisation of the 3-Bearing-Variants*. Dramstadt : Institut für Elektrische Energiewandlung, Technische Universität, 1997. Diploma Report No. 551.

[51] MTOI Wind Turbines. [WWW] http://www.mtoi.es (27.04.2015)

[52] Engström, S., Hernnäs, B., Parkegren, C., Waernulf, S. Development of NewGen – a New Type of Direct-Drive Generator. *In: Proceedings of European Wind Energy Conference, London*, 2004, 1–10.

[53] Enercon. [WWW] http://de.wikipedia.org/wiki/Enercon (25.04.2015)

[54] McDonald, A.S., Mueller, M.A., Polinder, H. Comparison of Generator Topologies for Direct-Drive Wind Turbines Including Structural Mass. *In: Proceedings of the XVII International Conference on Electrical Machines*, 2006, 361–367.

[55] Boulder Wind Power. [WWW] http://www.boulderwindpower.com (28.04.2015)

[56] Sway Turbine AS. [WWW] http://www.swayturbine.no (28.04.2015)

[57] Borgen, E. Direct Drive Generator/Motor for a Windmill/Hydropower Plant/Vessel where the Generator/Motor is Configured as a Hollow Profile and Method to Assemble Such a Windmill/Hydropower Plant. Patent NO: WO 2007/043894, 2007.

[58] Chin, Y.K., Kanninen, P., Maki-Ontto, P., Sakki, R., Lendenmann, H. Phenomenon of Magnetic Force in Permanent Magnet Wind Turbine

Generators. *In: Proceedings of International Conference on Electrical Machines and Systems, Tokyo*, 2009, 1–6.

[59] Pinilla, M. Martinez, S. Optimal Design of Permanent-Magnet Direct-Drive Generator for Wind Energy Considering the Cost Uncertainty in Raw Materials. – *Renewable Energy*, 2012, 41 (1), 267–276.

[60] Li, H., Chen, Z., Polinder, H. Optimization of Multibrid Permanent-Magnet Wind Generator Systems. – *IEEE Transactions on Energy Conversion*, 2009, 24 (1), 82–92.

[61] Sethuraman, L., Venugopal, V., Zavvos, A., Mueller, M. Structural Integrity of a Direct-Drive Generator for a Floating Wind Turbine. – *Renewable Energy*, 2014, 63, 597–616.

[62] Chun, Y.D., Wakao, S., Kim, T.H., Jang, K.B., Lee, J. Multiobjective Design Optimization of Brushless Permanent Magnet Motor Using 3D Equivalent Magnetic Circuit Network Method. – *IEEE Transactions on Applied Superconductivity*, 2004, 14 (2), 1910–1913.

[63] Sim, D.J., Cho, D.H., Chun, J.S., Jung, H.K., Chung, T.K. Efficiency Optimization of Interior Permanent Magnet Synchronous Motor Using Genetic Algorithms. – *IEEE Transactions on Magnetics*, 1997, 33 (2), 1880–1883.

[64] Pellegrino, G., Cupertino, F. IPM Motor Rotor Design by Means of FEA-Based Multi-Objective Optimization. *In: Proceedings of IEEE International Symposium on Industrial Electronics*, Bari, 2010, 1340–1346.

[65] Montgomery, D.C. *Design and Analysis of Experiments*. New York : John Wiley and Sons, 1997.

[66] Majak, J., Pohlak, M., Eerme, M., Küttner, R., Karjust, K. Artificial Neural Networks and Genetic Algorithms in Engineering Design. *In: Proceedings of International Conference on Engineering Optimization, Rio De Janeiro*, 2008.

[67] Gnana Sheela, K., Deepa, S.N. Review on Methods to Fix Number of Hidden Neurons in Neural Networks. – *Mathematical Problems in Engineering*, 2013, Article ID 425740. [WWW] http://dx.doi.org/10.1155/2013/425740

[68] Hecht-Nielsen, R. Theory of the Backpropagation Neural Network. *In: Proceedings of the International Joint Conference on Neural Networks, Washington*, 1989, 1, 593–605.

[69] Yin, H., Xiao, Y., Wen, G., Qing, Q., Deng, Y. Multiobjective Optimization for Foam-Filled Multi-Cell Thin-Walled Structures Under Lateral Impact. – *Thin-Walled Structures*, 2015, 95, 1–12.

[70] Velsker, T. *Design Optimization of Steel and Glass Structures* : PhD dissertation. Tallinn, Tallinn University of Technology, 2012.

[71] Majak, J., Pohlak, M. Decomposition Method for Solving Optimal Material Orientation Problems. – *Composite Structures*, 2010, 92 (8), 1839–1845.

[72] Majak, J., Pohlak, M. Optimal Material Orientation of Linear and Non-Linear Elastic 3D Anisotropic Materials. – *Meccanica*, 2010, 45 (5), 671–680.

[73] Majak, J., Hannus, S. Orientational Design of Anisotropic Materials Using the Hill and Tsai-Wu Strenght Criteria. – *Mechanics of Composite Materials*, 2003, 39 (6), 509–520.

[74] Kallaste, A., Järvik, J., Kilk, A. Permanent Magnet Axial-Flux Generator With Toroidal Winding. *In: Proceedings of 5th International Conference "Electric Power Quality and Supply Reliability", Tallinn*, 2006, 167–171.

[75] Gordon, P. *Aspects of, and New Approaches to, the Design of Direct Drive Generators for Wind Turbines* : PhD dissertation. Durham, University of Durham, 2004.

[76] Kallaste, A. *Low Speed Permanent Magnet Slotless Generator Development and Implementation for Windmills* : PhD dissertation. Tallinn, Tallinn University of Technology, 2013.

[77] Li, H., Chen, Z. Design optimization and comparison of large direct-drive permanent magnet wind generator systems. *In: Proceedings of International Conference on Electrical Machines and Systems, Seoul*, 2007, 685–690.

[78] Pyrhonen, J., Jokinen, T., Hrabovcova, V. *Design of Rotating Electrical Machines*. Chichester : John Wiley and Sons, 2008.

[79] Tuttelberg, K., Vaimann, T., Kallaste, A. Analysis of a Slow-Speed Slotless Permanent Magnet Synchronous Generator. *In: Proceedings of 4th International Youth Conference on Energy, Siofok*, 2013, 1–5.

[80] Bumby, J.R., Spooner, E., Jagiela, M. Equivalent Circuit Analysis of Solid-Rotor Induction Machines with Reference to Turbocharger Accelerator Applications. *In: IEE Proceedings - Electric Power Applications*, 2006, 153 (1), 31–39.

[81] Cheng, B., Qian, Q., Sun, H. Steel Truss Bridges with Welded Box-Section Members and Bowknot Integral Joints, Part I: Linear and Non-Linear Analysis. – *Journal of Constructional Steel Research*, 2013, 80, 465–474.

[82] Zavvos, A., McDonald, A.S., Mueller, M. Electromagnetic and Mechanical Optimisation of Direct-Drive Generators for Large Wind Turbines. *In: Proceedings of 5th IET International Conference on Power Electronics, Machines and Drives, Brighton,* 2010, 1–6.

[83] McDonald, A.S., Mueller, M.A. *Development of Analytical Tools for Estimating Inactive Mass*. University of Edinburgh, Scotland, UPWIND report, 2008.

[84] Krenk, S., Høgsberg, J. *Statics and Mechanics of Structures*. Dordrecht : Springer, 2013.

[85] ANSYS, Inc. ANSYS 14.5 Manual, 2014.

[86] Jangamshetti, S.H., Rau, V.G. Site Matching of Wind Turbine Generators: a Case Study. – *IEEE Transactions on Energy Conversion*, 1999, 14 (4), 1537–1543.

[87] Kallaste, A., Belahcen, A., Kilk, A., Vaimann, T. Analysis of the Eccentricity in a Low-Speed Slotless Permanent-Magnet Wind Generator. *In: Proceedings of 8th International Conference 2012 Electric Power Quality and Supply Reliability, Tartu*, 2012, 47–52.

[88] Mikrotrend d.o.o. [WWW] http://www.mikrotrend.com (18.05.2015)

ACKNOWLEDGEMENTS

I would like to express my utmost gratitude and appreciation to my supervisor Professor Martin Eerme for his encouragement and believing in me even when my own faith was failing. This dissertation would have not been possible without his supervision and guidance.

Secondly, I would like to thank my colleagues, Lead Research Scientist Jüri Majak and Senior Research Scientist Meelis Pohlak. Their invaluable guidance and support in optimisation methods and physical programming techniques have made this dissertation what it is.

Special thanks go to Professor Priit Kulu for his wise words and sharp eyes, which have enabled to refine the structure and format of the paper to match the highest required scientific standards.

Also, I would like to express my sincere gratitude to my colleagues Ants Kallaste, Tauno Tiirats and all other members of Goliath Wind for their support in the development of the generator concept and building the prototype.

My sincere gratitude goes to my friend Ms. Kristin Lillemäe, whose kindness and help with language corrections has enabled to make the dissertation readable.

Finally, I would like to thank my mother, girlfriend and grandparents for their patience and constants support during my studies and intense periods of writing, data collection and calculations. Their care and dedication cannot be underestimated.

This thesis is dedicated to my grandmother M. D. Silvia Pabut who passed away this year and is unfortunately not able to see me graduate.

ABSTRACT

Optimal Design of Slotless Permanent Magnet Generators

The topic of this dissertation is the development of a design and optimisation process of an electrical generator for wind turbine applications. The introduced methodology focuses on increasing the machine's energy yield and decreasing the overall system cost. As the design of an electrical generator is a complex task involving several different disciplines, emphasis is put on the simplification and decomposition of the initial problem into sub-tasks and routines. Furthermore, novel electromagnetic and structural concepts are introduced to reduce the transportation problems associated with direct-drive generators.

A state of the art review is composed to investigate the current trends in wind energy technologies and especially development directions of direct-drive generators. Based on the collected information, the basic layout for the machine is composed and the introduced novel concepts are superimposed. The fully defined concept is then taken as a basis for the proposed optimisation procedure.

The suggested design and optimisation approach is divided into three blocks: pre-analysis of the optimality criteria and constraints, electromagnetic optimisation and structural optimisation. The pre-analysis block focuses on the initial definition of design parameters, constraints and the design sensitivity towards the acting loads. The proposed approach enables to reduce the design space without compromising the accuracy of the end results. The electromagnetic optimisation block is carried out by developing simplified analytical equations for defining the learning data. Artificial neural networks and a hybrid genetic algorithm are utilised to generate the mathematical model of the machine and carry out the optimisation. The novel concept of a structural response characteristic is introduced to take into account the effect of different electromagnetic parameters on the mechanical layout. In the structural optimisation block, the multiple polynomial regression model is applied to the learning data in order to develop the meta-model of the generator. Besides the electromagnetic and structural parameters, the cost and energy production of various generator configurations are assessed.

The full procedure is carried out on an example machine featuring a slotless electromagnetic circuit and the novel lattice concept support structure. The minimal weight and increased operational profit of the generator are taken as the final objectives of the procedure. However, due to the contradicting nature of the generator's efficiency and cost, the Pareto optimality concept is introduced. This also enables to select other final objective functions, as all the solutions on the Pareto front are optimal to some aspect. With only one optimisation, run the machine's weight is decreased 14 % and the energy output is increased 1.6 %.

The introduced electromagnetic and structural concepts offer solutions to reduce the transportation restrictions of the direct-drive generator by modularisation. However, they also feature specific problems associated with

assembly precision and the handling of the electromagnetically active units. In order to investigate the described drawbacks, small scale and full scale machine prototypes are built and experimentally investigated. On the small scale model the effects of machine eccentricity are assessed and the dynamic form is found to be the most critical. The assembly precision of the active components is measured on the full scale machine and deemed to be acceptable as it does not contribute significantly to the overall deformation levels. Furthermore, the average value of the real air-gap complies with the set theoretical value. Handling of the active components is assessed in parallel and a novel device with corresponding method is introduced and successfully tested.

Therefore, it can be concluded that the main objectives of the study have been achieved and all of the proposed hypotheses have been determined to be consistent with the findings of the research. The methodology for the design and optimisation of a generator in a wind turbine is introduced and proven on a sample layout. Furthermore, various novel solutions are offered to reduce the transportation problems associated with direct-drive machines.

KOKKUVÕTE

Uurdevabade püsimagnetgeneraatorite optimeerimismeetodid

Antud väitekiri kirjeldab tuulegeneraatorites kasutatava elektrigeneraatori projekteerimise ja optimeerimise protseduuri väljatöötamist. Uudne metoodika keskendub masina energiatootlikkuse suurendamisele ning hinna vähendamisele. Kuna elektrigeneraatori arendus on mitut distsipliini hõlmav kompleksne tegevus, võetakse eesmärgiks protseduuri lihtsustamine ning väiksemateks osadeks ja tegevusteks jagamine. Lisaks kirjeldatud metoodikale uuritakse uudse elektromagnetilise ahela ning tugistruktuuri kasutamise võimalikkust. Töö eesmärgid tulenevad tuuleenergeetika kiirest arengust, mille käigus on jõutud teatud tehnoloogiliste barjäärideni. Kuigi otseajamiga generaatorid on töökindlamad kui käigukastiga lahendused, osutuvad need tihtipeale massilt liiga rasketeks ning hinnalt kulukateks. Mida suuremaks kasvavad tuulikute väljundvõimsused, seda teravamaks muutuvad ka generaatoritega seotud tehnilised probleemid. Sellest lähtuvalt kirjeldab töö nii olemasolevate tehnoloogiate optimeerimist kui ka uute tehniliste lahenduste juurutamist.

Kirjanduse ülevaatest lähtuvalt koostatakse algne generaatori mudel, millele rakendatakse uurdevaba elektromagnetiline ahel ning uudne sõrestikul baseeruv tugistruktuur. Pärast esialgset parameetrite määramist optimeeritakse masinat töös kirjeldatud metoodika alusel. Kuigi see protseduur on illustreeritud konkreetse lahenduse näitel, võib metoodikat rakendada erinevatele generaatoritele, muutes sisendparameetrite olemust ning väärtuseid.

Väljapakutud projekteerimise ja optimeerimise protseduur koosneb kolmest peamisest osast: esialgne rajatingimuste ning soovitud tulemuste põhjalik analüüs, elektromagnetilise ahela optimeerimine ja tugistruktuuri optimeerimine. Rajatingimuste analüüsi käigus määratakse peamised masinat kirjeldavad parameetrid ning nende piirväärtused. Lisaks sellele uuritakse põhjalikult generaatori tundlikkust mõjuvate jõudude suhtes, et vähem olulised tegurid analüüsist kõrvale jätta. Taoline lähenemine võimaldab vähendada kasutatavate parameetrite arvu ning seega ka vajaminevate eksperimentide ja arvutuste mahtu. Elektromagnetilise ahela optimeerimise käigus tuuakse välja analüütilised meetodid, mille abil on võimalik määrata masina parameetritele esialgsed väärtused ning koostada andmete kogum generaatori matemaatilise mudeli koostamiseks. Optimeerimisprotseduur viiakse läbi, kasutades tehislikke närvivõrke ja geneetilist algoritmi. Peamise uuendusena lisatakse üheks väljundparameetriks „struktuurne mõju". Taoline lähenemine võimaldab ilma sisendparameetrite hulga suurendamiseta hinnata elektromagnetilise ahela võimalikku mõju tugistruktuuri hilisemale massile. Struktuurne optimeerimine ja matemaatilise mudeli väljatöötamine teostatakse regressioonanalüüsiga. Lisaks mehaanilistele ning elektromagnetilistele parameetritele hinnatakse tehtud valikute mõju masina hinnale ning energia tootlikkusele.

Antud töös on lõplikuks eesmärgiks valitud masina minimaalne kaal ning suurenenud kasum energia tootmisest. Silmas tuleb pidada, et generaatori elektriline efektiivsus ning madal hind on vastuolulised funktsioonid ja ühe suurenedes kasvab ka teine. Seetõttu rakendatakse tulemuste kirjeldamiseks Pareto optimaalsuse printsiipi. Kuna kõik valikud Pareto väljal on teatud mõttes optimaalsed, on võimalik valida vastavalt vajadusele teistsuguseid optimeerimise lõppeesmärke. Kirjeldatud protseduuri ja metoodika abil väheneb masina esialgne kaal 14 % ning toodetud energia kogus suureneb 1.6 %. Majanduslikust aspektist oluline energiatootlikkuse kasum kasvab, kuigi masina esialgne hind suureneb.

Kasutatud uurdevaba elektromagnetiline ahel ning sõrestikul baseeruv tugistruktuur võimaldavad masina koostamist sarnastest moodulitest. Selle tulemusena muutuvad transpordist tulenevad gabariitmõõtmete piirangud ebaoluliseks. Kuid taolise kontseptsiooni kasutamisega kaasnevad uued praktilised probleemid nagu generaatori koostamise täpsus ning magnetiliselt aktiivsete moodulite käsitsemine. Ebapiisav aktiivsete elementide koostamise täpsus võib viia masina ekstsentrilisuseni, mis tekitab nii staatilisi kui ka dünaamilisi probleeme. Ekstsentrilisuse mõju uurimiseks ehitati töö käigus vähendatud mõõdus katsemasin. Selle abil tuvastati, et dünaamiline ekstsentrilisuse vorm on kõige ohtlikum, kuna suurendab masina õhupilu elementide liikumist nii raadiuse kui ka telje suunas. Õhupilu elementide reaalset paigutamise täpsust ja sellest tulenevaid ohte mõõdeti ning hinnati täisskaalas valmistatud masina prototüübil. Koostamistäpsuse parandamiseks kasutati töö käigus välja töötatud spetsiaalset seadet, mille abil saavutatud tulemused osutusid rahuldavaks. Arvutustele tuginedes tuvastati, et kirjeldatud täpsus ei mõjuta masina tööparameetreid. Magnetiliselt aktiivsete komponentide käsitsemist uuriti samuti testmasina koostamise käigus ning kasutatud seadme rakendamine aitas kardetud probleeme täielikult vältida.

Lõpetuseks võib väita, et töö alguses püstitatud eesmärgid saavutati täiel määral ning püstitatud hüpoteesid leidsid kinnitust. Välja töötati projekteerimise ja optimeerimise protseduur, mida rakendati edukalt elektrigeneraatori parameetrite optimeerimiseks. Väljapakutud uudne elektromagnetiline ahel ning tugistruktuur võimaldavad projekteerida kaalult kergeid modulaarseid generaatoreid, mida on võimalik koostada sarnastest segmentidest ning vajaliku täpsusega.

OTHER PUBLICATIONS

1. Aruniit, A.; Kers, J.; Krumme, A.; Antonov, M.; Allikas, G.; Herranen, H.; Pabut, O. Wear Resistance Influencers of Particle Reinforced Polymer Composite. *In: Proceedings of 19th International Conference on Composite Materials: 28 July – 2 August 2013, Montreal, Canada.*

2. Pabut, O.; Allikas, G.; Herranen, H.; Talalaev, R.; Vene, K. Model Validation and Structural Analysis of a Small Wind Turbine Blade. *In: Proceedings of the 8th International Conference of DAAAM Baltic Industrial Engineering 19–21 April 2012, Tallinn, Estonia,* 74 – 79.

3. Kallaste, A.; Vaimann, T.; Pabut, O. Slow-Speed Ring-Shaped Permanent Magnet Generator for Wind Applications. *In: 11th International Symposium "Typical Problems in the Field of Electrical and Power Engineering" and "Doctoral School of Energy and Geotechnology II": 16–21 January 2012, Pärnu, Estonia,* 66 – 69.

4. Herranen, H.; Kers, J.; Preden, J.; Talalaev, R.; Eerme, M.; Majak, J.; Pohlak, M.; Allikas, G.; Pabut, O.; Lend, H. The Influence of Embedded Electronics on the Structural Performance in Carbon Fibre Laminates. *In: Proceedings of Mechanics of Nano, Micro and Macro Composite Structures: 18–20 June 2012, Torino, Italy.*

5. Allikas, G.; Kers, J.; Aruniit, A.; Herranen, H.; Eerme, M.; Majak, J.; Pohlak, M.; Pabut, O. (2012). Design of light-weight sandwich panels for trailers. *In: Proceedings of the 15th European Conference on Composite Materials: June 24–28, 2012, Venice, Italy.*

6. Kallaste, A.; Vaimann, T.; Pabut, O. Aeglasekäiguline otsetoimeline püsimagnetgeneraator tuuleagregaatidele. *In: TEUK XIV: Taastuvate energiaallikate uurimine ja kasutamine - neljateistkümnenda konverentsi kogumik: 8. november, 2012, Tartu, Estonia,* 68 – 77.

7. Herranen, H.; Pabut, O.; Eerme, M.; Majak, J.; Pohlak, M.; Kers, J.; Saarna, M.; Allikas, G.; Aruniit, A. (2011). Design and Testing of Sandwich Structures with Different Core Materials. *Materials Science (Medžiagotyra), Kaunas University of Technology,* vol. 18, no. 1. 2012, 1 – 6.

8. Pabut, O.; Eerme, M.; Majak, J.; Pohlak, M. (2010). Design Optimization of Structural Components for Fatigue Loading. *In: Proceedings of 7th International Conference of DAAAM Baltic Industrial Engineering: 22–24 April 2010, Tallinn, Estonia,* 131 – 135.

APPENDIX A

Publications

Paper 1

Pabut, O.; Lend, H.; Tiirats, T. Load Sensitivity Analysis of a Large Diameter Permanent Magnet Generator for Wind Turbines. *In: Proceedings of the 9th International Conference of DAAAM Baltic Industrial Engineering: 24–26th April 2014, Tallinn, Estonia,* 59 – 64.

LOAD SENSITIVITY ANALYSIS OF A LARGE DIAMETER PERMANENT MAGNET GENERATOR FOR WIND TURBINES

Pabut, O.; Lend, H. & Tiirats, T.

Abstract: *Permanent magnet (PM) and electrically-excited direct-drive generators are usually described by their high mass and production costs. Studies have proved that when increasing generator's capacity, inactive mass increases faster than the active mass. In this paper, a load component sensitivity study for the inactive mass is performed on a direct-drive PM generator via Finite Element Analysis (FEA). Taguchi method is utilized for describing the relations between design parameters and the resulting stresses and deformations. Most influential load components are determined and general countermeasures are offered.*
Key words: sensitivity analysis, permanent magnet generator, finite element analysis, Taguchi method.

1. INTRODUCTION

During past decades a high number of research papers have been presented on the electromagnetic layout of an electrical generator in a wind turbine [1-2]. Despite the numerous solutions that have been offered, the geared drive train with an induction generator, still remains the dominant technology [3]. Alongside it, various alternative drive train solutions, like the PM synchronous generator, have emerged. Although, these machines offer higher reliability and power density, they are usually described also by their high mass and production costs [4].
With machines near megawatt scale, the final cost and mass of the generator has been largely associated with the active electrical parts. However, electrical machines also contain material that fulfils a structural role and works against a number of high forces. Studies have proved that when increasing the generator capacity, inactive mass increases faster than the active mass and begins to dominate [3, 5]. This, alongside the fact that price of the active materials has steadily been dropping, indicates that when dealing with higher capacity generators, more refined methods to reduce the inactive mass are necessary. This paper aims to provide insight to the relative importance of the acting forces on the generator, in order to provide information for the initial selection of design parameter values.

2. ANALYSIS DESCRIPTION

2.1 Generator
The machine subjected to the analysis is a PM ultra large direct-drive generator with an air-gap diameter of 12 meters and rated capacity of 3 MW. The machine consists of an inner rotor with permanent magnets and an air-cooled outer stator with electrical windings. Active elements are supported by a lattice structure consisting mainly of tubular steel beams. While the rotor is supported equally from both sides, the stator has one sided unsymmetrical support, like shown in Figure 1a. This is of interest when considering the acting gravity forces, which in this case result in an air-gap deforming rolling moment.
Electromagnetic setup of the generator is similar to the one that is described in the previous work [6]. The stator coils are located in the air-gap to reduce the normal component of Maxwell stress.
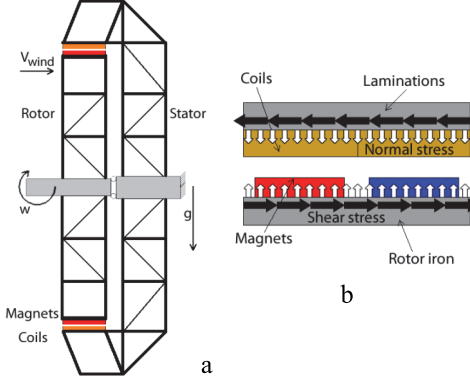
Fig. 1. Generator overall topology (a) and electromagnetic layout (b)

2.2 Acting forces

Forces present in an electrical machine are similar for most types of generators. In addition to those that can be found in regular electrical generators, effects from wind and tower top accelerations must be considered for a machine that is used in a wind turbine. As a result, in the presented analysis, following loads are considered: deadweight resulting from gravity, rotor rotational velocity, wind load on the structure, tower front-to-back acceleration and side-to-side acceleration, normal stress and generator torque.

Torque τ and rotational speed ω are proportional to the generator's electrical power output P_{el} and efficiency η (1). Therefore, they both cannot be subjected to minimization but their relation can be manipulated in a certain range if it turns out to be beneficial. The limits of this manipulation are set by maximum allowed rotational speed for the blades (tip speed limit ≈ 80 m/s). Meaning that for larger turbines and rotors, the rotational velocity is smaller.

$$P_{el} = \tau \cdot \omega \cdot \eta \qquad (1)$$

From an electromagnetic point of view, torque is a product of the tangential component of Maxwell stress, which is also designated as shear stress σ.

Therefore, torque of a rotating electrical machine can also be given as

$$\tau = 2\pi\sigma R^2 l \qquad (2)$$

where R is the machine air-gap radius and l axial length of the generator [4]. Torque is the useful force in an electrical machine and does not serve to close the air-gap.

In most generator topologies Maxwell stress has also a normal component (normal stress), which is caused by the attraction of the ferromagnetic surfaces of rotor and stator. Normal component can be a magnitude greater than the shear stress and directly acts to close the air-gap. Designers have long looked for ways how to reduce the normal stress in relation to the shear stress and as a result air-cored machines have been developed [7-8]. Presented machine is a hybrid solution, as the windings are located in the air-gap, like shown in Figure 1b.

Wind turbine towers have become highly optimized and in many cases extremely soft and flexible towers are used [9]. For geared drive trains this has a low impact but direct-drives with their high mass and material distribution on the outer perimeter are vulnerable to tower top accelerations. Depending on the topology of the support structure, considerable extra stresses and deformations can occur.

From (2) it can be seen that one option to increase the generator torque and therefore the power output, is to increase the air-gap radius. Many designers have taken advantage of this, which has led to generators with ultra large diameters. As the perimeters of the machines grow, so does the force that is resulting from wind acting on the generator's structure [10]. This can be found by

$$F_{wind} = \rho/2 \cdot v_{wind}^2 \cdot A \cdot c_p \qquad (3)$$

where ρ is the air density, v_{wind} the wind speed, A surface area of the generator that is perpendicular to the wind direction and c_p the shape parameter of the surface.

Therefore, depending on the actual surface that is exposed to wind, the force F_{wind} could become a significant factor that influences the generator design.

2.3 FEA model

Framework of the generator is modeled in ANSYS Workbench environment with two-node beam elements (BEAM188) having six degrees of freedom at each node. For the beam-to-beam connections it is assumed that they have the same carrying capacity as the profiles. Therefore, different beams are connected by shared nodes and automatically transmit all moments and forces.
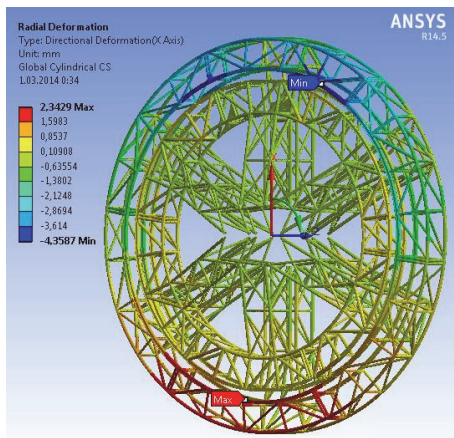

Fig. 2. FEA model of the generator

Only the framework of the generator is directly modeled while rest of the elements like magnets and coils are approximated by point masses. It is assumed that they do not add significantly to the structural stiffness of the machine. In addition, rotor shaft and stator king-pin are not modeled, as for direct-drive turbines they are mostly subjected to forces and moments from the rotor blades [7]. Therefore, their cost and end mass is not greatly influenced by the generator design parameters.

The setup and in particular the stiffness of the FEA model have been validated with an experimental study on the full scale generator structure. The dimensions of rotor and stator rings were measured with

and without magnetic forces and calculated deformations were found to be in good correlation with the FEA results.

3. SENSITIVITY STUDY

3.1 Initial parameter selection

In the first part of the analysis all the seven acting load components are applied to the structure one-by-one while resulting stresses and deformations are extracted. Results are compared with values from the nominal working situation where all the components are acting with the same values simultaneously. Overall stress and deformation values in the nominal working situation are within allowed limits to obtain reasonable results.
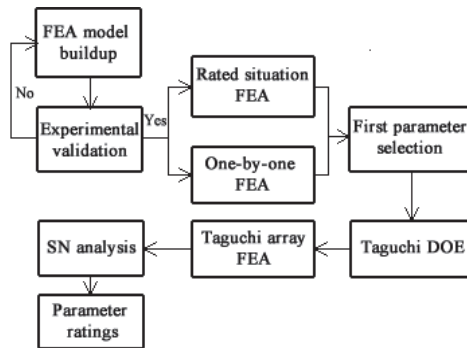

Fig. 3. Principles of the study

A cylindrical coordinate system is used to record the results and only rotor positive and stator negative radial deformations are investigated, as they serve to close the air-gap. The results of the FEA analysis are presented in Table 1, where the contribution of each component to the overall stress level is presented.

The initial study is performed to determine the most influential load components for further analysis. This enables to reduce the required number of experiments when investigating parameter interactions. From the comparison between the sum of components and actual results it is clear, that further analysis is required, as deformations differ about 20% and stresses 50%.

Only the parameters that contribute more than 5% to at least one of the outputs are selected for further investigation. These include: deadweight, front-to-back acceleration, normal stress and torque (marked green in Table 1).

Load	Rotor def	Stator def	Rotor stress	Stator stress
Deadweight	38%	64%	18%	42%
Rot speed	5%	0%	4%	0%
Side accel	4%	5%	2%	4%
Front accel	3%	2%	7%	5%
Norm stress	44%	23%	27%	21%
Torque	5%	4%	39%	26%
Wind	1%	1%	3%	2%
Sum	**1.3**	**4.8**	**109**	**185**
Actual total	**1.1**	**4.1**	**74**	**128**

Table 1. Load component contribution to overall stress level.

3.2 Taguchi analysis

Taguchi method for design of experiments is utilized to compose the mathematical model describing the relations between design parameters and the resulting stresses and deformations. Taguchi is chosen as it enables to reduce the number of required experiments even further. Five value levels are chosen for each input parameter: 100%, 60%, 80%, 120% and 140% of their rated value. The levels are chosen based on an assumption that for a defined output power the design characteristics would vary not more than ± 40%. This is important since conclusions drawn from small scale experiments are valid only over the particular experimental region [11].

Variation is applied to the rated value of the parameter, without considering the safety factor that needs to be applied to the loads [10]. The value of the parameter is changed according to the required percentage and only then multiplied with the safety factor. In case of the deadweight, only the mass of active material together with needed fixtures is varied, as only this can directly be influenced by designer's initial decisions.

Since there are four parameters and five levels, L25 orthogonal array is used. For each experiment, the stresses and deformations of rotor and stator are extracted as performance characteristics. The obtained FEM results are transformed into signal-to-noise (SN) ratios. The SN ratios are used as a measure of deviation from or nearness to the desired value. Goal of the analysis is minimization of performance characteristics. The needed SN ration are found with

$$SN_i = -10log\left(\sum_{u=1}^{N_i} \frac{y_u^2}{N_i}\right) \qquad (4)$$

where u is the trial number, N_i the number of trials for experiment i and y_u is the value of the performance characteristic for a given experiment. "After calculating the SN ratio for each experiment, the average SN value is calculated for each factor and level. In order to determine the effect of the variable on the process, Δ value (high SN – low SN) is found for each parameter." [11]

Response of the SN ratios for the rotor deformation can be found in Table 2. The rakings of all four parameters with their corresponding Δ values for all performance characteristics are presented in Table 3.

Level	Dead-weight	Front accel	Norm stress	Torque
100%	0.00	0.12	-0.08	-0.11
60%	1.19	0.13	1.82	0.09
80%	0.50	-0.04	0.81	0.15
120%	-0.59	-0.14	-0.89	0.03
140%	-1.11	-0.07	-1.66	-0.17
Δ	**2.30**	**0.28**	**3.48**	**0.32**
Rank	**II**	**IV**	**I**	**III**

Table 2. Response table for SN ratios for rotor deformation.

		Dead-weight	Front accel	Norm stress	Torque
Rotor def	Δ	2.30	0.28	3.48	0.32
	rank	II	IV	I	III
Stator def	Δ	3.65	0.19	1.72	0.19
	rank	I	III	II	IV
Rotor stress	Δ	0.98	0.39	0.82	4.19
	rank	II	IV	III	I
Stator stress	Δ	2.49	0.06	0.62	2.59
	rank	II	IV	III	I

Table 3. Rankings of all parameters for all performance characteristics.

4. DISCUSSION

According to results presented in Table 3, deadweight and normal stress are the most influential factors for the air-gap deformations. For rotor, normal stress prevails but for stator, deadweight has by far the biggest influence. This can be explained by cantilever nature of the stator structure (Figure 1a). It could be compensated by adding a frontal support structure. However, it would also make the mechanical construction and specially the assembly process more complex. For the stator the deadweight is not an alternating force. Therefore, the resulting deformations could be already factored into the shape of the structure prior to the assembly and later the machine would deform itself into right dimensions. Alternatively, after the stator assembly the windings could be adjusted in order to compensate for the static deformations after stator has been lifted into the vertical position. Another option could be also utilization of materials with better stiffness to weight ratio i.e. performing structural optimization [12-15].

Frontal acceleration has a minor significance for all of the performance characteristics. This can be explained by the mechanical setup of the frame structure. As it requires space to use material effectively, it also contributes to the axial stiffness of the machine and therefore reduces the acceleration influence. But it must be noted that for disc like sheet metal structures with their material located mostly on the outer rim, this most likely does not apply.

From Table 1 and 3 it can be summarized that for this type of generator, the key influential factor determining the levels of stress and deformation, is the mass of the material located at the air-gap radius.

When taking actions to reduce the mass on the air-gap radius, care has to be taken that these actions do not increase the normal stress, as any benefits would be then cancelled out. For example one of the possible solutions could be using higher grade PM's with better mass to field strength ratio. At the same time the air-gap could be extended to keep normal stress at acceptable level. The reduced mass would also be beneficial for the other turbine parts, as it would mean for example lower loads for the yaw system.

This conclusion indicates that solutions offered in literature to use heavy but cheap magnetic materials like ferrites [16] are most likely cost wise not beneficial. The savings on magnet material costs would be lost in the extra investment that is required for the structure reinforcement.

On the stress side, the designer's aim, in addition to reducing mass of the active material, should be also limitation of the torque value. Due to the torque's direct dependency on the output power (1) and constraints laid on the rotational speed, there is usually not much room left to play. However, as a rule of thumb, the blades should be always utilized at their maximum allowed rotational speed.

Finally, electromagnetic setups that offer either considerably lower mass or normal stresses could be considered. For example solution of an ironless design presented by Gordon and Spooner [8] would fulfil these criteria.

5. CONCLUSION

Experimentally validated FEA model of a large diameter PM generator for a wind turbine has been built in ANSYS environment. The main loads acting on the generator structure have been described. Their individual contribution to the overall stress and deformation levels has been determined. Taguchi method of design of experiments has been used to study interactions of the individual load components and their relation to structural stresses and air-gap deformations. The mass of material located on the air-gap radius appears to be the most influential component when looking at both stresses and deformations. When regarding only the

deformations, normal stress has to be strongly considered and when focusing on stresses, the generator torque is the dominant parameter.

The obtained results imply that all efforts must be focused on the reduction of mass at the air-gap radius as it would bring about further reduction of structural mass.

6. REFERENCES

[1] Bang, D., Polinder, H., Shrestha, G., Ferreira, J. A. Promising Direct-Drive Generator Systems for Large Wind Turbine. *Wind Power to the Grid – EPE Wind Energy Chapter 1st Seminar,* 2008, 1-10.

[2] Henriksen, M., Jensen, B. Induction Generators for Direct-Drive Wind Turbines. *Electric Machines Drives Conference,* 2011, 1125-1130.

[3] Zhang, Z., Chen, A., Matveev, A., Nilssen, R., Nysveen, A. High-Power Generators for Offshore Wind Turbines. *Energy Proc.,* 2013, **35(2013),** 52-61.

[4] McDonald, A. S., Mueller, M. A., Polinder, H. Structural Mass in Direct-Drive Permanent Magnet Electrical Generators. *IET Renewable Power Generator,* 2007, **2(1)**, 3-15.

[5] Shrestha, G., Poliner, H., Ferreira, J. A. Scaling Laws for Direct-Drive Generators in Wind Turbines. *Proc. IEMDC,* 2009, 797-803.

[6] Kallaste, A., Vaimann, T., Pabut, O. Slow-Speed Ring-Shaped Permanent Magnet Generator for Wind Applications. *11th Int. Symp.”Typ. Problems in the Field of Electrical and Power Engineering,* 2012, 66-69.

[7] Mueller, M. S., McDonald, A. S. A Lightweight Low Speed Permanent Magnet Electrical Generator for Direct-Drive Wind Turbines. *Wind Energy,* 2009, **12(8)**, 768-780.

[8] Spooner, E., Gordon, P., Bumby, J. R., French, C.D., Lightweight Ironless-Stator PM Generators for Direct-Drive Wind Turbines. *Proc. Inst. Elec. Eng. Elec. Pow. Appl.,* 2005, **152(1)**, 17-26.

[9] Erich, H. Wind Turbines: Fundamentals, Technologies, Application, Economics. *Springer,* 2006.

[10] Guideline for the Certification of Wind Turbines. *Germanischer Lloyd,* 2010.

[11] Phadke, S. M. Quality Engineering Using Robust Design. *Englewood Cliffs, N.J., Prentice Hall,* 1989.

[12] Pohlak, M., Küttner, R., Majak, J. Modeling and Optimal Design of Sheet Metal RP&M Processes. *Rapid Protot. Journal,* 2005, **11(5),** 304-311.

[13] Kers, J., Majak, J. Modeling a New Composite From a Recycled GFRP. *Mechanics of Composite Materials,* 2008, **44(4)**, 623-632.

[14] Majak, J., Pohlak, M. De-Composition Method for Solving Optimal Material Orientation Problems, *Composite Structures,* 2010, **92(8)**, 1839-1845.

[15] Majak, J., Pohlak, M., Eerme, M., Velsker, T. Design of Car Frontal Protection System Using Neural Networks and Genetic Algorithm. Mechanika, 2012, **18 (4)**, 453-460.

[16] Kallaste, A. Low Speed Permanent Magnet Slotless Generator Development and Implementation for Windmills. *Ph.D. Dissertation, TUT, Tallinn,* 2013.

7. ADDITIONAL DATA ABOUT AUTHORS

MSc. Ott Pabut
TUT, Department of Machinery
Ehitajate tee 5, 19086 Tallinn, Estonia
Phone: +372 51 644 57,
E-mail: ottpabut@hotmail.com
http://www.ttu.ee

Paper 2

Pabut, O.; Eerme, M.; Kallaste, A.; Vaimann, T. Multi-Criteria Design Optimization of Ultra Large Diameter Permanent Magnet Generator. *Elektronika ir Elektrotechnika*, vol. 21, no. 3, 2015, 43 – 48.

Multi-Criteria Design Optimization of Ultra Large Diameter Permanent Magnet Generator

Ott Pabut[1], Martin Eerme[1], Ants Kallaste[2], Toomas Vaimann[2]
[1]Department of Machinery, Tallinn University of Technology,
Ehitajate tee 5, 19086 Tallinn, Estonia
[2]Department of Electrical Engineering, Tallinn University of Technology,
Ehitajate tee 5, 19086 Tallinn, Estonia
ott.pabut@ttu.ee

Abstract—This paper presents a novel design optimization procedure for an ultra large diameter permanent magnet generator. As the machine features unorthodox electromagnetic and mechanical layouts, basic principles for determining structural loads together with material quantities for cost estimation are described. Finite element modelling with beam elements is used for retrieving stresses and deformations of the novel carrier structure. Mathematical system response model of the generator is created with artificial neural networks, while genetic algorithm with gradient method is utilized for determining the optimal solutions. Input dataset for the model build-up is constructed with a help of a full factorial experimental method. Achieved results are utilized for describing the relationship between the structural response and efficiency values of the generator. As the design of the machine has to fulfil contradicting technical and economical requirements, Pareto optimality concept is employed. As an example, a set of optimal solutions is determined for the particular case.

Index Terms—Artificial neural networks, finite element analysis, Pareto optimization, permanent magnet machine.

I. INTRODUCTION

Central issue in the development of wind energy conversion systems has been scaling up to higher turbine capacities and bigger rotor diameters [1]. Consequently more effort and innovation has been put into developing optimal solutions for subcomponents of wind turbines in order to comply with increasing technical and commercial requirements [2]. One of the favourite topics for analysis has become the layout of the electrical generator in terms of increasing its energy density and decreasing cost [3]. Various electromagnetic topology options have been presented and researchers have developed deterministic and probabilistic methods for prediction of structural properties including mass and overall dimensions [4], [5].

It also has become clear that design principles and restrictions which were suitable at lower power outputs have to be reviewed. For example the price of active materials has been in general declining and therefore its influence in determining the end cost of generators has also become less

important [6]. Some researchers have utilized various approximating methods known from other industries [7] to optimize existing concepts and provide better understanding for the selection of initial design parameters. For example Li and Chen [8] have successfully used improved genetic algorithm (GA) for design optimization and site matching of generators with different power ratings and rotational speeds. Isfahani *et al.* [9] have used GA to carry out simultaneous multiobjective optimization of the electromagnetic setup of a permanent magnet (PM) generator to minimize machine mass and increase annual energy output.

Present study proposes to use a novel design optimization procedure for an ultra large diameter permanent magnet generator and presents results based on an example machine. Aim of the described methodology is to find the most suitable design values in terms of structural response, cost and efficiency for a machine with novel electromagnetic and mechanical layout. Finite element modelling (FEM), artificial neural networks (ANN) and hybrid genetic algorithm (HGA) are combined to carry out the proposed procedure [10]–[13]. As the obtained design values are evaluated against multiple criteria, Pareto optimality concept is applied in the analysis phase.

II. METHODOLOGY

Design activities regarding an electrical generator extend throughout different disciplines, including electromagnetic and structural engineering. Therefore, a procedure of obtaining an optimal solution for the machine's layout demands taking into account multiple criteria from their specific fields. In current study various analytical methods and software tools are utilized to evaluate the considered complex large scale structure. The principle flow chart of the design procedure is given in Fig. 1. In engineering process commonly certain FEM, design of experiments (DOE), optimization and evaluation blocks are utilized to reach a qualified decision regarding the effectiveness of the design. Main novel and specific features of the proposed optimization procedure can be outlined as:

- Presence of the pre-design block containing thoroughgoing preliminary analysis and simplification of initial problem;
- Presence of electromagnetic modelling and structural

response modelling blocks, specific for the particular problem.

In next chapters, the basic blocks of the proposed optimization procedure are described.
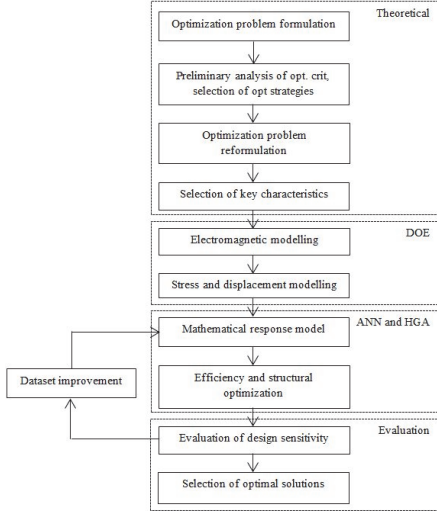

Fig. 1. Flow chart of the design procedure.

III. GENERATOR DESCRIPTION

The subject of optimization is a 3 MW ultra large diameter PM radial flux generator with concentrated electrical windings. The machine prototype built for testing is presented in Fig. 2 and basic characteristic figures are given in Table I.

Fig. 2. Full scale generator prototype.

TABLE I. GENERATOR CHARACTERISTICS.

Electrical power	P_{el}	kW	3000
Rotational speed	ω	rpm	15.3
Torque	τ	kNm	2090
Air-gap radius	R	m	6.3
Air-gap width	g_{air}	mm	9
Magnet height	h_m	mm	18
Magnet width	w_m	mm	100
Magnet length	l_m	mm	600
Coil height	h_c	mm	17
Coil width	w_c	mm	200
Coil length	l_c	mm	800

A. Electromagnetic Model

Detailed description of the electromagnetic conversion principles of the machine can be found in previous work [14]. Electrical layout of the generator describing one rotor pole and corresponding concentrated electrical stator winding is presented in Fig. 3. The loads induced for the carrier structure of the machine are directly influenced by the electromagnetic energy conversion principle. In [15] the authors have used FEM and Taguchi method to investigate the relative importance of main active forces for the initial selection of design parameters for the described generator solution. Mass of the material located on the rotor outer and stator inner radiuses, normal component of Maxwell stress and operational torque have been identified as they key driving factors for the stresses and deformations of the structure.
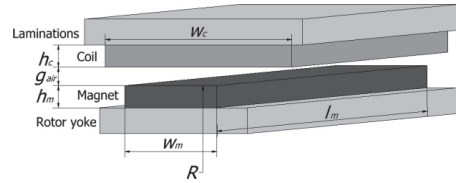

Fig. 3. Air-gap layout and symbols.

As the generator torque depends on the air-gap radius squared (1) and stator armature has a slotless design (resulting in low magnetic field density in the air-gap), the machine has unconventionally large air-gap radius. Torque τ of a radial flux generator can be given as [6]

$$\tau = 2\pi\sigma_{\tan}R^2 l, \qquad (1)$$

where $\sigma_{\tan}$ is tangential component of Maxwell stress, R generator air-gap radius and l generator axial length.

Normal component of Maxwell stress can be estimated by

$$q = n_m w_m l_m B_n^2 / (2\mu_o), \qquad (2)$$

where n_m is the magnet number, w_m magnet width, l_m magnet length, B_n normal direction air-gap flux density and μ_0 permeability of vacuum.

Mass on rotor outer radius m_{rot}^{oR} to be used in further structural simulations is found according to

$$m_{rot}^{oR} = m_{mag} + m_{yok} + m_{fixR}, \qquad (3)$$

where m_{mag} is the permanent magnet mass, m_{yok} rotor yoke mass and m_{fixR} constant lump sum mass of smaller structural fixing items and flanges for the rotor. It is considered that m_{fixR} is not dependent on the exact electromagnetic parameters and structural loading of the generator. The mass on stator inner electrical radius m_{stat}^{iR} is found according to

$$m_{stat}^{iR} = m_{con} + m_{lam} + m_{cprf} + m_{fixS}, \qquad (4)$$

where m_{con} is the conductor mass, m_{lam} lamination mass,

m_{cprf} cooling profile mass and m_{fixS} constant lump sum mass of smaller structural fixing items and flanges for the stator. It is considered that m_{fixS} is not dependent on the exact electromagnetic parameters and structural loading of the generator.

B. Structural Model

General description of the mechanical layout of the generator and corresponding beam model in ANSYS FEM software can be found in [15]. FEM model used in the simulation is given in Fig. 4. Time stepping method is used to realize all loading, while results are computed as stationary solutions. Mechanical behaviour of rotor and stator structures is assessed based on resulting deformations ε_{rot} and ε_{stat} and stresses σ_{rot} and σ_{stat}. For rotor only positive (maximum) and for stator only negative (minimum) deformation values in a cylindrical coordinate system are evaluated, as they describe most accurately closing of the generator air-gap. For stress characteristics, highest absolute value from the linear combination of direct stress and maximum local bending stress is used. Both stresses and deformations are kept within reasonable limits to avoid nonlinear effects of strain stiffening or unreasonable big air-gap deflections resulting in collision.

Fig. 4. FEM model of the generator.

C. Cost Model

Generator cost is approximated only based on the prices of active materials, as the investigation of exact relationship between the electromagnetic loading and needed structural mass is not considered to be part of the current research. In order to find the most optimal solution for the generator in terms of price, the cost of active materials p_{act} can be approximated as

$$p_{act} = p_{rot}^{act} + p_{stat}^{act}, \qquad (5)$$

where p_{rot}^{act} and p_{stat}^{act} are the active material costs for rotor and stator, respectively. For particular machine rotor active material cost can be found by

$$p_{rot}^{act} = p_{mag}m_{mag} + p_{yok}m_{yok} + p_{work}\left(m_{mag} + m_{yok}\right), \quad (6)$$

where p_{mag}, p_{yok}, and p_{work} are the specific costs of permanent magnets, rotor yoke and work done for assembly, respectively. For the generator under consideration, stator

active material cost is found according to

$$p_{stat}^{act} = p_{con}m_{con} + p_{lam}m_{lam} + p_{cprf}m_{cprf} +$$
$$+ p_{work}\left(m_{con} + m_{lam} + m_{cprf}\right), \qquad (7)$$

where p_{con}, p_{lam} and p_{cprf} are the specific costs of conductor, laminations and cooling profile, respectively.

Values for the specific costs (€/kg) of the materials used in cost approximation are described in Table II. Numbers are obtained as an average value of supplier quotations given for the actual parts of the prototype generator.

TABLE II. SPECIFIC MATERIAL COSTS.

Permanent magnets	56.5
Rotor yoke	5.0
Conductor	8.6
Laminations	1.6
Cooling profile	5.2
Assembly work	4.3

IV. OPTIMIZATION PROCEDURE

A. Preliminary Analysis of Optimality Criteria

In the case of complex multi-criteria optimization problems, the preliminary analysis of the optimality criteria and constraints is extremely important like pre-processing in FEM analysis. Preliminary theoretical analysis and simplification allows to avoid principal miscarriages in selection of optimization strategies, reduce computational time, complexity etc. [16]–[18].

The first question to be solved is the selection of objectives and constraints which can often be reformulated as "objectives vs. constraints", since certain characteristics can be often considered in form of an objective or a constraint. There are no unique rules available for latter task and the decisions should be made according to the character of each particular problem.

The objectives selected in the current study can be listed as: cost, efficiency and maximum values of four structural response characteristics (rotor deformation, stator deformation, rotor maximum stress, stator maximum stress). The most widely used approach - minimization of the strain energy density is not applied herein due to following considerations

− An attempt is made to control simultaneously both stiffness (max. strains) and strength (max. stresses) properties;
− In context of the current problem, the values of deformations are extremely important (in order to avoid collision) and an approach introduced allows for flexible separate handling of the characteristics.

The multi-criteria optimization problem described above can be formulated as:

$$\begin{cases} F\left(\overline{x}\right) = \left(F_C\left(\overline{x}\right), \dots, F_{SRn}\left(\overline{x}\right)\right) \to \min, \\ F_E\left(\overline{x}\right) \to \max, \end{cases} \qquad (8)$$

subjected to constraints:

$$\begin{cases} g_i\left(\overline{x}\right) \le g_i^*, \ i=1,\ldots,n_1, \\ h_j\left(\overline{x}\right) = h_j^*, \ j=1,\ldots,n_2, \end{cases} \qquad (9)$$

where $x_i \le x_i^*$, $x_{i*} \le x_i \le x_i^*$, $-x_i \le -x_{i*}$, $i=1,\ldots,n$, $F_c\left(\overline{x}\right)$ and $F_E\left(\overline{x}\right)$ stand for cost and efficiency, respectively. The objectives $F_{SR1}\left(\overline{x}\right),\ldots,F_{SRn}\left(\overline{x}\right)$ describe structural response of the construction (maximum rotor and stator deformations ε_{rot}^{max}, ε_{stat}^{max} and stresses σ_{rot}^{max}, σ_{stat}^{max}, characterizing stiffness and strength of the structure), $\overline{x}=[x_1,\ldots,x_n]$ is vector of design variables and g_i^*, h_i^*, x_{i*}, x_i^* are given constants.

The second question to be solved is the handling of multiple optimality criteria considered i.e. selection of optimization strategies. In order to compare and analyse optimality criteria, normalization should be performed, since the magnitudes and the units used to measure the objectives may be different. The objective functions subjected to maximum and minimum can be normalised by formulas (10) and (11) respectively:

$$f_E\left(\overline{x}\right) = \frac{\max F_E\left(\overline{x}\right) - F_E\left(\overline{x}\right)}{\max F_E\left(\overline{x}\right) - \min F_E\left(\overline{x}\right)}, \qquad (10)$$

$$f_{SRi}\left(\overline{x}\right) = \frac{F_{SRi}\left(\overline{x}\right) - \min F_{SRi}\left(\overline{x}\right)}{\max F_{SRi}\left(\overline{x}\right) - \min F_{SRi}\left(\overline{x}\right)}. \qquad (11)$$

Preliminary analysis performed for particular problem considered can be summarized as:

– The four structural response characteristics $f_{SRi}\left(\overline{x}\right)$ are not conflicting with each other and can be combined into one objective $f_{SR}\left(\overline{x}\right)$;

– The structural response characteristics and efficiency have conflicting character thus, the Pareto optimality concept can be applied to $f_{SR}\left(\overline{x}\right)$ and $f_E\left(\overline{x}\right)$;

– The small values of strains are safe, but the values nearing to the value of air-gap are critical i.e. risk is increasing with increasing value of the strains and this relation is not linear (higher order). Thus, the most widely used strategy for combining objectives – "weighted summation" is not satisfactory. The compromise programming technique can be employed, which provides that the larger distances from an ideal solution are penalized more than smaller distances $\left(c>1\right)$;

– The combined objective $f_{SR}\left(\overline{x}\right)$ and cost are not conflicting. The minimum value of the cost and $f_{SR}\left(\overline{x}\right)$ coincide. Thus, the cost as an objective can be omitted or combined with $f_{SR}\left(\overline{x}\right)$.

Finally, the posed optimization problem (8)–(9) can be reduced to minimization (due to normalization function (10) lower values of efficiency correspond to higher values in reality) of two objectives as

$$f\left(\overline{x}\right) = \left(f_E\left(\overline{x}\right), f_{SR}\left(\overline{x}\right)\right) \to \min, \qquad (12)$$

subjected to constraints given by (10). The combined objective $f_{SR}\left(\overline{x}\right)$ in (12) is defined as

$$f_{SR} = \left[\sum_{i=1}^{4}\left(w_i f_{SRi}\right)^c\right]^{1/c}, \qquad (13)$$

where $\sum_{i=1}^{4} w_i = 1$, $0 < w_i \le 1$.

In (13) the parameter $c \ge 1$ $i=1,\ldots,n$ and in the case of $c=1$, the compromise programming technique reduces to weighted summation technique. It can be noted that the reason, why the initial formulation of the optimization problem needs often improvement, is that large amount of theoretical and numerical analysis should be performed before corresponding decisions can be accomplished.

B. Design of Experiments

Full factorial experiment (FFE) technique is utilized to create numerous of electromagnetic configurations for optimization input with an aid of a spread sheet program. This enables to identify the effect each factor has on the response variables and also how different interactions between the factors influence the response variables [19]. Designs are created with nominal generator rotational speed, air-gap radius, ambient wind speed and same type NdFeB permanent magnets. In order to achieve comparable results, electrical output power P_{el} is kept constant while the required mechanical power P_{meh} varies due to the change in generator efficiency η. Consequently masses of required active material, total normal stress and torque are freely varying and can be used to investigate corresponding structural responses.

Number of factors k is selected to be 4: air-gap width g_{air}, magnet height h_m, magnet length l_m, and coil height h_c (see Table III). Based on the previous conducted research it is known that these factors have the highest influence on both the mechanical response of the support structure and efficiency of the generator. The number of levels n for each factor is set to be 3 in order to provide protection against potential nonlinearity in the factorial effects. It also enables to easily modify the method to perform further optimization with response surface modelling if desired. The dataset results in $3^4 = 81$ generator configurations.

TABLE III. FACTORS AND LEVELS USED IN FFE.

Factor	Symbol	Unit	Level 1	Level 2	Level 3
Air-gap width	g_{air}	mm	6	10	14
Magnet height	h_m	mm	18	22	26
Magnet length	l_m	mm	600	800	1000
Coil height	h_c	mm	14	18	22

C. ANN and HGA

Numerical modelling of the large scale structure considered, is extremely time consuming and complex task, even after simplifications introduced above (analysis of optimality criteria, key parameters selection, use of beam elements in FEM analysis, etc.). Furthermore, the

evolutionary algorithms in general and HGA need a huge number of function evaluations. For that reason the ANN and HGA are combined in optimization procedure. The response modelling is performed by employing feed forward ANN and the obtained mathematical model is used for evaluation of the four objective functions. The input and output data for ANN learning are gathered from FEM analysis. No unique rules are available in literature for determining the architecture of the ANN (should be configured for each particular problem). A criterion used in the current study is minimization of the mean square error (MSE), but the robustness of the network is also kept in mind. However, certain initial considerations about network architecture are needed for starting point and final decision. Review on methods to determine architecture of the ANN featured for function approximation is given in [20]. Hecht-Nielsen and others have proved that an ANN with a single hidden layer can approximate any continuous function to arbitrary accuracy on a compact set and an ANN with a two hidden layers can approximate any complex function to arbitrary accuracy [21]. By omitting the rules of thumb, the following formulas involving capacity of the training data are considered [20]:

$$N_h = \left(N_{in} + \sqrt{N_{tr}} \right) / L, \qquad (14)$$

$$N_h = C \left(N_{tr} / \left(N_{in} \log \left(N_{tr} \right) \right) \right)^{1/2}, \qquad (15)$$

where L is a number of hidden layers and N_{tr} the capacity of the training data, N_h, N_{in} stand for number of neurons in hidden and input layers, respectively. The expression (15) contains the parameter C, which should vary for determining N_h. For that reason, herein formula (14) is used as a starting point and the number of neurons in hidden layer is increased up to the upper bound determined by right hand side of the formula (15) (see [20])

$$N_h \leq N_{tr} / N_{in}. \qquad (16)$$

According to dataset size and (14) seven neurons in hidden layers are used as starting value in an ANN with two hidden layers. Next the number of neurons is increased by one until the MSE reaches a satisfactory level. Final configuration of the selected ANN, includes eight neurons, 5 and 3 in first and second hidden layers, respectively. ANN with one hidden layer was also considered. In that case the starting point and optimal configuration were found to include 13 and 14 hidden neurons, respectively. The ANN with two hidden layers and smaller number of neurons is used for design optimization. The hybrid genetic algorithm employed herein contains GA for global search and gradient method for local search. Local search is performed only for the individuals satisfying the following requirements:

− Individuals belong to first 15 % of population based on values of the fitness function;
− The distance between individuals is not less than given value (diversity condition).

The proposed HGA is less time consuming in comparison with traditional GA and also allows to overcome problems

with convergence to exact minimum (not near-minimum).

V. RESULTS AND DISCUSSION

In the following figures, output data are given in normalized form in order to retain collation determined by normalization and Pareto concept. In case of efficiency the lowest normalized values correspond to the highest non-normalized values as defined by (10). Results regarding the relation between efficiency and the structural response obtained from the DOE are depicted in Fig. 5. It can be seen that in general higher efficiencies tend to cause also higher stresses and deformations. This is to be expected, as stronger magnetic flux for the needed higher efficiency also tends to lead to larger normal stress values. But even for the higher efficiency values it is possible to keep the structural response close to the average value of entire population. In all of the efficiency ranges it is also possible to find bad designs with very high response values. Number of those configurations compared to general population is quite low and the overall spread of structural responses for a particular efficiency is not very high. The best efficiency values are obtained with large magnet thickness and length combined with medium to large air-gap and small coil thickness.
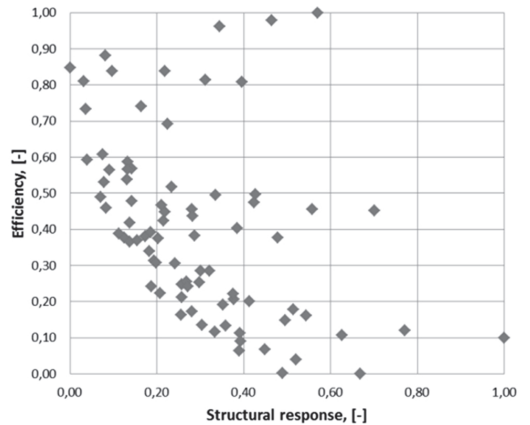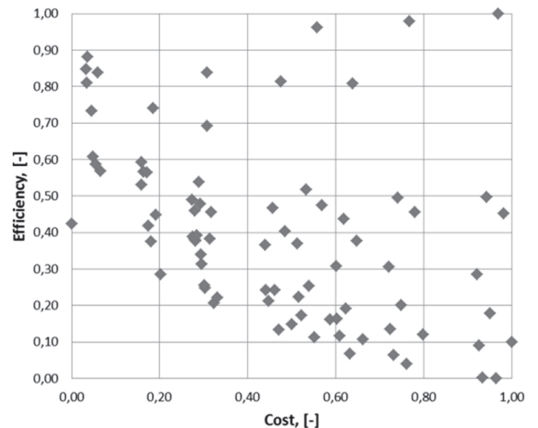

Fig. 5. Structural response vs. efficiency.

Fig. 6. Cost vs. efficiency.

Relation between the cost of active material and

efficiency depicted in Fig. 6, shows much clearer tendencies in the high efficiency area, although the overall scattering of design points is much larger. For cases with extremely high efficiency, the cost of active material cannot be kept low and a clear trade-off between the two variables exists. The higher the efficiency, the steeper the cost increase curve. For the medium high area, numerous designs with costs near the average values are possible. Due to large scattering, the possibility of having a bad design in terms of costs is higher. This is true for both high and low efficiency ranges and indicates that the relation between active material and air-gap needs to be carefully considered. It also has to be noted that some designs with over average efficiency and very low cost figures have to be discarded, as they are feasible only with the lowest air-gap value and even structural responses

slightly below average could cause an air-gap closure.

The Pareto front "structural response vs. efficiency" is depictured in Fig. 7. It can be seen that the increase rate of the efficiency is growing with decreasing values of the structural response. One possible/meaningful selection of the optimal solution in Pareto curve is (0.1; 0.5). In this point the structural response reached near possible minimum value and further improving structural response leads to extremely rapid increase (worsening) of the efficiency. The other interesting point in Pareto curve is (0.5; 0.11) where the efficiency reaches near ideal value and further improvement of the efficiency leads to rapid increase (worsening) of the structural response. The optimal set of design variables corresponding to selected points (0.1; 0.5), (0.5; 0.11) in Pareto front is presented in Table IV.
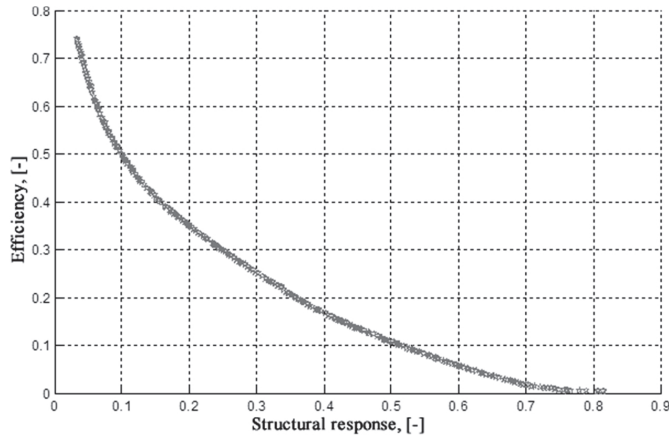

Fig. 7. Pareto front: structural response vs. efficiency.

TABLE IV. POSSIBLE OPTIMAL LAYOUTS.

Air-gap	Magnet thickness	Magnet length	Coil thickness	Comment
mm	mm	mm	mm	-
13.9	19.9	708	21.9	(0.1; 0.5) low resp, lower eff.
13.9	21.5	969	15.9	(0.5; 0.11) high eff., higher resp.

Thus, the Pareto front provides much more information in comparison to physical programming techniques. However, certain additional considerations are needed for selection of final design(s), as all solutions given by Pareto curve are optimal to some respect.

The relation between structural response and cost is found to be proportional as stated in section earlier. The cost as objective has been omitted from the multi-criteria optimization procedure. An alternate approach is to combine the cost with structural response $f_{SR}(\overline{x})$. However, it has been numerically verified, that including cost in combined objective has marginal impact on the final design.

VI. CONCLUSIONS

Current research has been performed on the Goliath Cyclos 16/3 generator. Novel optimization procedure is proposed to aid in the design procedure of an ultra large diameter permanent magnet generator. Specific features of

the proposed multi-criteria optimization procedure introduced include pre-design block for the analysis of optimality criteria and constraints, electromagnetic and structural modelling blocks. An analysis of the optimality criteria performed allows significant simplification of the initial optimization problem. The objective space is reduced from six to two.

An electromagnetic design tool together with a structural FEM model is used to generate multiple machine configurations at the same power level by varying magnet volume, generator axial length and air-gap width. Obtained structural responses, efficiencies and costs of the active material are used as an input for artificial neural networks to compose a mathematical response model of the machine. The optimization itself is realized by combining genetic algorithm with gradient method.

Performance characteristics of the objectives obtained during the DOE and optimization are evaluated against each other. The scattering of designs is larger for the "cost vs. efficiency" criteria, however also for the "structural response vs. efficiency" criteria it is possible to have so called bad designs and especially in the middle efficiency area.

REFERENCES

[1] H. Polinder, J. A. Ferreira, B. B. Jensen, A. B. Abrahamsen, K. Atallah, R. A. McMahon, "Trends in wind turbine generator systems", *IEEE Journ. of Emerg. and Select. Top. in Power Electr.*, vol. 1, no. 3, pp. 174–185, 2013.

[2] Z. Alnasir, M. Kazerani, "An analytical literature review of stand-alone wind energy conversion systems from generator viewpoint", *Renew. and* Sust. Energy Reviews, vol. 28, pp. 597–615, 2013. [Online]. Available: http://dx.doi.org/10.1016/j.rser.2013.08.027

[3] V. D. Colli, F. Marginetti, C. Attaianese, "Analytical and multiphysics approach to the optimal design of a 10-MW DFIG for direct-drive wind turbines", *IEEE Trans. on Industr. Electron.*, vol. 59, no. 7, pp. 2791–2799, 2012.

[4] C. Versteegh, "Design of the Zephyros Z72 wind turbine with emphasis on the direct drive PM generator", *Proc. of the Nordic Workshop on Power and Industrial Electronics,* Trondheim, 2004.

[5] G. Shrestha, H. Polinder, J. A. Ferreira, "Scaling laws for the direct drive generators in wind turbines", in *Proc. of IEMDC '09*, Miami, 2009.

[6] A. S. McDonald, M. A. Mueller, H. Polinder, "Structural mass in direct-drive permanent magnet electrical generators", *IET Renew. Pow. Gen.,* vol. 2, no. 1, pp. 3–15, 2008. [Online]. Available: http://dx.doi.org/10.1049/iet-rpg:20070071

[7] J. Kers, J. Majak, "Modelling a new composite from a recycled GFRP", *Mech. of Comp. Mat.,* vol. 44, no. 6, pp. 623–632, 2009. [Online]. Available: http://dx.doi.org/10.1007/s11029-009-9050-4

[8] H. Li, Z. Chen, "Design optimization and site matching of direct-drive permanent magnet wind power generator systems", *Renewable Energy,* vol. 34, no. 4, pp. 1175–1184, 2009. [Online]. Available: http://dx.doi.org/10.1016/j.renene.2008.04.041

[9] A. H. Isfahani, A. H. S. Boroujerdi, S. Hazanzadeh, "Multi-objective design optimization of a large-scale direct-drive permanent magnet generator for wind energy conversion systems", *Front. In Energy.,* vol. 8, no. 2, pp. 182–191, 2014.

[10] M. Pohlak, R. Kuttner, J. Majak, "Modelling and optimal design of sheet metal RP&M process", *Rapid Prototyping Journal,* vol. 11, no. 5, pp. 304–11, 2005. [Online]. Available: [Online]. Available: http://dx.doi.org/10.1108/13552540510623620

[11] J. Majak, M. Pohlak, M. Eerme, T. Velsker, "Design of car frontal protection system using neural networks and genetic algorithm", *Mechanika,* vol. 18, no. 4, pp. 453–460, 2012. [Online]. Available: http://dx.doi.org/10.5755/j01.mech.18.4.2325

[12] H. Herranen, O. Pabut, M. Eerme, *et al,* "Design and testing of sandwich structures with different core materials", *Materials Science=Medžiagotyra*, vol. 18, no. 1, pp. 1–6, 2012.

[13] K. Karjust, M. Pohlak, J. Majak, "Technology route planning of large composite parts", *Int. Jrn. Mat. Frm.*, vol. 3, no. 1, pp. 631–634, 2010. [Online]. Available: http://dx.doi.org/10.1007/s12289-010-0849-2

[14] A. Kallaste, T. Vaimann, O. Pabut, "Slow-speed ring-shaped permanent magnet generator for wind applications", *11th Int. Symp. Typical Problems in the Field of Electrical and Power Engineering,* Tallinn, 2012, pp. 66–69.

[15] O. Pabut, H. Lend, T. Tiirats, "Load sensitivity analysis of a large diameter permanent magnet generator for wind turbines", in *Proc. of the 9th Int. Conf. DAAAM Baltic Indust. Eng.* Tallinn, 2014, vol. 1, pp. 59–64.

[16] J. Majak, M. Pohlak, "Decomposition method for solving optimal material orientation problems", *Composite Structures,* vol. 92, no. 8, pp. 1839–1845, 2010. [Online]. Available: http://dx.doi.org/10.1016/j.compstruct.2010.01.015

[17] J. Majak, M. Pohlak, "Optimal material orientation of linear and non-linear elastic 3D anisotropic materials", *Meccanica*, vol. 45, no. 5, pp. 671–680, 2010. [Online]. Available: http://dx.doi.org/10.1007/s11012-009-9262-7

[18] J. Majak, S. Hannus, "Orientational design of anisotropic materials using the hill and Tsai-Wu strength criteria", *Mech. of Comp. Mat.,* vol. 39, no. 6, pp. 509–520, 2003. [Online]. Available: http://dx.doi.org/10.1023/B:MOCM.0000010623.38596.3e

[19] D. C. Montgomery, *Design and Analysis of Experiments.* New York: John Wiley and Sons, 1997, ch. 5.

[20] K. Gnana Sheela, S. N. Deepa, "Review of methods to fix number of hidden neurons in neural networks", *Math. Problems in Eng.,* vol. 2013, pp. 1–11, 2013. http://dx.doi.org/10.1155/2013/425740

[21] R. Hecht-Nielsen, "Theory of the back propagation neural network", *Proc. of Int. Joint Conf. on Neur. Net.*, 1989, vol. 1, pp. 593–608.

Paper 3

Pabut, O.; Kirs, M.; Lend, H.; Tiirats, T. Optimal Structural Design of a Slotless Permanent Magnet Generator. *In: Proceedings of the 10th International Conference of DAAAM Baltic Industrial Engineering: 12–13th May 2015, Tallinn, Estonia,* 1 – 7.

OPTIMAL STRUCTURAL DESIGN OF A SLOTLESS PERMANENT MAGNET GENERATOR

Pabut, O.; Kirs, M;. Lend, H. & Tiirats, T.

Abstract: *Most optimal mechanical layout of an electrical generator in a wind turbine is still under investigation. In current work, a novel lattice passed solution is presented together with corresponding design principles and optimization procedure. Finite element analysis and response surface modelling are used to create the mathematical model of the structure and carry out the design investigation and optimization. Generator layout is modelled at two turbine capacity levels and compared to a similar sheet metal structure. Results prove the suitability of the offered procedure and superiority of the lattice concept in terms of the generator structural mass.*
Key words: Design optimization, lattice structure, response surface modelling, permanent magnet machine.

1. INTRODUCTION

Wind energy sector has gone through a rapid commercial and technical revolution during past decades [1]. For many sub-systems clear technical standardization has taken place, while the concept of the most beneficial electrical generator is still under investigation [2]. Direct-drive generators have been gaining popularity but in terms of machine cost they are still inferior to the established combination of a double-fed induction generator and a gearbox [3]. Researchers have indicated that optimization and component integration of these machines could lead to a considerably lower energy cost, while keeping their known advantages [4]. Most of the cost and heavy mass of these units

can be attributed to the mechanical carrier structure of the machine [5].

Goal of the current work is to develop design principles and optimization procedure for a new type of mechanical carrier structure for a permanent magnet (PM) generator. Utilization of now available computational power together with various software tools and methods, including finite element modelling (FEM) and response surface modelling (RSM), is used to create the mathematical model of the generator structure. For comparison purposes two alternative mechanical structures are investigated to prove the superiority of the lattice concept against the more common sheet metal solution.

2. GENERATOR MODEL

2.1 Electromagnetic layout

Basic parameters of a direct drive generator are primarily determined by the wind turbine where the generator is used. The power P available in the wind for a wind turbine with given blades can be found according to [6]:

$$P = \frac{1}{2}\rho_{air}\pi r^2 v_{wind}^3 C_p, \qquad (1)$$

where ρ_{air} is the air mass density, r is the turbine rotor radius, v_{wind} is the given wind speed and C_p is the power coefficient. Rotational speed of the turbine is given as:

$$\omega = \frac{v_{tip}}{r}, \qquad (2)$$

where v_{tip} is the blade tip speed and ω is the rotational speed of the machine. Torque

resulting from the power and rotational speed is defined according to:

$$\tau = \frac{P}{\omega}. \qquad (3)$$

By combining equations (1), (2) and (3), torque of the turbine system can be expressed as:

$$\tau = \frac{\rho_{air}\pi r^3 v_{wind}^3 C_p}{2 v_{tip}}. \qquad (4)$$

In order to convert the kinetic energy of the wind into electrical energy, the used generator has to be able to produce equal torque [7] described by:

$$\tau = 2\pi\sigma_{tan}R^2 l, \qquad (5)$$

where σ_{tan} is the tangential component of Maxwell stress, R generator air-gap radius and l generator axial length. Value of σ_{tan} for a generator with defined electromagnetic configuration is a rather constant value over a large range of capacities and is given as [8]:

$$\sigma_{tan} = \frac{1}{2}A_s B_n cos\varphi, \qquad (6)$$

where A_s is the linear current density, B_n normal direction air-gap flux density and $cos\varphi$ is the power factor between active and apparent power. Air-gap flux depends largely on the chosen electromagnetic circuit of the machine. In present work concept developed by Kallaste [9] is utilized with air-gap windings and iron in the stator yoke leading to a magnetic flux density around 0.5 T. Allowed linear current density is limited by the heat dissipation properties of the machine. For passively cooled generators, values leading to high efficiencies range between 40 kA/m and 50 kA/m [10].

For a given generator type the most economic layouts in terms of active material vs. efficiency vs. acting forces are achieved at a constant electromagnetic aspect ratio k_a determined according to:

$$k_{a=}\frac{l}{R} . \qquad (7)$$

Based on previous research, value 0.125 is chosen for the particular machine [11]. By combining equations (5) and (7) the generator air-gap radius is expressed as:

$$R = \sqrt[3]{\frac{\tau}{2\pi\sigma_{tan}k_a}} . \qquad (8)$$

In order to assess the mechanical designs of machines in equivalent frame of reference, their electrical designs should fulfil certain similarity criteria. Following relative dimensions for the generator active components have been found to be most optimal in terms of cost vs. efficiency:

$$k_p = \frac{w_m}{w_p} = 0.65, \quad k_w = \frac{h_y}{w_p} = 0.32,$$

$$k_{mag} = \frac{h_m}{h_y} = 0.44, \quad k_{coil} = \frac{h_c}{h_y} = 0.29, (9)$$

where k_p is the magnet width and pole pitch ratio, w_m is the magnet width, w_p is the pole pitch, k_w is the total air-gap ratio to the pole pitch, h_y is the total air-gap height, k_{mag} is the magnet height ratio to the air-gap, h_m is the magnet height, k_{coil} is the coil height ratio to the air-gap and h_c is the coil height.
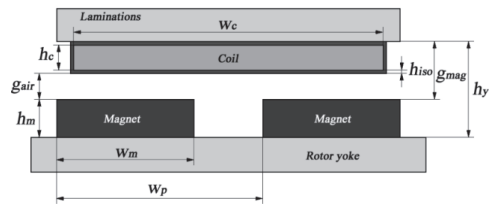

Fig. 1. Air-gap layout and parameters

For simplification purposes magnet length l_m is taken to be equal to the axial length l of the machine. Main parameters of the active components are described in Fig. 1. As common practice the value of generator mechanical air-gap g_{air} is predefined according to allowable mechanical deformations and assembly precision.

Magnet height h_m as a function of air-gap flux density can be found according to [12]:

$$h_m = \frac{B_n \mu_{rm} g_{eff}}{B_{rm}}, \qquad (10)$$

where μ_{rm} is the relative permeability of the PM material, B_{rm} is the remanent flux density of the magnet and g_{eff} is the effective air-gap. As the machine has no slots and coil units are located in the air-gap following simplification can be made:

$$g_{eff} = h_y + 2h_{iso}, \qquad (11)$$

where h_{iso} is the isolation layer height around the winding. Combining equations (9), (10) and (11) leads to:

$$h_m = \frac{g_{air} + 2h_{iso}}{\left(\frac{B_{rm}}{B_n \mu_{rm}} \cdot \frac{k_{coil}}{k_{mag}} - 1\right)}. \qquad (12)$$

Based on the above described similarity criteria and principles given in [9] two generator layouts with different capacities are defined and presented in Table 1.

Electrical power	P_{el}	MW	3	1
Rated wind speed	v_{wind}	m/s	11	11
Power coefficient	C_p	-	0.48	0.48
Rated tip speed	v_{tip}	m/s	81.5	81.5
Rotational speed	ω	rpm	15.3	26.5
Torque	τ	kNm	1983	385
Air-gap radius	R	m	6.3	3.65
Air-gap width	g_{air}	mm	11.5	8.5
Flux density	B_n	T	0.5	0.5
Current density	A_s	kA/m	40	40
Efficiency	η	%	94.5	93.5
Magnet height	h_m	mm	22	17.5
Magnet width	w_m	mm	100	79.5
Magnet length	l_m	mm	800	460
Magnet flux density	B_{rem}	T	1.34	1.34
Coil height	h_c	mm	14.5	11.5
Coil width	w_c	mm	200	160
Coil length	l_c	mm	1000	620

Table 1. Used generator layouts

2.2 Structural layout

Design of the mechanical carrier structure for a PM generator is in general driven by the allowable air-gap deflection. For machines with high flux densities

$(B_n = 1.1$ T) and large aspect ratios $(k_a > 0.4)$ well studied mechanical layouts can be found from literature. These structures are made up from thin walled $(0.001R$ to $0.0025R)$ discs, structurally profiled spokes, support arms and stiffness ribs [2]. For generator's with ultra large radiuses and small air-gap flux densities, more complicated solutions with pre-stressed tension rods and air-gap bearings have been employed [13]. One option not considered in the available literature is the utilization of a lattice structure. This has been used in bridge and crane structures for centuries and is generally characterized by its light weight, high loading capacity and high stiffness to length ratio [14], which makes it a good candidate for an optimal structural concept.
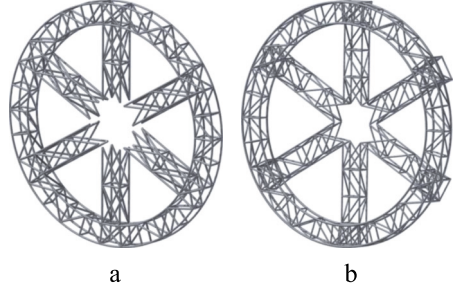

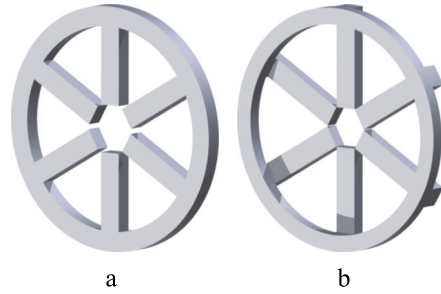Fig. 2. Layout of the lattice rotor (a) and the lattice stator (b)

Fig. 3. Layout of the sheet rotor (a) and the sheet stator (b)

Principle layouts of the employed lattice configurations for rotor and stator are depicted in Fig. 2a and Fig. 2b, respectively. In order to have a more direct

comparison to a sheet structure with similar size a corresponding sheet model is developed and analysed in parallel. Principle layouts of the rotor with internal support arms and stator with cantilever support beams are shown in Fig. 3a and Fig. 3b, respectively.

2.3 Mathematical model of the structure

Direct-drive generators with sheet metal structures are well studied and analytical formulas have been developed to determine the air-gap deflections for regular mechanical layouts [5]. As lattice structure has so far not been utilized for a generator, no ready-made analytical tools are available. It is possible to use known truss calculation methods like Maxwell-Cremona diagram for determining the internal forces and deflections of the members. In current study, FEM in conjunction with RSM technique is used to compose the mathematical models for different support structures. RSM technique is a combination of mathematical and statistical methods, which allows composing an objective function based on learning data. The obtained functions are represented by certain degree polynomial models. In current work quadratic model is used with following general form [15]:

$$Y = \beta_0 + \sum_{i=1}^{k} \beta_i X_i + \sum_{i=1}^{k} \beta_{ii} X_i^2 + \\ + \sum_i \sum_j \beta_{ij} X_i X_j, \qquad (13)$$

where Y is the measured response, k is the number of factors, β_0, β_i, β_{ii} and β_{ij} are the regression coefficients for intercept, linearity, square and interaction and X_i and X_j are the independent design variables. In present paper the procedure is carried out in *Design Expert 9* software environment.

Full factorial experimental (FFE) method is employed to create the initial population of designs for RSM. For both structure configurations the number of factors k is selected to be 4 and the number of levels n for each factor is set to be 5. As the sheet and lattice structures are different in nature, the used factors vary between the structure

types. Factors and their limit values are depicted in Table 2. General structural variables and variables specific for the sheet structure are described in Fig. 4a and variables used for the lattice structure in Fig. 4b.
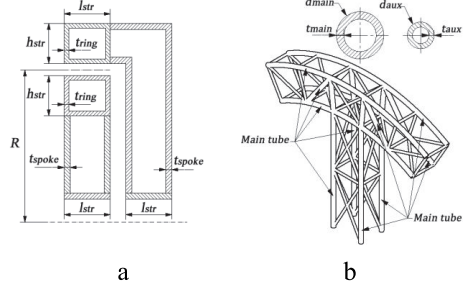

a   b

Fig. 4. General and sheet variables (a) and lattice structure variables (b)

For both of the structure types, the height of the rotor and stator rings h_{str} is varied as a state variable defined by:

$$h_{str} = k_{str} l_{str}, \qquad (14)$$

where k_{str} is the structure aspect ratio and l_{str} is the structure axial length.

Lattice structure bracing is subjected to following dependencies in order to keep the number of variables in a reasonable limit:

$$d_{aux} = 0.7 d_{main}, \quad t_{aux} = 0.5 t_{main}, \quad (15)$$

where d_{aux} is the bracing tube diameter, d_{main} is the main tube diameter, t_{aux} is the bracing tube wall thickness and t_{main} is the main tube wall thickness.

Calculations to compose the learning data are carried out on a parametric geometrical computer aided design model in *ANSYS Workbench* software. General description of the applied loads and the corresponding beam model can be found in [16].

3. OPTIMIZATION PROCEDURE

Generator structural mass $F_m(\bar{x})$ is chosen as an objective subjected to minimization while the air-gap deformation ε is defined

Factor	Symbol	Unit	3 MW lattice	3 MW sheet	1 MW lattice	1 MW sheet
Structure axial length	l_{str}	mm	700-1300	700-1100	400-700	385-585
Structure aspect ratio	k_{str}	-	0.7-1.3	0.5-0.9	0.7-1.3	0.5-0.9
Main tube diameter	d_{main}	mm	110-150	-	30-50	-
Main tube wall thick.	t_{main}	mm	10-18	-	4-8	-
Spoke sheet thick.	t_{spoke}	mm	-	6-18	-	4-10
Ring sheet thick.	t_{ring}	mm	-	6-18	-	4-10

Table 2. Factors and levels used in the FFE

as a constraint. Therefore, the optimization problem can be formulated:

$$F_m(\bar{x}) \rightarrow \min, \qquad (16)$$

subjected to linear constraints applied to the design variables vector $\bar{x}$:

$$x_i \leq x_i^*, \quad -x_i \leq x_{i*}, \quad i = 1, \dots, n, \quad (17)$$

and non-linear constraint applied to the sum of rotor and stator air-gap deflections ε^{max} as:

$$\varepsilon^{max}(\bar{x}) \leq \varepsilon^*, \qquad (18)$$

where indexes * in (17) and (18) refer to upper limit value of the variable.

For regular slotted generators the allowable air-gap deflection is in most cases fixed to 10% of the initial air-gap value, as larger deflections would result in unreasonable changes to flux densities and generated electromagnetic force. The machine under investigation has air-gap windings and as a result, the magnetic air-gap g_{mag} (see Fig. 1) and mechanical air-gap g_{air} are not equal. Consequently, the generator is electromagnetically less sensitive towards mechanical air-gap deformations. Therefore, a double criterion is applied to the deformations in order to allow for sufficient flexibility and guarantee both mechanical and electrical safety:

$$\varepsilon^{max} \leq 0.12 g_{mag}, \quad \varepsilon^{max} \leq 0.3 g_{air}, \quad (19)$$

As the stator is designed in a cantilever form and rotor is supported from both sides, rigidity of the rotor can be achieved with smaller weight penalty. The allowable deformations for rotor ε_{rot}^{max} and stator

ε_{stat}^{max} are found according to:

$$\varepsilon_{rot}^{max} = 0{,}25\varepsilon^{max}, \varepsilon_{stat}^{max} = 0{,}75\varepsilon^{max}. \quad (20)$$

Even though stress is observed as one of the outputs during the FFE, initially no criterion is applied to the resulting stresses. As the optimization is against single criteria with applicable constraints, no normalization of the inputs or outputs is necessary.

4. RESULTS AND DISCUSSION

Optimal configurations of the structures with respect to the criteria described in (19) and (20) together with corresponding values of the coefficient of determination for deformation (R_{def}^2) are listed in Table 3. At 3 MW level, total masses of the different generators are almost equal in terms of weight and for the 1 MW level, the lattice concept is about 17% lighter. Selection of the stiffness criteria was based on an assumption that structures designed for high rigidity are also optimal in terms of ultimate strength and fatigue resistance [17]. Evaluation of the determined optimal solutions against fatigue, linear buckling and additional tower top accelerations revealed this to be untrue. Found encumbrance can be mostly attributed to the fact that rigidity of such a large structure is a global property, while fatigue and buckling problems depend on local topology. For each structure type not compliant with the applied set of requirements, another optimization run was conducted with additional design criteria for maximum stresses and minimum load multiplier for buckling. The achieved results are presented in Table 4.

Factor	Unit	3 MW lattice		3 MW shell		1 MW lattice		1 MW shell	
		Stator	Rotor	Stator	Rotor	Stator	Rotor	Stator	Rotor
Structure ax. length	mm	700	1234	700	700	400	400	385	385
Aspect ratio	-	1.04	1.30	0.88	1.30	1.00	1.30	0.54	1.01
Deformation	mm	2.5	0.85	2.5	0.85	2.0	0.55	2.0	0.47
Stress	MPa	54	43	83	59	80	54	106	60
Part mass	t	16.85	13.74	15.77	13.64	2.22	2.08	2.79	2.38
Generator mass	t	30.59		29.41		4.30		5.17	
R^2_{def}	-	0.995	0.997	0.980	0.980	0.987	0.991	0.965	0.986

Table 3. Optimization – stiffness criteria

Factor	Unit	3 MW lattice		3 MW shell		1 MW lattice		1 MW shell	
		Stator	Rotor	Stator	Rotor	Stator	Rotor	Stator	Rotor
Structure ax. length	mm	700	1000	700	700	400	400	385	385
Aspect ratio	-	1.04	1.30	0.50	1.30	1.08	1.13	0.50	1.17
Deformation	mm	2.5	0.85	2.4	0.85	1.57	0.55	2	0.47
Stress	MPa	54	43	70	55	60	50	113	50
Mass	t	16.85	13.74	19.32	14.68	2.80	2.38	3.33	2.54
Generator mass	t	30.59		34.00		5.18		5.87	

Table 4. Optimization – stiffness, fatigue and buckling criteria

With the additional criteria the lattice generator is 10% lighter at 3 MW level and 12% lighter at 1 MW level. For lattice stators, smallest allowed axial lengths and aspect ratios around 1 lead to low weight structures. This is mainly caused by the cantilever nature of the stator, where additional overhang due to the increased axial length leads to large deformations. Increasing the aspect ratio beyond 1 does not yield any benefits, as the bending is mostly seen in the stator spokes. For the lattice rotors, higher aspect ratios are preferable as the angles of diagonal bracings are turned into better alignment with the vectors of normal stress. Similar phenomenon can be seen for the shell rotor and stator aspect ratios and axial lengths.

5. CONCLUSIONS

Analytical equations and optimization procedure are proposed for designing a PM generator with a novel type of carrier structure. Similarity criteria for a slotless air-gap winding generator are introduced and used to define two generator electromagnetic configurations at different power levels. The resulting loads and mechanical parameters are used as an input to set up a lattice type carrier structure for the generator and to compare it to a more common sheet metal solution. Due to the complex geometry of the lattice design, RSM approach is used to create the analytical models for both structure types with the aid of FEM. Obtained results are used as an input for RSM with quadratic curve fitting to optimize the structural mass for both concepts. Based on the process and achieved outcome it is concluded that:

• RSM with quadratic fitting can be used to predict the structural behaviour of generator support structures;

• when considering only stiffness criteria, conclusion regarding optimality of a generator structural concept cannot be made;

• if stiffness, fatigue, buckling and tower top acceleration criteria are considered, lower structural weights can be obtained with the lattice concept;

• stiffness criteria can be used for initial definition of the described generator structure, however fatigue resistance criteria has to be applied either simultaneously or as a next step in the optimization procedure.

6. REFERENCES

[1] Manwell, J. F., McGowan, J. G., Rogers, A. L. *Wind Energy Explained: Theory, Design and Application.* Wiley, Chichester, 2009.

[2] Stander, J. N., Venter, G., Kamper, M. J. Review of Direct-Drive Radial Flux Wind Turbine Generator Mechanical Design. *Wind Eng.,* 2012, **15**, 459-472.

[3] de Vries, E. Wind Turbine Drive Systems: A Commercial Overview. In *Electrical Drives for Direct Drive Renewable Energy Systems* (Mueller, M. and Polinder, H. eds). Woodhead, Oxford, 2013, 139-157.

[4] Bang, D., Polinder, H., Shrestha, G., Ferreira, J. A. Possible Solutions to Overcome Drawbacks of Direct-Drive Generator for Large Wind Turbines. *Proc. EWEC 2009*, 2009, 1-10.

[5] McDonald, A. S. Structural Analysis of Low Speed, High Torque, Electrical Generators for Direct Drive Renewable Energy Converters. *Ph. D. Dissertation,* Edinburgh University, 2009.

[6] Polinder, H., de Haan, S. W. H., Dubois, M. R., Slootweg, J. G. Basic Operation Principles and Electrical Conversion Systems of Wind Turbines. *EPE Jour.,* 2005, **15**, 43-50.

[7] McDonald, A. S., Mueller, M. A., Polinder, H. Structural Mass in Direct-Drive Permanent Magnet Electrical Generators. *IET Renew. Pow. Gen.,* 2008, **2**, 3-15.

[8] Polinder, H. Principles of Electrical Design of Permanent Magnet Generators for Direct Drive Renewable Energy Systems. In *Electrical Drives for Direct Drive Renewable Energy Systems* (Mueller, M. and Polinder, H. eds). Woodhead, Oxford, 2013, 30-50.

[9] Kallaste, A. Low Speed Permanent Magnet Slotless Generator Development and Implementation for Windmills. *Ph. D. Dissertation,* TUT, Tallinn, 2013.

[10] Pyrhonen, J., Jokinen, T., Hrabovcova, V. *Design of Rotating Electrical Machines*. Wiley, Chichester, 2008.

[11] Pabut, O., Eerme, M., Kallaste, A., Vaimann, T. Multi-Criteria Design Optimization of Ultra Large Diameter Permanent Magnet Generator. *Int. Conf. Elect. 2015 15-17 June*, 2015.

[12] Li, H., Chen, Z. Design Optimization and Comparison of Large Direct-Drive Permanent Magnet Wind Generator Systems. *Proc. Int. Conf. on Elec. Mach. and Sys.*, 2007, 685-690.

[13] Gordon, P. Aspects of, and New Approaches to, the Design of Direct Drive Generators for Wind Turbines. *Ph. D. Dissertation,* University of Durham, 2004.

[14] Cheng, B., Qian, Q., Sun, H. Steel Truss Bridges with Welded Box-Section Members and Bowknot Integral Joints. *Jour. of Const. Steel Research*, 2013, **80**, 465-474.

[15] Montgomery, D. C., *Design and Analysis of Experiments*. Wiley, New York, 1997.

[16] Pabut, O., Lend, H., Tiirats, T. Load Sensitivity Analysis of a Large Diameter Permanent Magnet Generator for Wind Turbines. *Proc. of the 9th Int. Conf. DAAAM Baltic Indust. Eng. Tallinn*, 2014, **1**, 59-64.

[17] Cervellera, P., Zhou, M., Schramm, U. Optimization Driven Design of Shell Structures Under Stiffness, Strength and Stability Requirements. *Proc. of 6th WCSMO,* 2005.

7. ADDITIONAL DATA ABOUT AUTHORS

MSc. Ott Pabut
TUT, Department of Machinery
Ehitajate tee 5, 19086 Tallinn, Estonia
Phone: +372 51 644 57,
E-mail: ott.pabut@ttu.ee
http://www.ttu.ee

Paper 4

Tiirats, T.; **Pabut, O.**; Kallaste, A.; Herranen, H.; Naar, H.; Vaimann, T. Analysis of Mechanical Vibrations Caused by Eccentricity in a Slow-Speed Slotless Permanent Magnet Generator. *In: Electric Power Quality and Supply Reliability Conference PQ 2014: 11–13th June, Rakvere, Estonia,* 237 – 241.

Analysis of Mechanical Vibrations Caused by Eccentricity in a Slow-Speed Slotless Permanent Magnet Generator

Tauno Tiirats, Ott Pabut, Ants Kallaste, Henrik Herranen, Hendrik Naar, and Toomas Vaimann

Abstract— **This paper focuses on the analysis of mechanical vibrations caused by different eccentricities in the rotor of a slow-speed slotless permanent magnet generator. The analysis of different eccentricities and their influences was carried out on a full scale laboratory test machine. Three most common mass center dislocation faults of a generator rotor that can occur in the production phase of the machine were investigated: asymmetrical rotor weight distribution, none coaxiality of rotor and stator, dislocated rotor. The analysis was conducted to obtain information on how different eccentricities influence vibrations and how to take this into account in production. Mentioned cases were chosen as they represent most common eccentricity faults caused by mistakes in production and assembly. Vibration measurements were carried out by non-contact optical measurement system. The measurement procedure and process are described in the paper as they are a crucial part of the analysis. The obtained results show that additional mechanical vibrations depend on the relation between eccentricity types. In addition, it was identified that rotor rotational speed affects the vibration amplitudes only slightly and the rate of influence is also dependent on the eccentricity type. Dynamic eccentricity was found to be the most dangerous case compared to the others.**

Index Terms— **Mechanical vibrations, eccentricity, slotless permanent magnet generator, non-contact optical measurement.**

I. Introduction

Multiple electrical generator types are used in modern day wind turbines [1]. One of the options is a slow-speed slotless permanent magnet generator [2]. It has many positive aspects, for example no need for gearbox, light weight and no cogging torque [3].

Producing this kind of a generator is straightforward and low-cost, but mentioned machine has a large radius and is relatively thin. It is expected that problems could occur due

to the eccentricity issues rising from the low mechanical stiffness of the generator construction in axial direction. Direct outcome of the eccentricity faults is a change in operational parameters of the generator such as the induced voltage waveform and output current [4]. Less investigated effects are the mechanical stress acting on the machine and possible air-gap closing. Low stiffness of the generator makes possible eccentricity an important issue to take into account during the design process.

As soon as rotor eccentricity appears, additional loads are generated in the machine. These loads are represented by excessive mechanical vibrations. The vibrations affect the bearings lifetime and fatigue strength of the generator. In the worst case it can lead to rotor-stator rub or air-gap closure that can destroy the whole machine.

Current work investigates different cases of eccentricities from the structural side in a slow-speed slotless permanent magnet generator. A more thorough understanding of mechanical vibrations that are caused by eccentricity problems is presented. Paper is used to further optimize the generator by analyzing the dangerous situations that could be caused by different eccentricity faults.

II. Problem Statement

Air-gap eccentricity is mainly caused by mistakes in the assembly procedure or inaccurate manufacturing. Therefore, usually these types of mistakes are present already in the first run of the generator and can be discovered by machine diagnosis [5], [6] and eliminated when necessary. Eccentricities that are caused by working state are less common, but may be present due to increased wear or incorrect fatigue calculations [7]. Fig. 1 shows possible types of air-gap eccentricities: healthy machine (a), static eccentricity (b), elliptic eccentricity (c) and dynamic eccentricity (d). Only the basic center dislocation faults are investigated. That means elliptic eccentricity is discarded from this analysis and replaced with asymmetrical weight distribution situation. All these faults can occur during production phase by wrong assembly procedure, too big tolerances or uneven mass distribution in the parts. Type and relative size of the fault greatly influences whether the machine is still able to operate the required period with required parameters.

Generator can be optimized by knowing and considering the eccentricity caused faults. Vibration calculations in finite element method (FEM) software can be used for generator optimization and for prediction of eccentricity effects on similar structures.
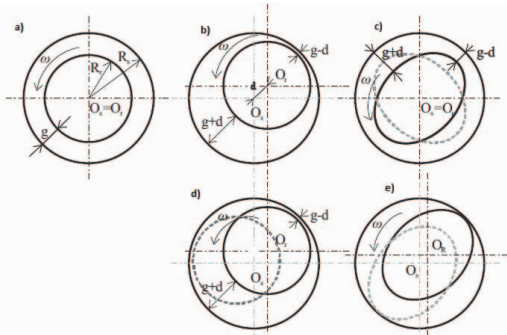
Fig. 1. Type of eccentricities of an electrical machine. a) healthy machine, b) static , c) elliptic, d) dynamic and e) mixed eccentricity [4] (O$_r$ and O$_s$ are rotor and stator symmetry centers, g is the width of the air-gap and d represents the eccentricity magnitude).

III. TEST SETUP

All described fault situations were achieved by modifying the machine in a way that rotor or its mass center is shifted 1 mm from original position. This value was chosen because the air-gap of the prototype machine is 2.5 mm and bigger eccentricity could risk damaging the machine. Smaller might not give clear results as the inherent level of static or dynamic eccentricity is typically within 10% of the air-gap [8], [9].

Asymmetrical weight distribution was achieved by adding certain mass to the rotor spoke with a certain distance in a manner that the mass center shifts 1 mm from the rotor's center.

Static eccentricity, known as none coaxiality of rotor and stator, was achieved by lowering the stator yoke, regarding to the rotor by 1 mm.

Dynamic eccentricity, known as dislocated rotor, was achieved by lowering the rotor 1 mm, regarding to the shaft and stator axis, see Fig. 1).

All cases were investigated at three different rotational speeds: 115 rpm – half the speed of nominal speed, 230 rpm – nominal working situation and 290 rpm – little over the maximum allowed speed of 280 rpm. First, healthy machine vibrations were measured and later results from faulty situations were obtained and compared to the healthy machine in order to cancel out the error caused by prototype's own structural peculiarities.
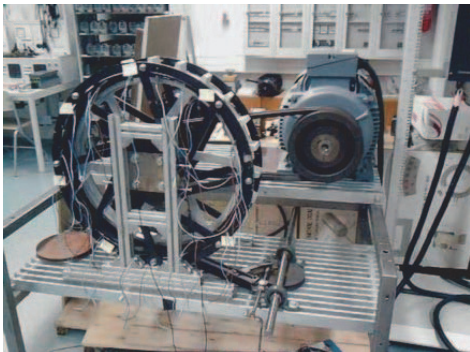

Fig. 2. Generator in the test-bench.

Tests were carried out on a full scale laboratory test machine [2]. It was connected to a heavy metal desk via specially made stand and turned by a 30 kW induction motor. Fig. 2 shows the testing machine attached to the stand and the external drive. Generator was not electrically loaded, so in actual working condition results are different and should be investigated in the future.

IV. TESTING AND RESULTS

Measurements were carried out with a non-contact optical measurement system PONTOS [10]. These systems are widely spread in automotive, aviation and space industries and are proven to be a reliable alternative for conventional displacement measuring systems and accelerometers. The method was chosen instead of standard acceleration sensors because no modification of test machine is necessary, it is easy to prepare the machine for measurements and multiple measurement points can be chosen. Preciseness with this method was enough for needed analysis, although results showed that for more thorough analyses like fast Fourier transform (FFT) bigger frame rate is needed.

The machine was covered with approximately 100 measuring points that were marked with reflector stickers like shown on Fig. 3. These points were distributed evenly around the stator ring, around the rotor ring and on the stand. Four separated points were marked on a nearby separated object, to get fixed reference points for later analyses. Fig. 3 shows how each point is identified by the PONTOS software.
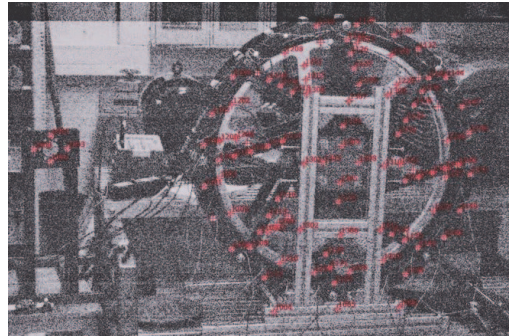

Fig. 3. Measuring points identified by the PONTOS software.

In optical measurements, camera should cover all the points in each measuring stage, but with current structure stator spokes block some of the points from the camera during rotation. Therefore, in post processing of rotor results, usage of interpolation was needed. Additionally, some small loose moving objects, like wires, might block the measuring reflector and ruin the data for that point. In that case the point data is not reliable and cannot be used for analysis.

Preciseness of the measurements was 0.011 mm, which was achieved by exact calibration procedure. PONTOS measures displacements in camera based Cartesian coordinates. For post processing results were transferred to cylindrical coordinates because of rotational movement and ring shaped air-gap. Coordinate's origin was set in the center of the stator ring by using stator's measuring points.

Optical motion measuring is a good solution to measure this kind of a generator because of multiple data points, good accessibility and no modification needed solution. Big diameter and open construction allows reasonable access to the rotor for the camera.

It was estimated that the biggest motion will be on the outer ring of stator and rotor. Main force for excessive motion comes from rotor that is turning with a certain speed. Therefore, it is reasonable to assume that transition of measurement points takes place with certain frequency and moves according to a sine function that is determined by the rotational speed.

Results show that it is true for the rotor, but not so clear for the stator. Both structure elements are analyzed separately. Motions in axial and radial directions, during half a second period, are investigated. Cylindrical coordinates are used due to suitability with generator structure.

A. Stator

Measurements showed that stator vibrations were low and they were not influenced by rotor rotation directly. Fig. 4 shows measurement results for 230 rpm with dynamic eccentricity. Four points are selected to represent points with the lowest vibrations (1112 and 1138) and points with highest vibrations (1130 and 1119) on the generator. Even though the figure contains two full rotations we cannot distinguish any kind of waveforms. Probably the stator was responding to the rotation movement of dislocated rotor, but the effect is very low and gets lost in the high frequencies with low amplitudes that are caused by multiple different structural parts in the machine. Different parts have different vibration modes and when combined, they give a complex sum of vibrations. These vibrations can be determined by FFT analyses, but more dense data is needed and it is not in the scope of current research.
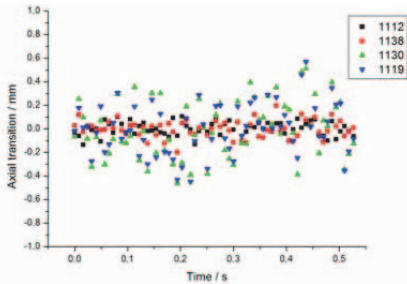

Fig. 4.   Stator measurement results for 230 rpm with dynamic eccentricity.

All cases with different speeds show similar results. There is no significant difference between different speeds and eccentricity situations. Highest axial vibrations stay between –0.8 to 0.8 mm. Also, healthy machine results were varying in the same area. This shows that there is no direct influence between rotor eccentricities and stator vibrations for this machine. Motion in radial direction stayed under 0.1 mm, which shows no big forces were applied to the stator in radial direction.

One cause for so low amplitudes can be the stiffness of the stand. Compared to the wind turbine conditions, test bench has extra fixing points. It is made in a way that it does not allow excessive movement in radial direction. In axial direction, movement should be apparent, but pretension and profile stiffness of the supporting frame can be high enough to cancel out the excessive vibrating effect. Also, bearings can muffle a lot of rotor movement. This is a good case for structure fatigue, but vibration effect on bearings should be investigated further.

All in all, it shows that investigated eccentricity situations do not affect stator and do not pose any danger to the stator itself. Stator can be looked as one solid part of the machine.

B. Rotor

Rotor measurements provide more interesting results. It is clear that the rotor has a direct influence from the eccentricity and being made from thin metal sheet, it is apparent in the results. Nonlinear regression method is used to investigate rotor vibrations. Sine function curve is fitted onto the captured data.

On Fig. 5 movement of four equally spaced healthy machine points in axial direction during two full rotations with nominal speed is presented. These vibrations can be looked as movements that are present always with this kind of structure and assembly procedure. It is taken as a base (ZERO) for different eccentricity comparisons.
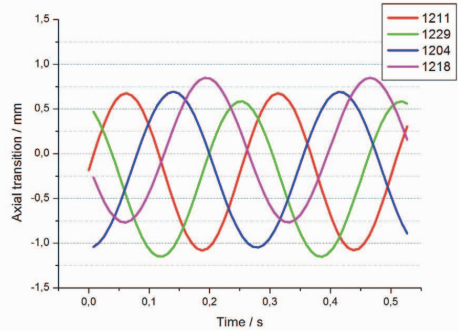

Fig. 5.   Healthy machine rotor measurement points movement in axial direction while working with nominal speed.

All fault cases with the speed of 230 rpm were investigated and results are presented in Fig. 6. It is clear that each type of eccentricity affects the dominating vibration mode by increasing the amplitude as shown in Table I. Extra mass fault (EMAS) and static eccentricity (STAT) have a small influence, but dynamic eccentricity (DYN) has a mayor influence. Rotor ring moves in axial direction about 2.14 mm more than in a healthy situation. This should not significantly affect the electrical side of the generator, but it shortens the lifetime of bearings and rotor structure remarkably. Comparing the differences with mass center dislocation fault, which is around 0.42 mm, it is clear that dynamic eccentricity is the most dangerous situation for this kind of generator. Other eccentricities have significantly smaller influence.
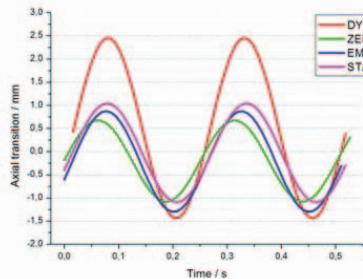

Fig. 6.   Rotor vibrations in axial direction caused by different eccentricities during nominal speed.

In Fig. 7 lower rotational speed (115 rpm) comparison is shown. One full rotation is represented and it is again clear that dynamic eccentricity is the most dangerous situation. Amplitude is almost the same as with nominal speed and difference between dynamic and healthy is 2.06 mm. That makes the vibration's amplitude two times bigger than of the healthy machine.

Static eccentricity caused vibration amplitudes are 0.1 mm bigger from healthy case, that is a smaller increase than with 230 rpm. The biggest difference regarding to nominal speed situation comes while looking at the extra mass caused vibrations, which are 0.88 mm bigger than zero based vibration as shown in Table I. Mass center dislocation influences the structure more while working with lower speeds, oppositely to the other eccentricities.
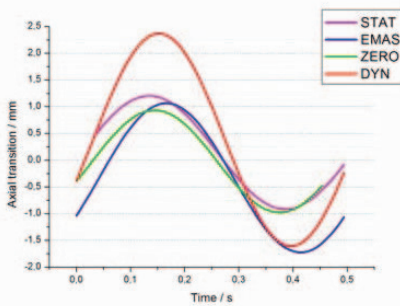

Fig. 7. Rotor vibrations in axial direction caused by different eccentricities during 115 rpm.

290 rpm test results are represented in Fig. 8 and in Table I. Increase in rotational speed changed the worst case situation amplitudes slightly. Dynamic eccentricity caused vibrations were now 2.2 mm bigger than the healthy case ones. Also, static eccentricity situation has only a bit higher amplitudes than compared to the 230 rpm case. From that we can conclude that rotational speed influences vibrations caused by dynamic and static eccentricities, although the increase is small and insignificant. However, the difference of 0.32 mm in mass center dislocation caused vibrations proves the previously stated fact: vibrations caused by extra mass on rotor are influenced by rotational speed in the opposite way to the static and dynamic cases. The lower the speed is the higher are the vibrations.
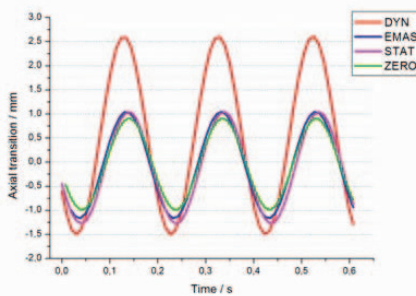

Fig. 8. Rotor vibrations in axial direction caused by different eccentricities during 290 rpm.

TABLE I.   ECCENTRICITY CAUSED VIBRATION AMPLITUDE DIFFERENCES FROM HEALTHY MACHINE AMPLITUDES

Amplitude difference ΔA			
Rotational speed	EMAS	STAT	DYN
rpm	mm	mm	mm
115	0.88	0.10	2.06
230	0.42	0.38	2.14
290	0.32	0.42	2.20

Vibrations in axial direction pose danger to the structure fatigue and bearings lifetime, but radial vibrations can have a direct outcome by influencing the magnetic forces [11] and in worst case closing the air-gap and damaging the electrical windings.

All radial deformation results are analyzed by referring to the healthy machine. The main issue is how much the air-gap changes between healthy and faulty situation.

Fig. 9 shows radial the difference of vibrations from the healthy situation on nominal rotational speed. It is clear that dynamic eccentricity is the only one that really poses any danger in terms of a serious air-gap change. Regarding the fact that the rotor was already shifted by 1 mm, additional vibrations with amplitude of 1.5 mm become a problematic issue. In no case it is safe to operate the machine in this condition. Stator eccentricity and mass dislocation caused radial vibrations pose no serious effect to the machine.
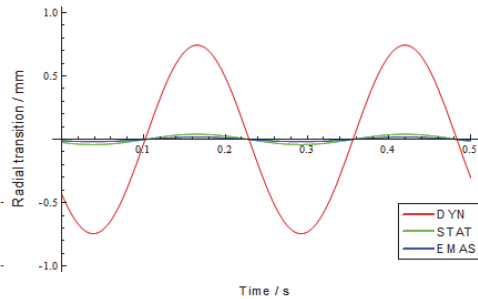

Fig. 9. Radial vibration difference from the healthy machine at nominal speed.

290 rpm situations are explained by Fig. 10. Compared to the nominal speed graph, nothing significant has changed. Dynamic eccentricity caused vibrations are at the same level and other vibration amplitude differences are still not more than 0.2 mm. Therefore, it can be said that vibration amplitudes did not increase more with higher rotational speed. This proves that in radial direction, rotational speed has almost no impact to the eccentricity caused vibrations.
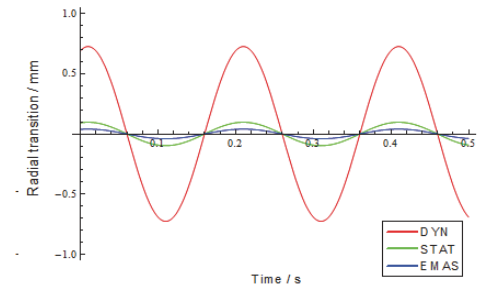

Fig. 10. Radial vibration difference from the healthy machine during 290 rpm.

Tests with 115 rpm showed the same differences in amplitudes, proving the stated hypothesis that speed has no influence and only dynamic eccentricity poses a real threat for the generator structure and to the air-gap uniformity. However, all eccentricity fault situations influence magnetic field. Therefore, output voltage is always influenced by the rotor eccentricities and extra forces are generated between the rotor and stator that could lead to unsymmetrical structural deformations and premature bearing fatigue failure.

V. Conclusion

An overview of slotless slow-speed permanent magnet generator rotor eccentricities has been presented. Method for measuring the mechanical vibrations via non-contact optical measurement system has been explained. Mechanical vibrations caused by mass center dislocation, static and dynamic eccentricities have been analyzed. Different rotational speeds have been included in the investigation. Results have been presented for rotor and stator separately and conclusions have been made.

Dynamic eccentricity is the most dangerous eccentricity situation for this machine. It amplifies the normal vibration amplitudes by factor of two and has a serious risk of air-gap closure. Uneven weight distribution and static eccentricity have an effect on the rotor, but it can be considered small and do not pose direct danger to the machine. Stator and rotor are affected differently, rotor has a direct influence with eccentricity, but stator has no increase of vibrations during eccentricity situations. Different rotational speeds affect the vibrations by amplitude increase in axial direction, however uneven mass distribution situation has higher amplitudes with lower speeds. Contrary to axial direction, rotational speed has no impact to vibration amplitudes in radial direction.

Relations between vibration magnitudes are used as an input for FEA model calibration. The model is used for further optimization of generator geometry and manufacturing methods in terms of eccentricity related faults.

References

[1] N. Bianchi, A. Lorenzoni, "Permanent magnet generators for wind power industry: an overall comparison with traditional generators," Int. Conf. on Opport. And Advant. In Int. Electric Power Gen., Durham, 1996, pp. 49–54.

[2] A. Kallaste, Low Speed Permanent Magnet Slotless Generator Development and Implementation for Windmills, Tallinn University of Technology. Doctoral Dissertation, 2013, 141 p.

[3] E. Spooner, P. Gordon, J. R. Bumby, and C. D. French, "Lightweight ironless-stator PM generators for direct-drive wind turbines," Electrical Power Applications, IEEE proceedings, vol. 152, no. 1, January 2005, pp. 17–26.

[4] A. Kallaste, A. Belahcen, A. Kilk, and T. Vaimann, "Analysis of the eccentricity in a low-speed slotless permanent-magnet wind generator," Proceedings of 8th International Conference 2012 Electric Power Quality and Supply Reliability, Tartu, June 11–13, 2012. IEEE, 2012, pp. 47–52.

[5] H. Merabet, T. Bahi, and Y. Soufi, "Fault detection and diagnosis of eccentricity in a wind generator," 8th International Conference and Exhibiton on Ecological Vehicles and Renewable Energies (EVER), (2013).

[6] B. M. Ebrahimi, J. Faiz, M. J. Roshtkari, "Static-, dynamic- and mixed eccentricity fault diagnoses in permanent-magnet synchronous motors," Industry Application Conference, 38th IAS Annual Meeting, vol. 3, 2003, pp. 1833–1838.

[7] J. K. H. Shek, D. G. Dorell, D. E. Macpherson, and M. A. Mueller, "Reducing bearing wear in induction generators for wave and tidal current energy devices," Renewable Power Generation (RPG 2011), IET Conference (2011).

[8] J. Cameron, W. Thomson, and A. Dow, "Vibration and current monitoring for detecting airgap eccentricity in large induction motors," Proceedings of IEE − Pt. B, May 1986, vol. 133, no. 3, pp. 155–163.

[9] S. Nandi, S. Ahmed, and H. Toliyat, "Detection of rotor slot and other eccentricity related harmonics in a three phase induction motor with different rotor cages," IEEE Transactions on Energy Conversion, September 2001, vol. 16, no. 3, pp. 253–260.

[10] http://www.gom.com/metrology-systems/3d-motion-analysis.html March 2013

[11] Y. K. Chin, P. Kanninen, P. Maki-Ontto, R. Sakki, and H. Lendenmann, "Phenomenon of magnetic force in permanent magnet wind turbine generarors," Electrical Machines and Systems, 2009. ICEMS 2009. pp. 1–6.

Paper 5

Patent application: EP14192176, Priority date 06.07.14: Placement and Replacement System and Method for Placing and Replacing the Electrical Components of Electromagnetic Rotary Machine. Owner: Goliath Wind OÜ, Inventors. **Pabut, O.**; Zingg, R.; Kisseljov, I.

5 **Title:** Placement and replacement system and method for placing and replacing the electrical components of
electromagnetic rotary machine

10 **Placement and replacement system and method for placing and replacing the electrical components
of electromagnetic rotary machine**

Field of the invention

The present invention belongs to the field of devices and methods for changing the electrical components,
more specifically coils and magnets, of electromagnetic rotary machines, more specifically electromagnetic
15 rotary machines with air-gap windings.

Background of the invention

The core of a generator are its coils and magnets, both situated at the outer-diameter of the generator on the
static and rotating parts respectively. Coils and magnets are critical components, which have to be inspected
and serviced on a regularly basis and if necessary replaced for the generator to maintain its integrity and
20 performance. Usually the permanent magnets are assembled on the generator structure with heavy machinery
in factory environment.

Preassembly of the magnets makes the generator sectors magnetically active during transportation phase.
Mounting and replacing coils and magnets in-situ may be at certain cases even more than in 100 m height.

Well known generators that exist on the market are transported in one piece, their electrical elements are
25 mounted in the factory and in case of premature failure the whole machine is replaced or lifted down from the
tower for repair or maintenance.

There are number of issues that the prior art does not solve. None of the known devices and methods can be
used for placing and replacing both coils and magnets. Having one method and device for both elements
significantly reduces the need for investment in materials and service personnel training. Furthermore, only
30 one device would need to be taken up to the generator on the wind turbine tower, if both coils and magnets
have failed. It is also suitable for handling the coils and magnets either in the factory, on the generator
assembly site or up tower. A configuration of a device which could be reasonably and efficiently operated in all
of the above mentioned conditions would result in reduced training time and material costs for various
configurations of equipment that is essentially performing the same task.

35 The prior art devices allow only initial placement of either coils or magnets into the generator. The way that the
devices are designed, handled and the fixing is performed allows no easy replacement of the electrically
active elements. With this configuration the initial cost of assembly is reduced but future failures on the active
elements would cause substantial problems and costs in servicing the machines.

The known devices require presence of rotor for placing or replacing coils on stator and presence of stator for
40 placing or replacing magnets on rotor. This implies that the modules cannot be placed or replaced while the
rotor and stator of the generator have not been inserted to each other and certain corresponding positioning is
needed between the two elements. Furthermore, in some cases it is required to rotate rotor or even stator to a
specific position, so the placement or replacement could take place. This is an action that significantly
increases time for needed operations and complicates the entire procedure by demanding extra tools or
45 design features. Therefore, a tool which could be operated on all stator and rotor positions would have
numerous advantages over the known solutions. Also, in certain cases it would be desired to conduct the
assembly of either coils or magnets without having either stator or rotor present, as this provides more space
for persons carrying out the actions and offers freedom in selecting assembly steps.

The prior art tooling in terms of coil placement and replacement is mostly suitable for replacing modules of
50 conventional slotted stator windings. However, as it is technically difficult to modularize this electromagnetic
configuration, the developed modules are heavy and cannot be handled by one or two persons. Due to the
weight of the modules, the equipment needed to manipulate them is also heavy and requires extra devices
and lifting hoists to be attached to the generator. Even though, this is more cost efficient than removing the
whole generator for maintenance or replacement, the extra equipment unnecessarily complicates the whole
55 procedure compared to a solution where the module and the device could be handled by one or two persons
without extra tooling. One also has to acknowledge that devices and methods which are meant for slotted
continuous stator windings, do not suit and cannot be adapted with reasonable effort for air-gap winding.

The closest known prior art solutions to avoid the placement and replacement and transportation issues and heavy machinery for electrical machines used in wind turbines are described as follows.

US patent application US20120073118A1 describes a module-handling tool for facilitating installation, servicing and dismantling of an electromagnetic rotary machine, having a modularized active portion. The handling tool itself is very complicated in terms of structure, operation procedure and fixing system. Due to the complexity and heavy weight, it needs to be hoisted up to the wind turbine by a crane and requires usage of an auxiliary turning mechanism on ground. Substantial workforce is needed to carry out the module replacement operation. Necessity for a crane adds considerable cost and time to the entire operation. Usage and fixing of the system requires presence of the generator rotor. During initial assembly this could be undesirable as the rotor would restrict access to the stator area. Furthermore, only few places at the rotor can accommodate the fixtures of the handling tool and therefore the rotor needs to be rotated to a module receiving location before the actual servicing can take place. This has considerable negative effects on the replacement time and unnecessarily complicates the entire procedure. Usage of the tool requires removal of permanent magnets in the vicinity of the replaceable coil modules. Therefore, another tool is needed to first remove the magnets and then further equipment is required to store them safely. Both of which are undesirable as they add cost and complexity to the entire operation and propose serious safety risks.

The known devices and method require large amount of assembly hours and sophisticated technology for mounting the electrical parts, i.e. coils and magnets, on the generator; increase the maintenance time and propose additional concerns related to safety; the known tools can be used only for insertion or removing of either magnet modules or coil modules and cannot be used removal or replacement or insertion of both modules; due to the heavy weight the additional hoisting equipment is required, which increases time for needed operations and complicates the entire procedure by demanding extra tools and design features; the known solutions cannot be handled by one or two persons, due to the complexity the special personnel training is needed; and complicated positioning systems are needed to achieve correct position between rotor and stator. These drawbacks make the prior art solutions complicated, expensive and unsafe to use.

Brief description of the invention

The purpose of the present placement and replacement system is to enable safe and controlled placement and replacement of coil modules and corresponding magnets on an electromagnetic rotary machine (for example generator of wind motors, generator of marine current turbines, motor of marine propulsion devices), which could be but does not have to be located on the top of the wind turbine tower with minimum time, prior training and physical effort. The design of the present placement and replacement system allows replacing individual elements of the electromagnetic rotary machine in case of electrical component (for example coils, magnets) failure, instead of replacing the whole machine. Replacing whole generator requires high capacity cranes, special personnel training and considerable amount of time, during which the machine and correspondingly the turbine cannot be operated.

The present placement and replacement system for placing and replacing the coils and magnets of electromagnetic rotary machine enables to carry out the placement or replacement procedure with a crew of maximum 2 persons without using hoisting machines (e.g. cranes, etc.) or other external assembly devices (winches, jigs, turntables etc.). The same principal procedure and very same device can be used for both coils and magnets. However, when using the placement and replacement system on the stator, no engagement or removal of rotor and its elements is necessary. Same applies for placing or replacing magnets on rotor. Furthermore, the same device can be used efficiently in factory, at the turbine assembly site or up tower after full or partial installment of the electromagnetic rotary machine and even without having the ability to turn the rotor to a predefined module receiving location.

The electromagnetic rotary machine utilizes concentrated air-gap windings in contrast to known machines, which use continuous windings with slots. This enables to design and build the coil and magnet modules fully independent of each other and light enough to be handled by a crew of maximum 2 persons also for machines with capacities in the multi-megawatt range.

The separated coil and magnet modules are fitted with a heat exchanger having a geometrical shape that creates a cavity between the main part of the module and attachment point to the generator structure. This cavity is used for placing the placement and replacement system through the coil or magnet module. As the rails, upon which the modules are fixed, are same for both rotor and stator and over the rotor and stator perimeter, fixing and positioning of the placement and replacement system is similar for all positions and for both rotor and stator. As the geometrical locking between the placement and replacement system and magnet or coil module heat exchanger is not gravity direction dependent, the system is used at all positions in similar manner without having to deal with changing gravity.

As the present placement and replacement system is placed through the coil or magnet module in such a manner that it extends away from the generator air-gap, only the coil and magnet modules are respectively affected by the replacement action and no interaction between rotor and stator is necessary. Furthermore, the usage of non-magnetic materials and the manner of geometrical locking between the system and coil or magnet modules enables to use the placement and replacement system under the influence of magnetic field

of the electromagnetic rotary machine while keeping full functionality and control over the system behavior. This means that the placement or replacement action can take place at any phase of the assembly process as soon as at least one of the generator support structure modules has been manufactured. As the system is not affected by the machine's relative position towards the gravity direction, it can be used at any phase of the
5   assembly process with same effectiveness in the factory, at the generator assembly site or up tower.

The differences between the present placement and replacement system and prior art devices:
- Same method and system for both coil and magnet;
- The present placement and replacement system can be used on generator configurations with air-gap winding;
10   - The present placement and replacement system and modules can be handled with a crew of maximum 2 persons without having to use other external assembly devices like winches, jigs, turntables, cranes etc.;
- The present placement and replacement system does not require the presence or preadjustment of rotor when handling the coils and presence of preadjustment of stator when handling the magnets;
15   - The present placement and replacement system can be used in the same manner at any positions of the electromagnetic rotary machine and also in a factory, assembly site or up the wind turbine tower;
- The present placement and replacement system is lighter, less expensive, easier to mount, easier to remove and faster to operate than any other know prior art solution;
- The present placement and replacement system is not affected by the magnetic forces of electromagnetic rotary machine.

20   **Description of the drawings**

The present invention is explained more precisely with references to figures added, where:
FIG. 1 shows a preferred embodiment of a placement and replacement system according to present invention;
FIG. 2 shows an example of electromagnetic rotary machine with replaceable coil and magnet modules;
FIG. 3 illustrates a front view of the present placement and replacement system shown on FIG. 2 with magnet
25   module;
FIG. 4 illustrates a front view of the present placement and replacement system shown on FIG. 2 with coil module;
FIG. 5 illustrates a cross-sectional view of the placement and replacement system and attachment profile, bearing assemblies and main body in the preferred embodiment;
30   FIG. 6 shows an alternative embodiment of attachment profile, bearing assemblies and main body;
FIG. 7 shows second alternative embodiment of attachment profile, bearing assemblies and main body;
FIG. 8 to FIG 10 show an example of a procedure concerning electrical component removal and replacing with the placement and replacement system according to present invention.

Detailed description of the invention

35   The placement and replacement system according to present invention for placing and replacing the electrical components of electromagnetic rotary machine, comprising frame, multiple of system fixing means to attach the system to the electromagnetic rotary machine, moving means for inserting electrical components to the electromagnetic rotary machine and extracting the electrical components from the electromagnetic rotary machine to place or replace the electrical components.

40   The frame of the system comprises a movable carriage 1 and main body 2 comprising guiding means. The system fixing means comprises first mounting bracket 3 and second mounting bracket 4, multiple of nut block fixing means 5, at least one adjustment mean 6, at least one bracket mounting element 7. The moving means comprises movable carriage 1, screw mechanism 8 including locking mean, nut block, preferably threaded nut block 9, crank block assembly 10, first bearing assembly 11 and second bearing assembly 12 connecting the
45   main body 2 and movable carriage 1, turning head 13, support bearing 14, multiple of support bearing fixing means 15, and attachment profile 16.

The placement and replacement system according to present invention comprises a movable carriage 1, screw mechanism 8, threaded nut block 9, crank block assembly 10, main body 2, first bearing assembly 11 and second bearing assembly 12 connecting the main body 2 and movable carriage 1, turning head 13,
50   support bearing 14, adjustable mounting bracket 3, at least one adjustment mean 6 (for example bolts), fixed mounting bracket 4, multiple of nut block fixing means 5, multiple of support bearing fixing means 15.

FIG. 2 shows an example of electromagnetic rotary machine for which the present placement and replacement system is used having a stator 27 and rotor 28. Both of which are supported by main shaft and king-pin assembly 29. To use the present placement and replacement system, the rotor 28 of electromagnetic
55   rotary machine is preferably located radially inward from the stator 27 however, in the alternative embodiments the placement and replacement system is used in configuration where stator 27 is located radially inward from the rotor 28. Both stator 27 and rotor 28 are made up from plurality of stator structure segments 30 and rotor structure segments 31 which functionally complete the stator 27 and rotor 28 carrier structures. These carrier structures feature generator fixing rails 22, having the same cross-sectional
60   geometry.

The present placement and replacement system in the preferred embodiment is applicable, wherein the rails feature preferably H-shaped geometry, however in alternative embodiments the placement and replacement system is applicable for various other geometrical shapes that feature at least one extending edge like L, Z or T-bars; the stator and rotor fixing rails 22 feature the same cross-sectional geometry; the electrical component, coil and magnet, modules 17 feature a similar geometry in terms of features relevant for achieving fixing and the electrical component, coil and magnet, modules 17 can be handled with a crew of maximum two persons.

The stator rails 22 are used to carry the stator coil modules 17 and rotor rails 22 are used to carry the rotor magnet modules 17. Modularity of stator 27 is achieved by using concentrated air-gap windings which do not specifically require that the stator active parts form a circumferentially tight structure in order to achieve reasonable electromagnetic efficiency figures for the rotary machine. Furthermore, the utilization of air-gap winding concept has a number of advantages, for example the possibility to design and build the modules relatively light and fully independent of each other, which makes it possible to replace them in case of dielectric break down. This is of significant importance when considering electromagnetic rotary machines placed in wind power units. There the maintenance and repair works can be very difficult and expensive especially when large cranes and crews are needed. Therefore, the present placing and replacement system which can be handled by a crew of maximum 2 persons without additional lifting equipment or jigs helps to achieve large economic impact.

FIG. 1 shows a preferred embodiment of the present placement and replacement system for placing and replacing the electrical component modules 17, wherein the component modules are coil and magnet modules, which are to be engaged with the movable carriage 1. In order to facilitate translational movement a screw mechanism 8 is attached to the movable carriage 1 via threaded nut block 9. As the threads of the screw mechanism 8 and nut block 9 become engaged, the movable carriage 1 will be translated along the rotational axis of the screw mechanism 8 while the mechanism is being turned. The threaded nut block 9 is fixed to the movable carriage 1 by nut block fixing means 4.

To combat the acting forces and block the rotational movement of the movable carriage 1, it is guided on the surface of the main body 2 by a first bearing assembly 11 and second bearing assembly 12. In the present embodiment, preferably pair of linear ball bearing rails are positioned on the main body 2, in alternative embodiments various other guiding means to facilitate the needed manner of guiding, like sliding bearings, multiple of attached roller bearings or full block anti friction materials, are possible. By the movable carriage 1, main body 2 and first bearing assembly 11 and second bearing assembly 12 is formed a system exhibiting stiffness properties that allow the system to withstand the magnetic and gravity forces without compromising the system's ability to facilitate translational movement for example due to the blockage of the first bearing assembly 11 and second bearing assembly 12 by deformations.

During the operation of the present placement and replacement system, it experiences a number of forces varying in strength and direction. In the preferred embodiment, to avoid involuntary movement of the carriage 1 while under the influence of these forces, the screw mechanism 8 comprises locking mean, for example trapezoidal or square thread profiles. In alternative embodiments the involuntary movement is avoided by application of braking systems, usage of high ratio gearing or application of bearings, with high friction, to support the screw mechanism 8.

To generate translational movement the screw mechanism 8 can be driven by a suitable drive mechanism via the crank block assembly 10 by applying force or a tool, capable of generating such force, to the turning head 13 (for example hexagonal wrench, hand-crank, pneumatic or electric or hydraulic mechanism or another tool capable of generating rotational force to move the movable carriage 1). The crank block assembly 10 is supported by a support bearing 14, which enables the crank block to turn around its rotational axis while blocking all other movements. The support bearing 14 is attached to the main body 2 by support bearing fixing screws 5.

Adjustable mounting bracket 3 and fixed mounting bracket 4 are attached to the main body 2 in order to make it possible for the system to become engaged with stator rails and rotor rails 22 (FIG. 2). The fixed mounting bracket 4 is attached to the main body 2 by means of welding or utilization of screws and bolts. The adjustable mounting bracket 3 is fixed to the main body via at least one adjustment mean 6 in order to allow necessary adjustment movements described in following paragraphs.

FIG. 3 illustrates a front view of the placement and replacement system's engagement with the electrical component module 17, for example magnet module, comprising attachment profile 16, base plate 32 and permanent magnet blocks 33, wherein the attachment profile 16 is magnet attachment profile, having a cavity 21 in the middle of the profile with inner mounting surfaces 18, vertical mounting surfaces 19 and outer mounting surfaces 20.

FIG. 4 illustrates the system's engagement with the electrical component module, for example coil module 17, comprising attachment profile 16 and embedded winding module 34, wherein the attachment profile 16 is coil attachment profile, having a cavity 21 in the middle of the profile with inner mounting surfaces 18, vertical mounting surfaces 19 and outer mounting surfaces 20.

Due to that, the magnet module and coil module comprise attachment profile 16 with the exactly same inner geometry, the system's engagement with the module is therefore only illustrated based on the example of the magnet module 17.

5   In addition to the placement and replacement action the attachment profile 16 serves also as a passive heat exchanger by dissipating heat generated during energy production of the electromagnetic rotary machine. The heat exchanger for the modules is required from the operational side of the machine, while only the inner geometry of it is shaped in a form suitable for placement and replacement action. Therefore, the attachment profile 16 is utilized for two functions, bringing savings in material and production costs.

10   Referring to FIG. 3 and FIG. 4, to facilitate the placement or replacement action, the system is slid through the cavity 21 in the attachment profile 16. This features inner mounting surfaces 18, vertical mounting surfaces 19 and outer mounting surfaces 20, which form an enclosed space in a manner that once the movable carriage 1 has been inserted into the cavity 21, only translational movement along the screw mechanism's 8 length wise axis remains possible. This degree of freedom is removed by placing at least two mounting elements 23 (for example screws, bolts, etc.) through the apertures 35 of attachment profile 32 into the apertures 36 of

15   movable carriage 1.

Geometrical locking between placement and replacement system and attachment profile 16 is facilitated in such a manner that the movable carriage 1 fully supports the attachment profile 16 despite the particular direction of gravity or magnetic forces acting in the view plane. For example, if the major force component is acting in the vertical direction of the view plane, the module is supported by inner mounting surfaces 18 or

20   outer mounting surfaces 20. When the major force component is acting in the horizontal direction of the view plane, the module is supported by vertical mounting surfaces 19. The particular feature makes it possible to use the placement and replacement system at any position of the electromagnetic rotary machine if proper mounting of the system to the rails 17 can be facilitated.

25   The ability to use the system at any position of the electromagnetic rotary machine with same effectiveness allows performing the needed replacement action without having to employ complicated positioning systems to achieve correct position between rotor and stator.

Handling and initial positioning of the system under the influence of magnetic forces is complicated and labour intensive work. In general, the influence of magnetic forces can be avoided for the placement of coil modules 17 but must be taken into account for magnet modules 17. Therefore, to use one system for both of the

30   electrical component modules 17 the elements of the present placement and replacement system are composed of non-ferromagnetic materials, such as austenitic stainless steel, ceramics, plastic, fiberglass or other composite materials. This allows using the same system for both electrical component, coil and magnet, modules 17 with same effectiveness.

35   FIG. 5 illustrates cross-sectional view of the placement and replacement system with the attachment profile 16. In this alternative embodiment the inner mounting surfaces 18 and outer mounting surfaces 20 in the profile are horizontal while the vertical supporting surfaces 19 are vertical. All these surfaces come in contact with the movable carriage 1 and facilitate the geometrical locking between elements. The movement of the carriage 1 relative to the main body 2 is facilitated by the first bearing assembly 11 and second bearing assembly 12, wherein the first and second bearing assembly are linear ball bearing.

40   FIGS. 6 and 7 show both alternative embodiments of attachment profile 16 and first bearing assembly 11 and second bearing assembly 12 designs. On FIG. 6 the movement of the carriage 1 relative to the main body 2 is facilitated by bearing assemblies 11 and 12 consisting of screwed on blocks of antifriction material (for example polyamide).

45   On FIG. 7 the bearing assemblies 11 and 12 consist of numerous screwed on roller bearings while the inner mounting surfaces 18 and outer mounting surfaces 19 are non- horizontal and the geometrical locking between the movable carriage 1 and attachment profile 16 is achieved by fishtail like elements.

The method, according to the present invention, for placing and replacing the electrical components of electromagnetic rotary machine with the system comprising frame, multiple of system fixing means to attach the system to the electromagnetic rotary machine, moving means for inserting electrical components to the

50   electromagnetic rotary machine and extracting the electrical components from the electromagnetic rotary machine to place or replace the electrical components. The method comprises attaching the system to the electromagnetic rotary machine to place and/or replace the electrical components, removing the electrical component to replace the electrical component and inserting the electrical component to the electromagnetic rotary machine.

55   Attaching the system to the electromagnetic rotary machine comprises following steps: sliding the system through the cavity 21 in the electrical component 17 attachment profile 16; clamping initially the system to the extending edges of stator sector rails 22 by first mounting bracket 3 and second mounting bracket 4; once initial clamping is achieved, moving the first adjustable mounting bracket 3 forward towards the extending edge of the stator rail 17 and fixing to it by at least one bracket mounting element 7 and by securing at least

60   one adjustment element 6 to the main body 2.

Removing the electrical component from the electromagnetic rotary machine comprises following steps: positioning and placing of the system; translating the movable carriage 1 into the attachment profile 16 by crank block assembly 10 and geometrically locking the attachment profile 16 and the system; locking the mounting elements 23 into place and removing module mounting elements 24 and engaging the electrical

5   component 17 with the placement and replacement system and transporting out of the electromagnetic rotary machine air-gap 25 by using the crank block assembly 10; transporting the electrical component 17 out of the electromagnetic rotary machine air-gap 25 to the end position and removing the mounting elements 23; finalizing the removing procedure by sliding the electrical component 17 off the placement and replacement system.

10   Removing the placement and replacement system by unclamping the first mounting bracket 3 and second mounting bracket 4 from the rails 22 or inserting the electrical component to the electromagnetic rotary machine, wherein inserting the electrical component comprises following steps: inserting new electrical component 17 by sliding the electrical component 17 onto the movable carriage 1 and locking into place by mounting elements 23; translating the electrical component 17 into end position of the placement and

15   replacement system via crank block assembly 10; fixing the electrical component 17 onto the rails 22 by module mounting elements 24; releasing the placement and replacement system by removing the mounting elements 23 from the attachment profile 16 and main body 2; translating the movable carriage 1 into the start position via crank block assembly 10; loosening the adjustment elements 6 and removing the bracket mounting elements 7; moving the first mounting bracket 3 away from the rail 22 and sliding the placement and

20   replacement system out of the attachment profile 16.

As follows the present method is described in more detailed. FIG. 8, FIG. 9 and FIG. 10 show an example of a procedure concerning electrical component, for example coil module, 17 removal with the placement and replacement system. In the preferred embodiment referring to FIG. 8, the system has been slid through the cavity 21 in the electrical component, for example coil module, 17 attachment profile 16. Adjustable mounting

25   bracket 3 and fixed mounting bracket 4 are used to achieve the initial clamping between the system and the extending edges of stator sector rails 22. The possibility to use the attachment profile 16 in order to slide the system into correct position for fixing is crucial, when considering the effort required to manipulate the system. Although, it can be handled by one person, less effort is required to position the system correctly, when it can be initially supported by the coil profile.

30   Once initial clamping has been achieved, the adjustable mounting bracket 3 is moved forward towards the extending edge of the stator rail 22 and fixed to it by at least one bracket mounting element 7. Final position and placement of the system is achieved by securing at least one adjustment element 6 to the main body 2.

FIG. 9 describes a situation where the movable carriage 1 has been translated into the attachment profile 16 by the use of crank block assembly 10. By this action the initial geometrical locking between the attachment

35   profile 16 and placement and replacement system is achieved. Once the mounting elements 23 are locked into place and module mounting elements 24 have been removed, the electrical component, for example coil module, 17 is fully engaged only with the placement and replacement system and can be transported out of the electromagnetic rotary machine air-gap 25 by the use of the crank block assembly 10.

FIG. 10 illustrates the phase where the electrical component, for example coil module, 17 has been

40   transported out of the electromagnetic rotary machine air-gap 25 to the end position and the mounting elements 23 (FIG. 9) have been removed. At this position the coil module 17 does not experience any magnetic forces and therefore is safe to handle without use of extra equipment. Now the module can be slid off the placement and replacement system and thus the removal procedure can be considered finalized. In the final position of the coil module 17, the support offered by the movable carriage 1 reduces the amount of

45   manual labour required to handle the module, which makes it possible to handle it with a crew of maximum two persons.

After removal of coil the module 17 either the placement and replacement system can be removed by unclamping the adjustable mounting bracket 3 and fixed mounting bracket 4 from the stator rails 22 or a new coil module 17 can be inserted by reversing the previously described steps. New module is slid onto the

50   movable carriage 1 and locked into place by mounting elements 23. After locking, the module will be translated into end position of the placement and replacement system via crank block assembly 10. There the plurality of module mounting elements 24 are utilized to fix the coil module 17 onto the stator rails 22. In order to remove the placement and replacement system the mounting elements 23 are removed from the attachment profile 16 and main body 2. The movable carriage 1 is translated into the starting position via

55   crank block assembly 10. Adjustment elements 6 are loosened and bracket mounting elements 7 are removed. The adjustable mounting bracket 3 is moved away from the stator rail 22 and the placement and replacement system is slid out of the attachment profile 16.

In an alternative embodiment initial positioning of the placement and replacement system is attached to the stator rails 22 without having an electrical component, for example coil module, 17 on the site of placement. In

60   that particular situation the system is clamped to the stator structure segment 30 in similar manner, however the initial positioning of the system is achieved via bracket mounting elements 7. The correctness of the positioning is confirmed by insertion and alignment of module mounting elements 24. In case of erroneous or

undesired positioning, the whole coil module 17 and placement and replacement system assembly can be relocated by slightly loosening the bracket mounting elements 7 without compromising any of safety related requirements.

Low weight of the system, simple and fast operation principles make it possible and also technically reasonable to utilize the system for both coil and magnet placement and replacement up tower, in the factory and on the wind power unit erection site.

Furthermore, due to the fact that for example only rotor rails 22 are required to achieve system placement, neither the existence of stator or even full rotor structure is necessary. As outer diameters of directly driven electromagnetic rotary machines in wind power units are growing as capacities grow, ultimately mechanical segmentation of the carrier structures for such machines is necessary in order to avoid transportation issues. In such cases, the final assembly of machines would take place on the wind power unit erection site. As it is dangerous and economically unjustified to transport highly magnetized segments of electromagnetic rotary machines, the permanent magnet modules would ultimately have to be assembled also on that erection site. Therefore, a device and method which could be used to assemble coil and magnet modules at wind power unit erection site with needed efficiency and without demands for infrastructure can be regarded as highly beneficial.

Claims

1. A placement and replacement system for placing and replacing the electrical components of electromagnetic rotary machine, comprising frame, multiple of system fixing means to attach the system to the electromagnetic rotary machine, moving means for inserting electrical components to the electromagnetic rotary machine and extracting the electrical components from the electromagnetic rotary machine to place or replace the electrical components, **characterized** in that,
    −   the frame of the system comprises a movable carriage (1) and main body (2) comprising guiding means;
    −   the system fixing means comprises first mounting bracket (3) and second mounting bracket (4), multiple of nut block fixing means (5), at least one adjustment mean (6), at least one bracket mounting element (7);
    −   the moving means comprises screw mechanism (8) including locking mean, nut block (9), crank block assembly (10), first bearing assembly (11) and second bearing assembly (12) connecting the main body (2) and movable carriage (1), turning head (13), support bearing (14), multiple of support bearing fixing means (15), and attachment profile (16), wherein
    a screw mechanism (8) is attached to the movable carriage (1) via nut block (9), which is fixed to the movable carriage (1) by nut block fixing means (5), the movable carriage (1) is translated along the rotational axis of the screw mechanism (8) while the mechanism is being turned, the movable carriage (1) is guided on the surface of the main body (2) by a first bearing assembly (11) and second bearing assembly (12), the crank block assembly (10) is supported by a support bearing (14), the support bearing (14) is attached to the main body (2) by support bearing fixing means (15) and the electrical components to be replaced are engaged with the movable carriage (1).

2. The placement and replacement system according to claim 1, **characterized** in that, the electrical component is stator coil module or rotor magnet module (17).

3. The placement and replacement system according to claim 1, **characterized** in that, the first mounting bracket (3) is adjustable and second mounting bracket (4) is fixed.

4. The placement and replacement system according to claim 1, **characterized** in that, the guiding mean of main body (2) is pair of linear ball bearing rails, sliding bearings, multiple of attached roller bearings or full block anti friction materials.

5. The placement and replacement system according to claim 1, **characterized** in that, by the carriage (1), main body (2) and first bearing assembly (11) and second bearing assembly (12) the system exhibiting stiffness properties is formed.

6. The placement and replacement system according to claim 1, **characterized** in that, the screw mechanism (8) comprises locking mean, which is trapezoidal thread profile, square thread profiles, braking system, usage of high ratio gearing or application of bearings, with high friction.

7. The placement and replacement system according to claim 1, **characterized** in that, the turning head (13) can be engaged with hexagonal wrench, hand-crank, pneumatic, electric or hydraulic mechanism or another tool capable of generating rotational force to move the movable carriage (1).

8. The placement and replacement system according to claim 1, **characterized** in that, the first mounting bracket (3) and second mounting bracket (4) are attached to the main body (2).

9. The placement and replacement system according to claim 1, **characterized** in that, the first mounting bracket (3) is fixed to the main body via at least one adjustment mean (6).

10. The placement and replacement system according to claim 1, **characterized** in that, the bearing assemblies (11) and (12) are linear ball bearing, screwed on blocks of antifriction material or screwed on roller bearings.

11. The placement and replacement system according to claim 1, **characterized** in that, the movable carriage (1) comprises inner mounting surfaces (18), vertical mounting surfaces (19) and outer mounting surfaces (20), forming an enclosed space in a manner that once the movable carriage (1) has been inserted into the cavity (21), only translational movement along the screw mechanism's (8) length wise axis remains possible and the geometrical locking between the movable carriage (1) and attachment profile (16) is achieved.

12. The placement and replacement system according to claim 11, **characterized** in that, the inner mounting surfaces (18) and outer mounting surfaces (20) in the profile are horizontal and the vertical supporting surfaces (19) are vertical.

13. The placement and replacement system according to claim 11, **characterized** in that, the inner mounting surfaces (18), outer mounting surfaces (20) are non- horizontal.

14. The placement and replacement system according to claim 11, **characterized** in that the geometrical locking between the movable carriage (1) and attachment profile (16) is achieved in contact of inner mounting surfaces (18), supporting surfaces (19), outer mounting surfaces (20) with movable carriage (1).

15. The placement and replacement system according to claim 11, **characterized** in that, the geometrical locking between the movable carriage (1) and attachment profile (16) is achieved by fishtail like elements.

16. A method for placing and replacing the electrical components of electromagnetic rotary machine with the system comprising frame, multiple of system fixing means to attach the system to the electromagnetic rotary machine, moving means for inserting electrical components to the electromagnetic rotary machine and extracting the electrical components from the electromagnetic rotary machine to place or replace the electrical components, **characterized** in that the method comprises attaching the system to the electromagnetic rotary machine to place and/or replace the electrical components, removing the electrical component to replace the electrical component and inserting the electrical component to the electromagnetic rotary machine, wherein

Attaching the system to the electromagnetic rotary machine comprises following steps:
   – Sliding the system through the cavity (21) in the electrical component (17) attachment profile (16);
   – Clamping initially the system to the extending edges of stator sector rails (22) by first mounting bracket (3) and second mounting bracket (4);
   – Once initial clamping is achieved, moving the first mounting bracket (3) forward towards the extending edge of the stator rail (22) and fixing to it by at least one bracket mounting element (7);

Removing the electrical component from the electromagnetic rotary machine comprises following steps:
   – Positioning and placing of the system;
   – Translating the movable carriage (1) into the attachment profile (16) by crank block assembly (10) and geometrically locking the attachment profile (16) and the system;
   – Locking the mounting elements (23) into place and removing module mounting elements (24) and engaging the electrical component (17) with the placement and replacement system and transporting out of the electromagnetic rotary machine air-gap (25) by using the crank block assembly (10);
   – Transporting the electrical component (17) out of the electromagnetic rotary machine air-gap (25) to the end position and removing the mounting elements (23);
   – Finalizing the removing procedure by sliding the electrical component (16) off the placement and replacement system.

Removing the placement and replacement system by unclamping the first mounting bracket (3) and second mounting bracket (4) from the rails (22) or inserting the electrical component to the electromagnetic rotary machine, wherein inserting the electrical component comprises following steps:
   – Inserting new electrical component (17) by sliding the electrical component (17) onto the movable carriage (1) and locking into place by mounting elements (23);
   – Translating the electrical component (17) into end position of the placement and replacement system via crank block assembly (10);
   – Fixing the electrical component (17) onto the rails (22) by module mounting elements (24);
   – Releasing the placement and replacement system by removing the mounting elements (23) from the attachment profile (16) and main body (2);
   – Translating the movable carriage (1) into the start position via crank block assembly (10);
   – Loosening the adjustment elements (6) and removing the bracket mounting elements (7);
   – Moving the first mounting bracket (3) away from the rail (22) and sliding the placement and replacement system out of the attachment profile (16).

17. The method according to claim 16, **characterized** in that the electrical component (17) is stator coil module or rotor magnet module.

18. The method according to claim 16, **characterized** in that, to generate translational movement the screw mechanism (8) is driven by a drive mechanism via the crank block assembly (10) by applying force or a tool, capable of generating such force, to the turning head (13).

Abstract

A placement and replacement system and method for placing and replacing the electrical components of electromagnetic rotary machine, wherein the system comprises a frame, multiple of system fixing means to attach the system to the electromagnetic rotary machine, moving means for inserting electrical components to the electromagnetic rotary machine and extracting the electrical components from the electromagnetic rotary machine to place or replace the electrical components.
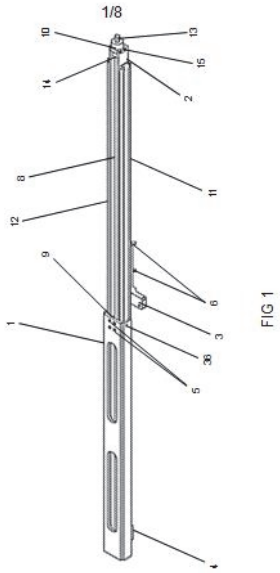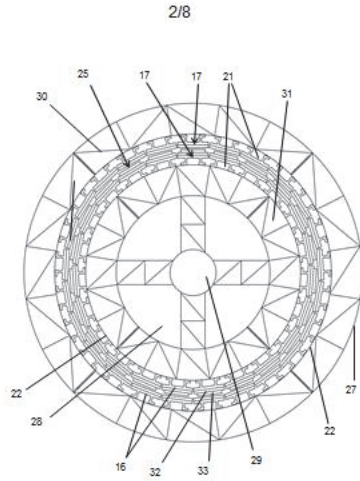
1/8

FIG 1
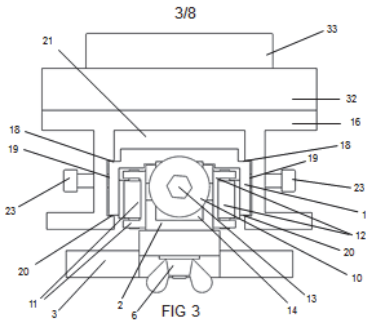

2/8

FIG 2

3/8

FIG 3

4/8

FIG 5

FIG 4

FIG 6

5/8

FIG 7

6/8

FIG 8

7/8

FIG 9

8/8
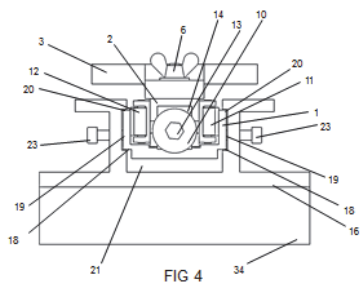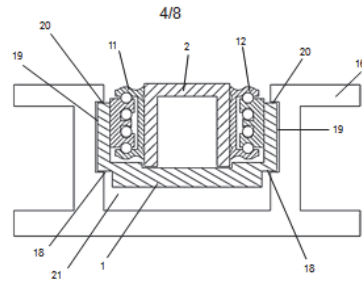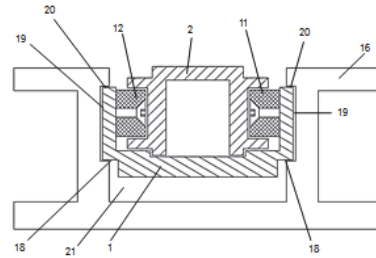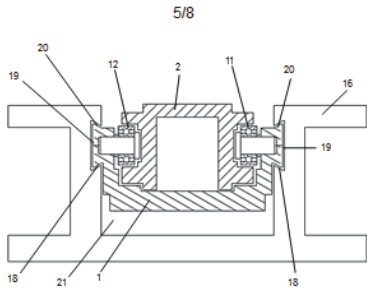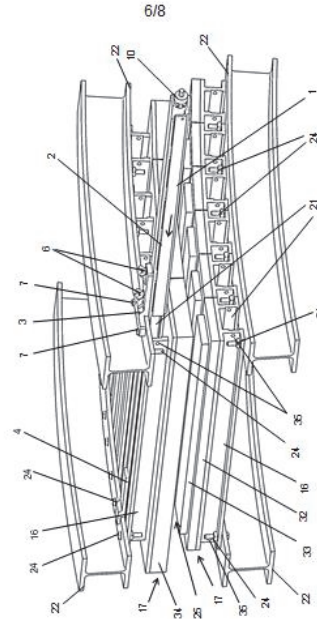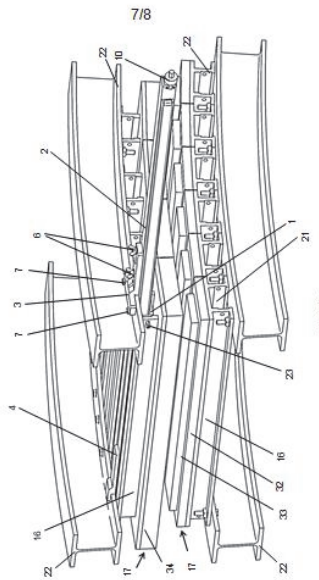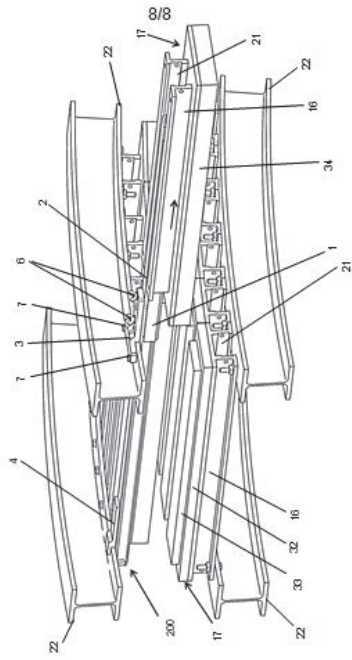
FIG 10

Curriculum Vitae

1. Personal data

Name	Ott Pabut
Date and place of birth	01.02.1986 Rakvere, Estonia
Nationality	Estonian
E-mail address	ott.pabut@ttu.ee

2. Education

Educational institution	Graduation year	Education (field of study/degree)
Tallinn University of Technology	2009	Product development and Production Engineering, MSc
Tallinn University of Technology	2008	Product development and Production Engineering, BSc
Tallinn Mustamäe Gymnasium	2005	Secondary education

3. Language competence/skills (fluent, average, basic skills)

Language	Level
Estonian	Fluent
English	Fluent
German	Basic
Russian	Basic

4. Special courses

Period	Educational or other organisation
02.2009	ANSYS V12.1 software training, Process Flow Ltd OY, Finland
09.2009 – 04.2010	Product development project, Aalto University, Finland
05.2015	Autodesk Product Design Suite 2015 software training, CAD360 OÜ, Estonia

5. Professional employment

Period	Organisation	Position
2010 – …	Goliath Wind OÜ	Managing Engineer
2009 – 2010	Tallinn University of Technology, Department of Machinery	Technician
2007 – 2007	JOT Automation OÜ	Trainee
2003 – 2003	North Estonia Medical Centre	Operating room assistant

6. Supervisions

- Tauno Tiirats, Bachelor of Science, "Analysis of Mechanical Vibrations Caused by Eccentricity in a Slow-Speed Slotless Permanent Magnet Generator", Tallinn University of Technology, 2014.

7. Projects

- Goliath OÜ wind generator, Lep10023, 01.02.10–16.04.10.
- The optimal design of constructions, products and production processes of composite and functional materials, SF0140035s12, 01.01.12–31.12.14.
- The analysis and development of digital direct production processes, ETF9441, 01.01.12–31.12.15.

8. Main research areas:

- applications of finite element analysis in design optimisation;
- enhancement of optimisation procedures;
- analysis and enhancement of computational models for permanent magnet generators;
- fatigue resistance of structures;
- modelling and analysis of frame structures;
- topology optimisation;
- wind energy technologies.

Elulookirjeldus

1. Isikuandmed

   Ees- ja perekonnanimi   Ott Pabut
   Sünniaeg ja -koht   01.02.1986 Rakvere, Eesti Vabariik
   Kodakondsus   Eesti
   E-posti aadress   ott.pabut@ttu.ee

2. Hariduskäik

Õppeasutus (nimetus lõpetamise ajal)	Lõpetamise aeg	Haridus (eriala/kraad)
Tallinna Tehnikaülikool	2009	Tootearendus ja tootmistehnika, Tehnikateaduste magistri
Tallinna Tehnikaülikool	2008	Tootearendus ja tootmistehnika, Tehnikateaduste bakalaureuse
Tallinna Mustemäe Gümnaasium	2005	Keskharidus

3. Keelteoskus (alg-, kesk- või kõrgtase)

Keel	Tase
Eesti keel	Kõrgtase
Inglise keel	Kõrgtase
Saksa keel	Algtase
Vene keel	Algtase

4. Täiendusõpe

Õppimise aeg	Täiendusõppe korraldaja nimetus
02.2009	ANSYS V12.1 kasutajakoolitus, Process Flow Ltd OY, Soome
09.2009 – 04.2010	Product development project, Aalto Ülikool, Soome
05.2015	Autodesk Product Design Suite 2015 kasutajakoolitus, CAD360 OÜ, Eesti

5. Teenistuskäik

Töötamise aeg	Tööandja nimetus	Ametikoht
2010 – …	Goliath Wind OÜ	Projektijuht
2009 – 2010	Tallinna Tehnikaülikool, Masinaehituse instituut	Tehnik
2007 – 2007	JOT Automation OÜ	Praktikant
2003 – 2003	Põhja-Eesti Regionaalhaigla	Operatsioonitoa abiline

6. Juhendamised

- Tauno Tiirats, bakalaureuse kraad, „Püsimagnetgeneraatori ekstsentrilisusest tingitud mehaaniliste vibratsioonide analüüs", Tallinna Tehnikaülikool, 2014.

7. Projektid

- Goliath OÜ tuulegeneraator, Lep10023, 01.02.10–16.04.10.
- Komposiit- ja funktsionaalsetest materjalidest konstruktsioonide, toodete ja tootmisprotsesside optimaalne projekteerimine, SF0140035s12., 01.01.12–31.12.14.
- Digitaalsete otsetootmisprotsesside analüüs ja arendus, ETF9441, 01.01.12–31.12.15.

8. Teadustöö põhisuunad:

- lõplike elementide meetodi rakendused optimaalses projekteerimises;
- optimeerimismudelite täiustamine;
- püsimagnetgeneraatori arvutusliku mudeli analüüs ja täiustamine;
- struktuuride väsimustugevuse hindamine;
- sõrestikstruktuuride analüüs ja modelleerimine;
- topoloogia optimeerimine;
- tuuleenergeetika tehnoloogiad.

DISSERTATIONS DEFENDED AT
TALLINN UNIVERSITY OF TECHNOLOGY ON
MECHANICAL ENGINEERING

1. **Jakob Kübarsepp**. Steel-Bonded Hardmetals. 1992.

2. **Jakub Kõo**. Determination of Residual Stresses in Coatings &Coated Parts. 1994.

3. **Mart Tamre**. Tribocharacteristics of Journal Bearings Unlocated Axis. 1995.

4. **Paul Kallas**. Abrasive Erosion of Powder Materials. 1996.

5. **Jüri Pirso**. Titanium and Chromium Carbide Based Cermets. 1996.

6. **Heinrich Reshetnyak**. Hard Metals Serviceability in Sheet Metal Forming Operations. 1996.

7. **Arvi Kruusing**. Magnetic Microdevices and Their Fabrication methods. 1997.

8. **Roberto Carmona Davila**. Some Contributions to the Quality Control in Motor Car Industry. 1999.

9. **Harri Annuka**. Characterization and Application of TiC-Based Iron Alloys Bonded Cermets. 1999.

10. **Irina Hussainova**. Investigation of Particle-Wall Collision and Erosion Prediction. 1999.

11. **Edi Kulderknup**. Reliability and Uncertainty of Quality Measurement. 2000.

12. **Vitali Podgurski**. Laser Ablation and Thermal Evaporation of Thin Films and Structures. 2001.

13. **Igor Penkov**. Strength Investigation of Threaded Joints Under Static and Dynamic Loading. 2001.

14. **Martin Eerme**. Structural Modelling of Engineering Products and Realisation of Computer-Based Environment for Product Development. 2001.

15. **Toivo Tähemaa**. Assurance of Synergy and Competitive Dependability at Non-Safety-Critical Mechatronics Systems design. 2002.

16. **Jüri Resev**. Virtual Differential as Torque Distribution Control Unit in Automotive Propulsion Systems. 2002.

17. **Toomas Pihl**. Powder Coatings for Abrasive Wear. 2002.

18. **Sergei Letunovitš**. Tribology of Fine-Grained Cermets. 2003.

19. **Tatyana Karaulova**. Development of the Modelling Tool for the Analysis of the Production Process and its Entities for the SME. 2004.

20. **Grigori Nekrassov**. Development of an Intelligent Integrated Environment for Computer. 2004.

21. **Sergei Zimakov**. Novel Wear Resistant WC-Based Thermal Sprayed Coatings. 2004.

22. **Irina Preis**. Fatigue Performance and Mechanical Reliability of Cemented Carbides. 2004.

23. **Medhat Hussainov**. Effect of Solid Particles on Turbulence of Gas in Two-Phase Flows. 2005.

24. **Frid Kaljas**. Synergy-Based Approach to Design of the Interdisciplinary Systems. 2005.

25. **Dmitri Neshumayev**. Experimental and Numerical Investigation of Combined Heat Transfer Enhancement Technique in Gas-Heated Channels. 2005.

26. **Renno Veinthal**. Characterization and Modelling of Erosion Wear of Powder Composite Materials and Coatings. 2005.

27. **Sergei Tisler**. Deposition of Solid Particles from Aerosol Flow in Laminar Flat-Plate Boundary Layer. 2006.

28. **Tauno Otto**. Models for Monitoring of Technological Processes and Production Systems. 2006.

29. **Maksim Antonov**. Assessment of Cermets Performance in Aggressive Media. 2006.

30. **Tatjana Barashkova**. Research of the Effect of Correlation at the Measurement of Alternating Voltage. 2006.

31. **Jaan Kers**. Recycling of Composite Plastics. 2006.

32. **Raivo Sell**. Model Based Mechatronic Systems Modeling Methodology in Conceptual Design Stage. 2007.

33. **Hans Rämmal**. Experimental Methods for Sound Propagation Studies in Automotive Duct Systems. 2007.

34. **Meelis Pohlak**. Rapid Prototyping of Sheet Metal Components with Incremental Sheet Forming Technology. 2007.

35. **Priidu Peetsalu**. Microstructural Aspects of Thermal Sprayed WC-Co Coatings and Ni-Cr Coated Steels. 2007.

36. **Lauri Kollo**. Sinter/HIP Technology of TiC-Based Cermets. 2007.

37. **Andrei Dedov**. Assessment of Metal Condition and Remaining Life of In-service Power Plant Components Operating at High Temperature. 2007.

38. **Fjodor Sergejev**. Investigation of the Fatigue Mechanics Aspects of PM Hardmetals and Cermets. 2007.

39. **Eduard Ševtšenko**. Intelligent Decision Support System for the Network of Collaborative SME-s. 2007.

40. **Rünno Lumiste**. Networks and Innovation in Machinery and Electronics Industry and Enterprises (Estonian Case Studies). 2008.

41. **Kristo Karjust**. Integrated Product Development and Production Technology of Large Composite Plastic Products. 2008.

42. **Mart Saarna**. Fatigue Characteristics of PM Steels. 2008.

43. **Eduard Kimmari**. Exothermically Synthesized B_4C-Al Composites for Dry Sliding. 2008.

44. **Indrek Abiline**. Calibration Methods of Coating Thickness Gauges. 2008.

45. **Tiit Hindreus**. Synergy-Based Approach to Quality Assurance. 2009.

46. **Karl Raba**. Uncertainty Focused Product Improvement Models. 2009.

47. **Riho Tarbe**. Abrasive Impact Wear: Tester, Wear and Grindability Studies. 2009.

48. **Kristjan Juhani**. Reactive Sintered Chromium and Titanium Carbide-Based Cermets. 2009.

49. **Nadežda Dementjeva**. Energy Planning Model Analysis and Their Adaptability for Estonian Energy Sector. 2009.

50. **Igor Krupenski**. Numerical Simulation of Two-Phase Turbulent Flows in Ash Circulating Fluidized Bed. 2010.

51. **Aleksandr Hlebnikov**. The Analysis of Efficiency and Optimization of District Heating Networks in Estonia. 2010.

52. **Andres Petritšenko**. Vibration of Ladder Frames. 2010.

53. **Renee Joost**. Novel Methods for Hardmetal Production and Recycling. 2010.

54. **Andre Gregor**. Hard PVD Coatings for Tooling. 2010.

55. **Tõnu Roosaar**. Wear Performance of WC- and TiC-Based Ceramic-Metallic Composites. 2010.

56. **Alina Sivitski**. Sliding Wear of PVD Hard Coatings: Fatigue and Measurement Aspects. 2010.

57. **Sergei Kramanenko**. Fractal Approach for Multiple Project Management in Manufacturing Enterprises. 2010.

58. **Eduard Latõsov**. Model for the Analysis of Combined Heat and Power Production. 2011.

59. **Jürgen Riim**. Calibration Methods of Coating Thickness Standards. 2011.

60. **Andrei Surzhenkov**. Duplex Treatment of Steel Surface. 2011.

61. **Steffen Dahms**. Diffusion Welding of Different Materials. 2011.

62. **Birthe Matsi**. Research of Innovation Capasity Monitoring Methodology for Engineering Industry. 2011.

63. **Peeter Ross**. Data Sharing and Shared Workflow in Medical Imaging. 2011.

64. **Siim Link**. Reactivity of Woody and Herbaceous Biomass Chars. 2011.

65. **Kristjan Plamus**. The Impact of Oil Shale Calorific Value on CFB Boiler Thermal Efficiency and Environment. 2012.

66. **Aleksei Tšinjan**. Performance of Tool Materials in Blanking. 2012.

67. **Martinš Sarkans**. Synergy Deployment at Early Evaluation of Modularity of the Multi-Agent Production Systems. 2012.

68. **Sven Seiler**. Laboratory as a Service – A Holistic Framework for Remote and Virtual Labs. 2012.

69. **Tarmo Velsker**. Design Optimization of Steel and Glass Structures. 2012.

70. **Madis Tiik**. Access Rights and Organizational Management in Implementation of Estonian Electronic Health Record System. 2012.

71. **Marina Kostina**. Reliability Management of Manufacturing Processes in Machinery Enterprises. 2012.

72. **Robert Hudjakov**. Long-Range Navigation for Unmanned Off-Road Ground Vehicle. 2012.

73. **Arkadi Zikin**. Advanced Multiphase Tribo-Functional PTA Hardfacings. 2013.

74. **Alar Konist**. Environmental Aspects of Oil Shale Power Production. 2013.

75. **Inge Roos**. Methodology for Calculating CO_2 Emissions from Estonian Shale Oil Industry. 2013.

76. **Dmitri Shvarts**. Global 3D Map Merging Methods for Robot Navigation. 2013.

77. **Kaia Lõun**. Company's Strategy Based Formation of e-Workplace Performance in the Engineering Industry. 2013.

78. **Maido Hiiemaa**. Motion Planner for Skid-Steer Unmanned Ground Vehicle. 2013.

79. **Dmitri Goljandin**. Disintegrator Milling System Development and Milling Technologies of Different Materials. 2013.

80. **Dmitri Aleksandrov**. Light-Weight Multicopter Structural Design for Energy Saving. 2013.

81. **Henrik Herranen**. Design Optimization of Smart Composite Structures with Embedded Devices. 2014.

82. **Heiki Tiikoja**. Experimental Acoustic Characterization of Automotive Inlet and Exhaust System. 2014.

83. **Jelena Priss**. High Temperature Corrosion and Abrasive Wear of Boiler Steels. 2014.

84. **Aare Aruniit**. Thermoreactive Polymer Composite with High Particulate Filler Content. 2014.

85. **Dmitri Gornostajev**. Development of the Calculation Method for Barge Hull. 2014.

86. **Liina Lind**. Wear of PVD Coatings on Fineblanking Punches. 2014.

87. **Nikolai Voltšihhin**. Design and Technology of Oxides-Containing Ceramic-Based Composites. 2014.

88. **Aleksander Šablinski**. RANS Numerical Modelling of Turbulent Polydispersed Flows in CFB Freeboard. 2015.

89. **Tanel Aruväli**. Wireless Real-time Monitoring of Machining Processes. 2015.

90. **Andrei Bogatov**. Morphological Changes on Diamond and DLC Films During Sliding Wear. 2015.

91. **Raimo Kabral**. Aero-Acoustic Studies and Innovative Noise Control with Application to Modern Automotive Gas Exchange System. 2015.

92. **Jevgeni Sahno**. Dynamic Management Framework for Continuous Improvement of Production Processes. 2015.